Fachbereich
Ingenieurbaukunst

Lateral Load Bearing Systems of High-Rise Buildings Based on a Case Study

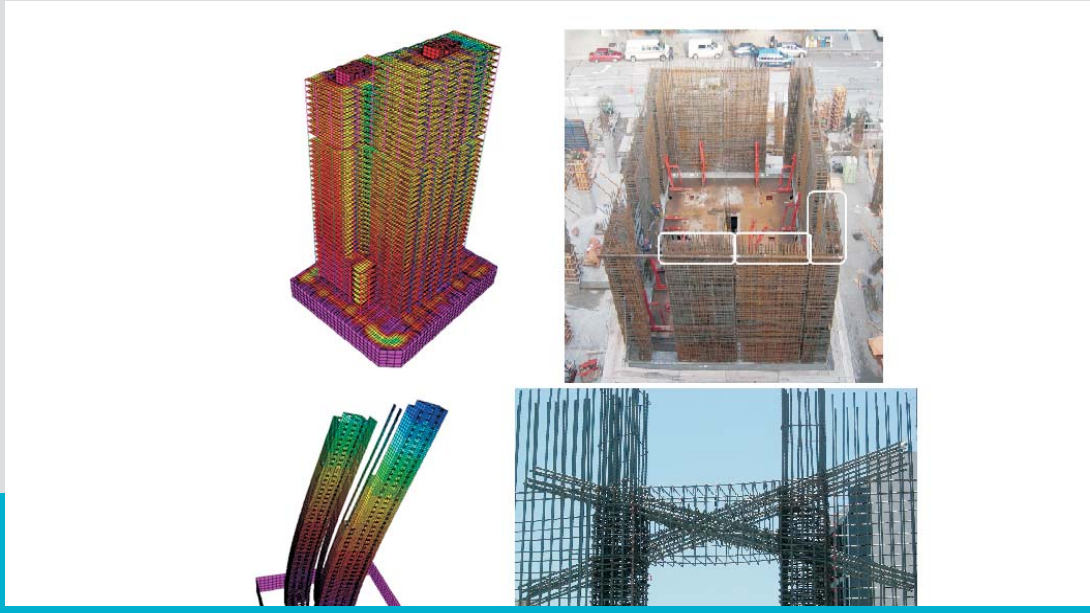

D-3-04/2014

Verfasser: **Yashar Pirayesh Rasteh**

Betreuer: **Nguyen Viet Tue, Univ.-Prof. Dr.-Ing. habil.**
Mitbetreuer: **Nguyen Duc Tung, Dr.-Ing.**

eingereicht am: **Institut für Betonbau**
Technische Universität Graz

Masterarbeit

Lateral Load Bearing Systems of High-Rise Buildings Based on a Case study

ausgeführt zum Zwecke der Erlangung des akademischen Grades eines Diplomingenieurs der Studienrichtung Bauingenieurwissenschaften

unter der Leitung von

O. Univ.-Prof. Dr.-Ing. habil. Viet Tue Nguyen

Betreuer

Dr. Duc Tung Nguyen

Institut für Betonbau

eingereicht an der Technischen Universität Graz

Fakultät für Bauingenieurwissenschaften

von

Yashar Pirayesh Rasteh, BSc

Graz, 02.10.2014

Eidesstattliche Erklärung

Ich erkläre an Eides Statt, dass ich die vorliegende Arbeit selbstständig verfasst, andere als die angegebene Quellen/Hilfsmittel nicht benutzt, und die in den benutzten Quellen wörtlich und inhaltlich entnommenen Stellen als solche kenntlich gemacht habe.

Graz, am …02.10.2014…… ……

(Unterschrift)

Acknowledgments

First of all, I would like to express my sincere gratitude to Prof habil. Viet Tue Nguyen, for his supervision, patience, support and friendly approach towards me throughout this thesis.

I owe special thanks to concrete faculty members, Dr. Duc Tung Nguyen, M.Sc. Katrin Turner, M.Sc. Werner Theiler for their support during my Master thesis in M.Sc. course in the Graz University of Technology.

I want to express my love and gratitude to my wife Tannaz and my family; for their understanding, supporting & endless love, through the duration of my study. If they weren't behind me I wasn't today here.

Abstract

The objective of this thesis is to study the feasibility of lateral load bearing system of a high-rise building in Vietnam which the architectural layout is given. For this purpose first the preliminary given layout has been analyzed and then improved to control the inter-story drift and to dimension the core walls in a way that they be able to bear and withstand the assumed loading properly without failure.

As a framework Euro codes are used. For loading EC1-1, EC1-4 and EC8 were used and for analysis and design EC8 and EC2.

For analysis ETABS program is utilized which is suitable for buildings and performs all dynamic analysis required for high-rise structures under wind and earthquake loadings. A 3D model is constructed to capture torsional effects.

A dual lateral structural system (exterior perimeter columns with core) is adopted to control inter-story drift and top displacement under seismic action in ultimate limit state with combining shear deflection mode and flexural deflection mode. The top level acceleration and displacement is also checked for serviceability limit state under wind load action.

High-strength concrete is extensively used in the columns and core walls to withstand high compressive stress at lower zones and building is designed for DCM ductility level.

Finally some designed details of core walls sections and coupling beams between them at three levels (base, midpoint, top) are illustrated.

Keywords: High-rise buildings, lateral load bearing systems, core systems, coupled shear walls

Kurzfassung

Das Ziel dieser Arbeit ist es, die Machbarkeit der Aussteifungssysteme von einem Hochhaus in Vietnam, die deren architektonische Gestaltung gegeben ist, zu studieren. Zu diesem Zweck wurde zunächst die vorläufige gegebenen Layout analysiert und dann verbessert um die Relative Verschiebung der Stockwerke ein zu schränken und die Kernwände in einer Weise zu dimensionieren und bemessen, dass sie in der Lage sein die angenommene Belastung ohne Versagen zu tragen und ordnungsgemäß zu widerstehen.

Als Rahmen wurde Euro Codes verwendet. Zum Belastungszweck kommt EC1-1, EC1-4 und EC8 zum Einsatz und für die Analyse und Bemessung EC8 und EC2.

Für die Analyse wurde ETABS Programm verwendet, der für hohe Gebäuden geeignet ist und führt alle erforderliche dynamische Analyse für Hochhäuser unter Wind und Erdbebenbelastung. Ein 3D-Modell ist konstruiert, um die Torsion effekt zu erfassen

Ein Mischsystem als Aussteifungssystem (Außenumfang Säulen mit Kern) wird adoptiert.um die gegenseitigen Stockwerksverschiebung und die Kopfauslenkung unter Erdbeben Einwirkung zu beschränken. Der Kopf Beschleunigung und Vervormung unter WindBelastung wurde zur Bewertung der Gebrauchstauglichkeit geprüft

Hochfestem Beton wird weitgehend in den Stützen und Kernwände verwendet um hohe Druckspannung bei niedrigeren Zonen zu widerstehen. Gebäude ist für DCM Duktilität konzipiert.

In letztem Abschnitt wurden einige bemessene Details der Kernwände Abschnitte und Kupplung-Balken zwischen ihnen auf drei Ebenen (Basis, Mitte, oben) veranschaulicht.

Schlüsselwörter: Hochhäuser, Aussteifungssysteme, Kernsysteme, gegliederte Wandscheiben

Table of Contents

Acknowledgments …… iii

Abstract …….. iv

Chapters

1 Introduction 1

1.1 General 2

1.2 Approach 2

1.3 Description of the Reinforced Concrete building project 4

1.4 Preliminary Structural System 11

2 An Overview on Structural Systems of High-Rise Buildings 14

2.1 Structural Forms and Concepts 14

2.2 Braced Frames 14

2.3 Behavior of Braced Frames 15

2.4 Rigid Frame Structures 16

2.5 Rigid Frame Behavior 17

2.6 Infilled-Frame Structures 18

2.6.1 Behavior of Infilled Frames 18

2.7 Shear Wall Structures 20

2.7.1 Behavior of Shear Wall Structures 20

2.8 Coupled Shear Wall Structures 23

2.8.1 Behavior of Coupled Shear Wall Structures 23

1.1.1 Analysis Methods of Coupled Shear Walls 26

2.9 Wall-Frame Structures 28

2.9.1 Behavior of Wall-Frame Structures 29

2.9.2 Analysis Methods of Wall-Frame Structures 31

2.10 Tubular Structures 32

2.10.1 Behavior of Tubular Structures 32

2.11 Core Structures 35

2.11.1 Behavior of Core Structures 35

2.11.2 Methods of Analysis of Core Structures 38

2.12 Core-Outrigger Systems 39

3 Gravity Loading 43
3.1 Loading Criteria 43
3.2 Dead Loads 43
3.3 Live Loads 43
3.3.1 Live Load Reduction 44
4 Wind Loading 44
4.1 Design Consideration 44
4.2 Definition, Nature and Classification of Wind 45
4.3 Variation of Wind Profile with Height 47
4.4 Terrain Roughness Effect 47
4.5 Mean Wind Velocity 49
4.6 Wind Turbulence 49
4.7 Peak Velocity Pressure 50
4.8 Wind Pressure Acting On Building 50
4.9 Structural Factor $c_s c_d$ 53
4.10 Background Factor 54
4.11 Resonance Response Factor 55
4.12 Peak Factor 58
4.13 Wind Forces 60
4.13.1 Wind Forces Using Force Coefficient 60
4.13.2 Wind Forces Using Surface Pressure 61
4.13.3 Comparison of Two Methods for Wind Forces 63
4.14 Vortex Shedding 64
4.15 Galloping Effect 66
4.16 Along Wind Response and Serviceability Control 67
4.17 Maximum Along-Wind Acceleration 67
5 Earthquake Loading 69
5.1 Seismic Actions 69
5.2 Earthquake 69
5.3 Seismic Requirements 69
5.4 Ground Types 70
5.5 Importance Factors and Classes of Structures 70
5.6 Response Spectrum 71
5.6.1 Elastic Response Spectrum in Euro Code 8 71
5.6.2 Design Spectrum 74
5.7 Methods of Structural Analysis 75

5.7.1 Modal Response Spectrum Analysis 76
5.7.2 Combination of Modes 80
5.8 Accidental Torsional Effects 81
6 Modeling and Analysis 83
6.1 Structural Model 83
6.2 Preliminary Analysis 86
6.3 Improved Structural System 86
6.4 Model Parameters 89
6.5 Material Properties 89
6.6 Effective Widths of Beams 89
6.7 Structural Regularity 90
6.8 Structural Analysis Method 90
6.8.1 Seismic Parameters 90
6.8.2 Seismic Mass 91
6.8.3 Ductility Class 91
6.9 Structural Type and Torsional Rigidity 92
6.10 Behavior Factor 93
6.11 Load Combination 94
7 Analysis Results and Design 96
7.1 Overview 96
7.2 Periods and Modal Shapes 96
7.3 Displacements 99
7.4 Damage Limitation 101
7.5 Shear Forces 103
7.6 Second Order Effects 104
7.7 Shear Wall and Spandrel Positions 107
7.8 Internal Forces from Dynamic Analysis 108
7.9 Internal Force Pattern 111
7.10 Design Envelopes 114
7.11 Failure Modes of Structural Walls 119
7.12 Local Ductility Parameter 119
7.13 Design of Walls at Base Section 120
7.14 Boundary Elements 120
7.15 Flexural Design 124
7.16 Shear Design 126
7.17 Detailing for Local Ductility 128

7.18 Failure Mechanisms and Behavior of Coupling Beams..... 136
7.19 Wall and Spandrel Design at Midspan and Top of Building 140
8 Conclusions and Recommendations 145
9 Recommendations for Further Studies 147

1 Introduction

From the beginning of the 20th century, and with densification of human activities in large cities, occupying the altitude has been one of the solutions for the space shortage in large cities. Also, it has been always challenging and ambitious for designers to build higher buildings and show their skills and abilities. Nowadays the regularity of building plan is no more a concerning point in design and computers have given the structural engineer the tools to respond challenging architectural layouts with sound structural solutions.

With developing computational ability of computers and programs it is now easier to analyze and compare huge alternative structures for a single project and find a more optimal solution.

Beside these computational abilities a deep insight in structural systems, which are developed dramatically during the time, is needed to choose a sound structural form satisfying the requirements of owner within the framework of national and sometimes international codes. A good comprehensive understanding of these structural forms also allows us to develop or combine different systems into hybrid systems and use the advantages of both systems.

To get a realistic result structure should be modeled in a way that the results represent the real behavior of structure. Modeling of structure is arguably the most difficult task facing structural analyst, requiring critical judgment and a sound knowledge of structural behavior of tall building components and assemblies. Also the results should be interpreted for use with the real structure, in order to serve as reasonable basis for design decisions.

As usual in high-rise buildings two challenging issues which include lateral building stiffness and ductility of main structural parts in earthquake regions should be solved with sound dimensioning, design and detailing of lateral and gravity load bearing systems of building.

In this thesis chapter 1 introduces the examined project based on given plan; chapter 2 includes an overview on lateral load bearing systems of high-rise buildings, their behavior and methods to their analysis; chapter 3 gives the evaluates loading parameter's values based on EC1-1; chapter 4 shows the calculation of wind loading and serviceability control under wind effect due to EC1-4; chapter 5 clarifies how the earthquake loading is considered in building analysis based on EC8; modeling procedure and used model parameters is the subject of chapter 6; chapter 7 is dedicated to structural analysis results and checked requirements due to EC8 and EC2, in this chapter also core of tower 1 is designed in three levels to check the structural elements capacity and strength under delivered loads.

1.1 General

The given project has been checked within the framework of euro codes. For loading EC1-1, EC1-4 and EC8 were used and for analysis and design EC8 and EC2.

For analysis ETABS program is used which is suitable for buildings and performs several dynamic analysis needed for high-rise structures under wind and earthquake loadings. A multi modal response spectrum analysis is conducted for analyzing the system.

A 3D model is constructed to capture torsional effects. The model is constructed with simplification of structure and only main load carrying parts have been modeled to decrease the stiffness matrix size and also computation time. Car ramps are not included in model also instead of foundation supports are assigned at the connection points with foundation slab as simplification. The forces from structural analysis should be exported to SAFE program to design the foundation.

As structural system a dual lateral system (exterior perimeter columns with core) is adopted to control inter-story drift and top displacement under seismic action in ultimate limit state with combining shear deflection mode and flexural deflection mode. The top level acceleration and displacement is also checked for serviceability limit state under wind load action.

High-strength concrete is extensively used in the columns and core walls to withstand high compressive stress at lower zones but in the next design stages concrete strength could be adopted and altered in 3 levels along the height. Building is designed for DCM ductility.

Since the collapse of such a high-rise structure is related with dramatic consequences for human life the importance class III is considered for the building in the dynamic analysis based on EC8.

1.2 Approach

For analysis and design purpose first the loading values and parameters are calculated for investigated structure. To this aim, formulas and recommendation of euro codes have been used and no national annex have been considered.

To have a deep insight into structural behavior, for first stage of design multi modal response spectrum analysis method is chosen, in which the structure is considered to be in the elastic range and the superposition rule is applicable. So we can trace the load portion and effect of each load case in load combinations and a reasonable countermeasure could be chosen based of these interpretations if needed.

The accidental torsional effect is considered based on EC8 recommendations to have more realistic evaluation of shear forces in shear walls.

For dynamic analysis 40 modes are considered in analysis to count for modes dependency. To encounter with numerical solutions problem Ritz vectors are utilized for determining of periods and modal shapes. These values are obtained based on cracked section of members.

Iteration is an inherent characteristic of design procedure, to converge on the final and optimal dimensions of structural elements several analyses have been run and each time the structural elements capacities and building displacements are checked and afterwards a new run is conducted based on new dimensions.

The flexural design of shear walls are based on interaction diagram of section and calculation of demand/capacity ratio of section based on iteration and trying to keep this ratio below 1. To calculate boundary elements every channel or U shape are disassembled into individual walls and boundary element are calculated for each straight wall. The flexural reinforcement is tried to be concentrated at extremities within boundary elements to gain higher flexural capacity.

Shear design is normally governing the shear walls design. To be on the safe side strut inclination is considered to be 45° which leads in a dense shear reinforcement. Since the shear walls are the main elements against shear forces and a shear failure could eventuate in serious consequences of a brittle failure, this consideration seems to be rational.

To keep the walls over the base in elastic range bending moment and shear walls envelopes have been constructed based on EC8 and used in design. Plastic hinges is assumed to be formed at the base with a length equal to critical length defined in EC8.

1.3 Description of the Reinforced Concrete building project

The investigated building project is a high-rise reinforced concrete structure. This building has commercial, office and residential utilization and consists of two towers where the tower one has 45 stories above the ground level and tower 2 has 41 stories, including elevator mechanical room on the roof. Both of towers have 5 common basement stories as parking, storage and mechanical rooms. These towers are connected together with floor slabs at all stories except stories 24, 28, 32, 36. Towers 1 and 2 have 160.35 and 147.15 m height respectively. Tower 1 is located with 5° inclination to the x axis in the plane which it makes the modeling more difficult.

First 7 stories have commercial utilization, with 6 m height at first floor and 4.5 m at other 6 stories above. From story 8 there is a setback and 7 columns are omitted at axes R, S, L, A. From this story two towers are separated in internal rooms at the necked part of floor slab by doors and partitions. Typical floor height above story 7 is 3.3 m.

The rest of stories above 7^{th} floor, have office or residential usage, where from 8^{th} story up to story 29 have office usage and rest of them are residential. Story 30 is the mechanical room with a height of 5.25 m. Stories 41 and 45 are also mechanical floors for elevators and ventilations at tower 2 and 1 respectively.

Basement floors are typical in main structural elements layout, and only parking ramps are different. As typical basement plan, 3^{rd} basement floor plan is shown in figure 1.1. 1^{st} storey is shown in figure 1.2. 2^{nd} to 8^{th} stories have also the same structural and architectural layout, for illustration purpose second floor plan has been shown in figure 1.3. From story 9 up to end the main structural elements layout is identical, only there is setbacks in shear walls. In some floors a sky garden has been considered in floor plans of stories 24, 28, 32 and 36. This causes a separation of floor slab between towers in these stories. Floor plan of story 9 is shown in figure 1.4 as a schematic illustration for the case that floor slabs are not separated between two towers. For case which floor slabs of are separated because of sky garden, floor plan of story 24 in figures 1.5 is shown. Building dimensions in figures are in mm.

This building has a glass facade connecting to building with its special framing system at floor slab levels. Every tower has a service shaft for elevators, staircase and also ducts, where is used for pipes and ventilation channels. These shafts are surrounded by concrete shear walls composing structure main lateral load bearing systems as cores.

Periphery and middle columns plus girders composing frames in y direction serve as elements which transfer gravity loads around the building and also contribute in horizontal load bearing system interacting with walls.

Foundation is considered as a mat thick foundation to be able to transfer high axial stresses to the ground below. All elements are fixed in foundation and the whole system works as a cantilever. An elevation of building is shown in figure 1.6.

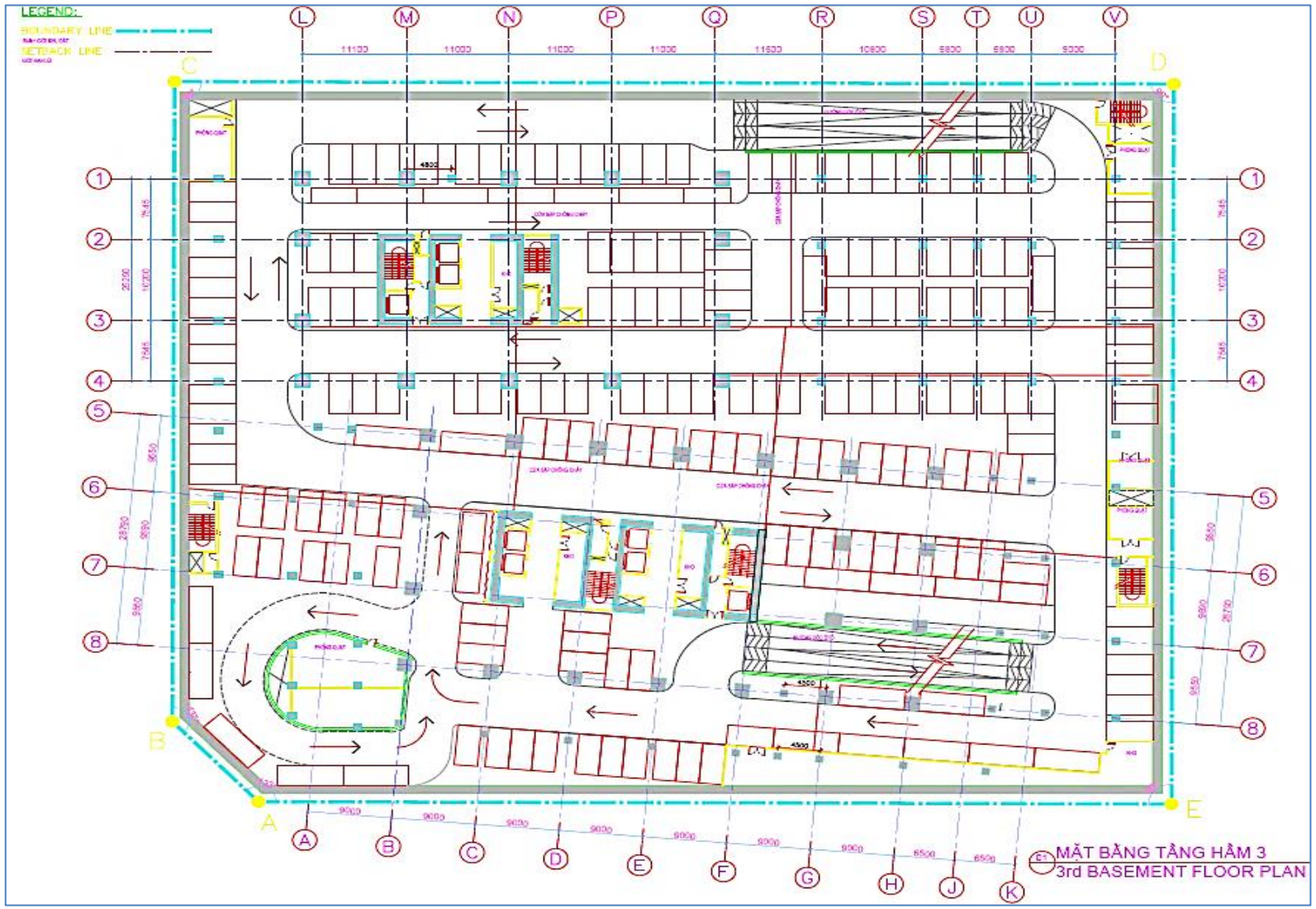

Figure 1.1: 3rd basement floor plan

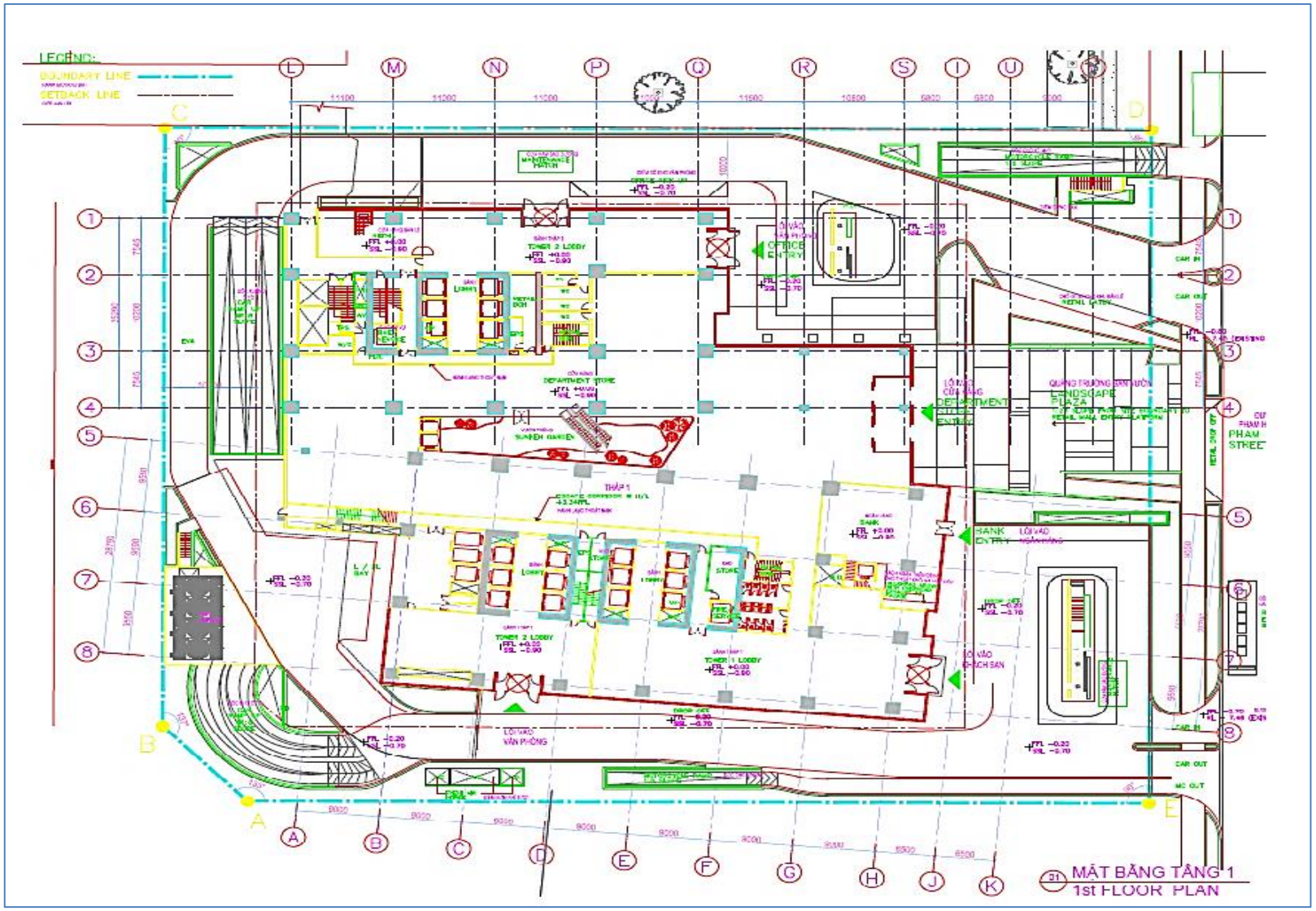

Figure 1.2: Typical floor plan from 1st to floor plan

Figure 1.3: Typical floor plan from 2nd to 8th story

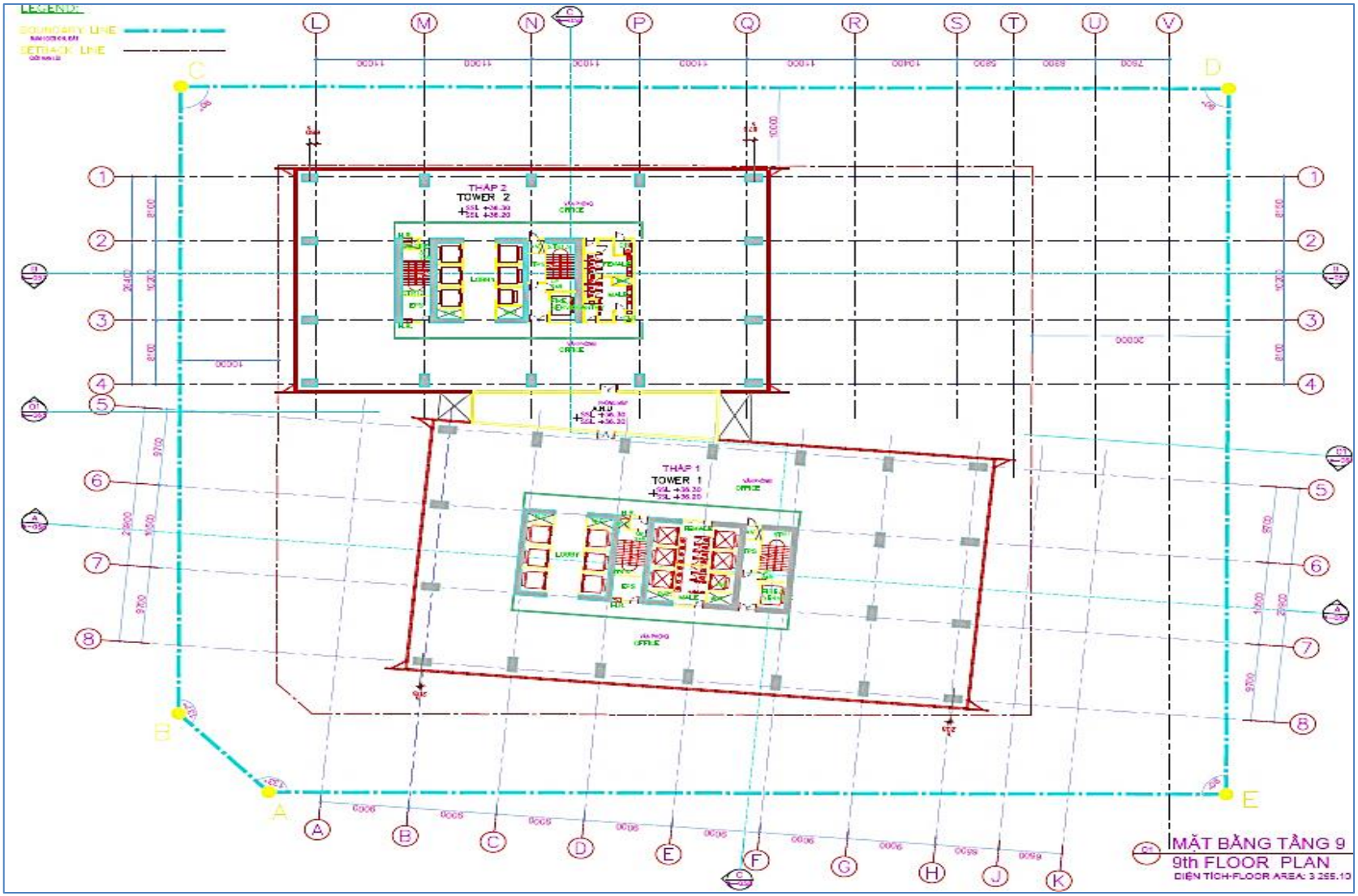

Figure 1.4: Typical floor plan from 9th up to end story, excluded story 24,28, 32, 36, connected floor slabs

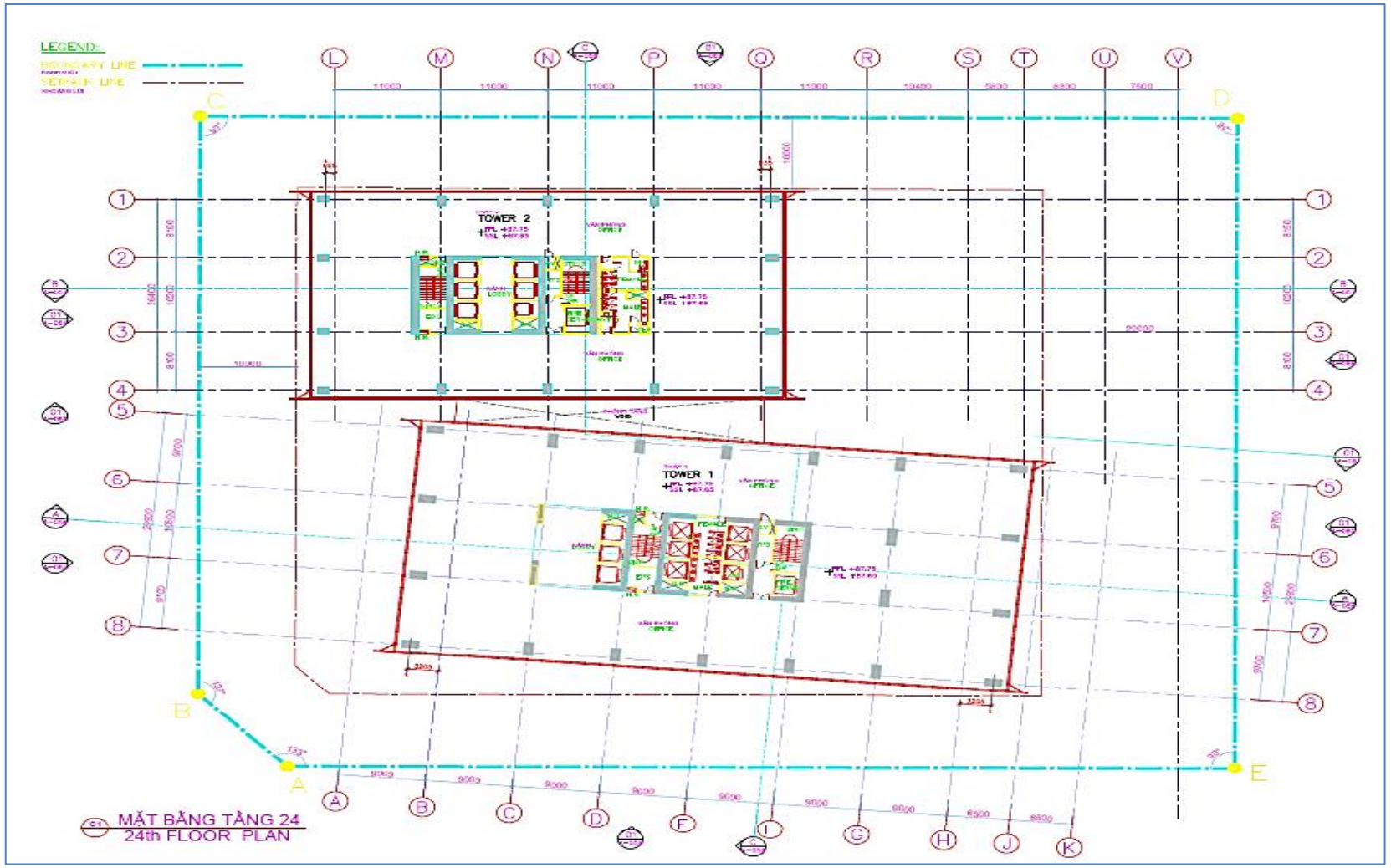

Figure 1.5: Typical separated floor slabs of 24, 28, 32, 36th floors

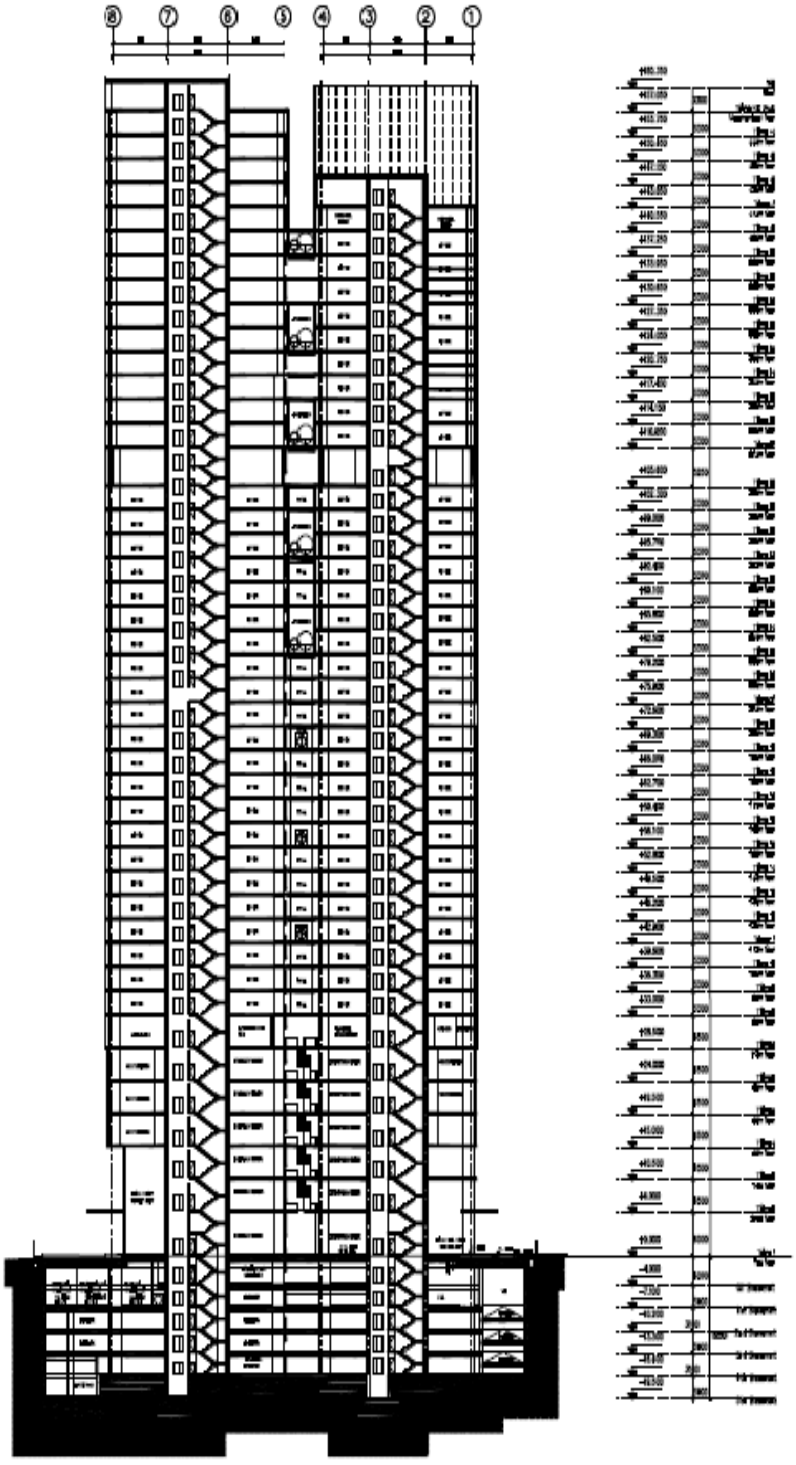

Figure 1.6: Elevation c-c

1.4 Preliminary Structural System

The preliminary structural system given by architectural design was based on two concrete cores around service shafts with periphery columns with concrete flat slabs. In the preliminary model the columns was assumed with pinned connections at stories and fixed at foundation, carrying only gravity loads and cores as a cantilever, fixed at the base and bracing the system, where resists against lateral and gravity loads.

Cores have access openings for elevators and staircases. In this case in one direction we have coupled shear walls consisted of piers and spandrels and in the other direction shear walls without openings. Openings height has been considered as 2.2 m and the widths vary with architectural plan.
Setbacks occur in shear walls in tower 1 at floor 22, 31, 44 and in tower 2 at floor 41. First setback occurs in floor 22 and second one in floor 31, between axes C and D, for comparison floors 21without setback and floors 22 and 31 with setback is illustrated in figure 1.7. The part with setbacks is specified in a red sign and only tower 1 is illustrated (there is no setback in core of tower 2). Setbacks at stories 41 and 44 are due to mechanical rooms for elevators and ridges at these levels.
Foundation is not considered in the computer model; at the base we assumed fixed supports under columns and walls. In later design stages forces from structural analysis could be extracted and used for foundation design. In the case of such a high-rise building normally foundation are assumed as a mat thick foundation which could be supported additionally with piles. Using piles depend on soil characteristic under structure and load magnitude which should be transmitted to the soil.
Periphery concrete walls are considered at basement stories to have a rigid basement at these levels, firstly against lateral loads and secondly against soil pressure acting on basement wall surfaces. Large lever arms between opposite walls of basement in each direction, makes this part able to withstand torsional and translational forces with negligible displacement. For this reason and due to (EN 1998-1) seismic action can be assumed to act from ground level in case of rigid concrete basement.
The structural elements dimensions are considered typical in three steps, first type from 3rd basement to 15th story, second type from 16th to 35th story and last type from 36th to 45th story. For our preliminary model walls width and columns dimensions are shown in table 1.1. Slab thickness has been considered equal to 20 cm.

Stories	Columns dimensions (cm)	Shear walls width (cm)
3rd basement to 15	120x60	50
16to 35	100x60	40
36 to 45	80x60	30

Table 1.1: Columns dimensions and walls width classification for preliminary model

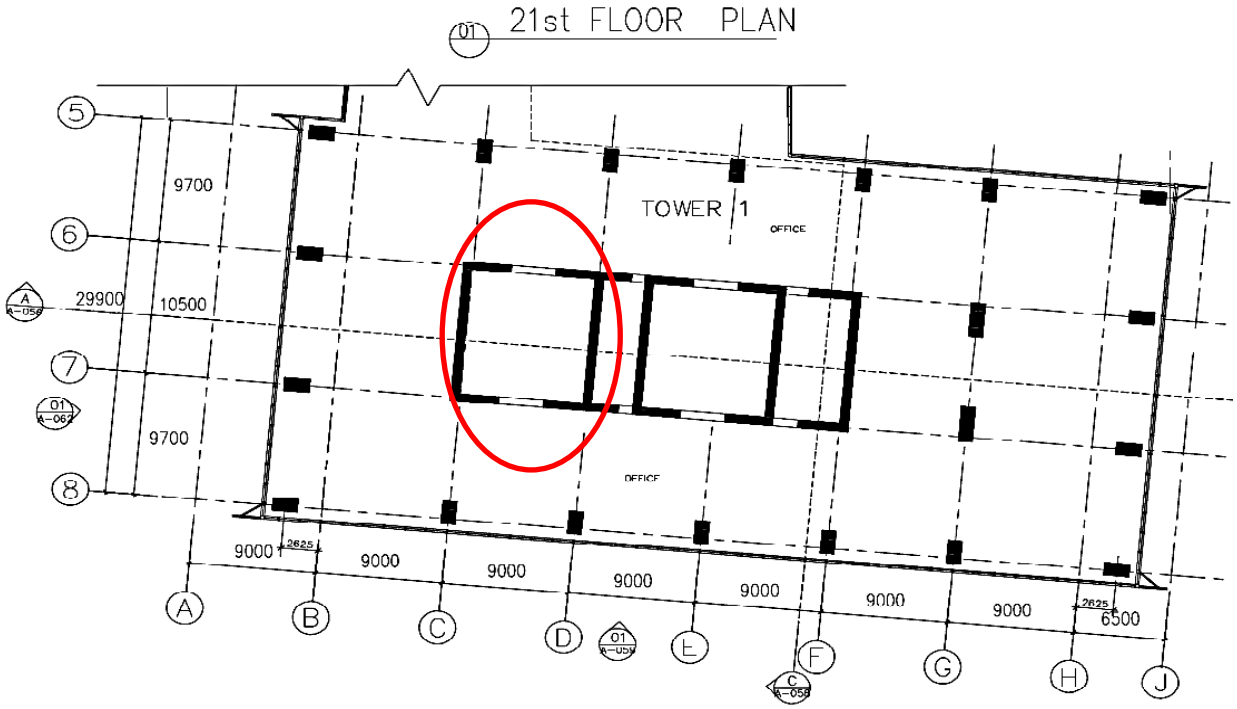

(a): wall without curtailment

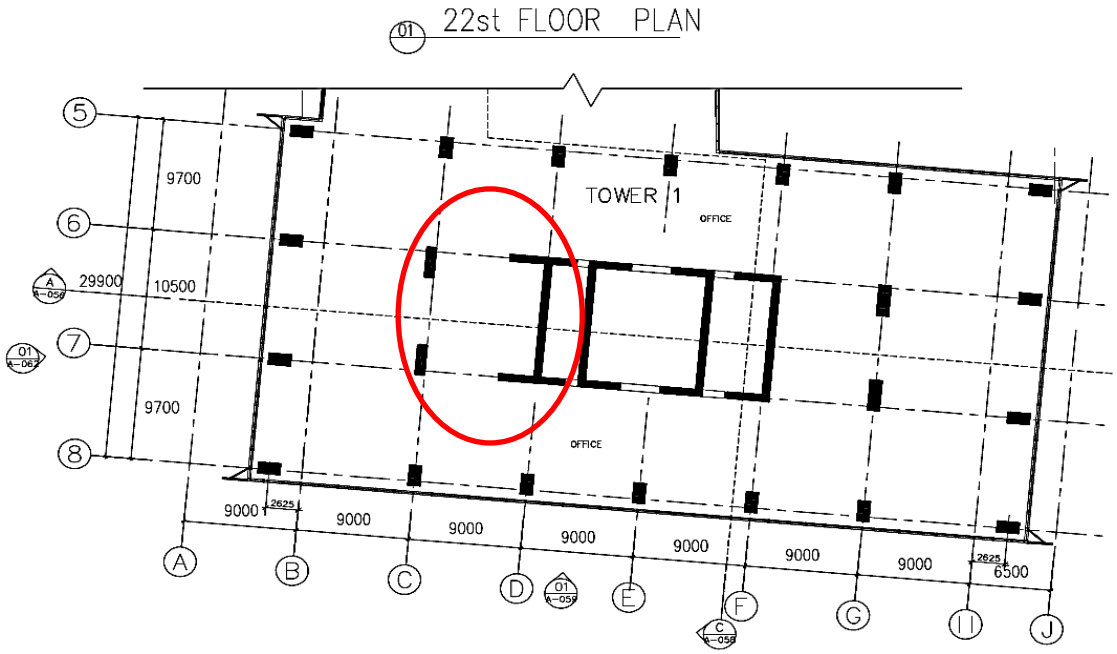

(b): Story 22

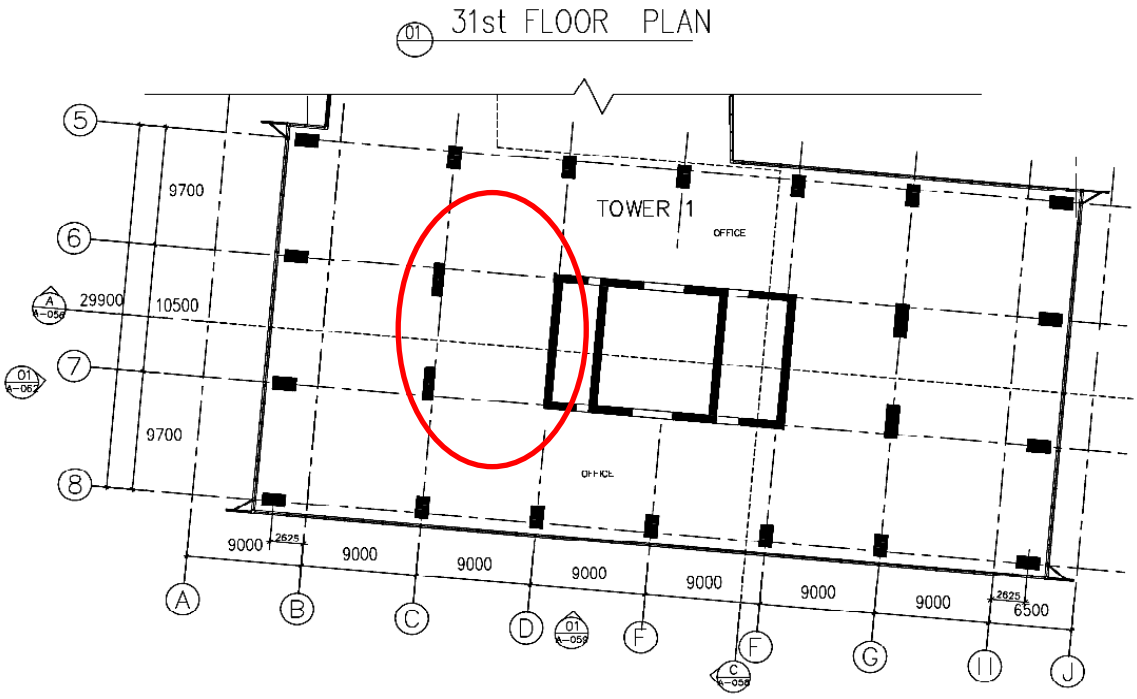

(c) Story 31

Figure 1.7: (a) Story 21 without setback; (b) shear wall setbacks at story 22; (c) curtailment at story 31 in tower 1(dimensions in mm)

2 An Overview on Structural Systems of High-Rise Buildings

2.1 Structural Forms and Concepts

The choice of structural form of a tall building is not only affected by selection and arrangement of the major structural elements to resist efficiently the various load combinations of lateral and gravity loads, but also is influenced by architectural, mechanical and electrical demands of building. Factors that has to be considered in deciding the structural form includes the internal planning, construction method, materials, external architecture, routing and location of service systems, horizontal loading and the height and proportion of building.

Function of building is another important factor affecting the structural form. Office buildings need large open floor area that could be subdivided easily with lightweight partitioning based on individual tenant's need. Consequently the structural concept differs depending on function and main structural components are generally arranged as far as possible around the periphery of the plan and, internally, in groups around the elevator and service shafts. Such an arrangement is more suitable for core and tube-type structures. In residential buildings or hotel, areas are subdivided permanently and usually repetitively from storey to storey. Therefore, continuously vertical elements like walls and columns could be adjusted and distributed in a way in plan to form, or fit within the partitioning. This arrangement is more suitable for shear wall or frame structures.

Different structural systems are developed through recent decays based on architectural and structural engineering demands. The choice, development and design of these systems against lateral loads and enhancing the stiffness and the lateral respond of structure, need a thorough understanding of structural behavior of each system.

In this chapter the behavior and features of some important structural systems are summarized.

2.2 Braced Frames [39], [40]

Braced systems are highly efficient and economic structures in resisting horizontal loads. This efficiency is gained by eliminating of the shear racking component of deflection due to bending of columns and girders which causes the drift to be too large. In this system the lateral shear is carried by web members. These members carry the lateral shear predominantly through axial forces, thus minimizing bending of beams and columns, which results in more economic profile size in these elements.

A brace bent consist of usual columns and girders whose primary goal is to transfer gravity loading, and diagonal bracing members that are connected so that the total

set of members forms a vertical cantilever truss. The braces and girders act as the web while columns as the chord of the truss.

Historically bracing systems has been used in majority of world's tallest buildings, like Chrysler Building with 319 m height and 77 storeys in New York built in 1930, and Empire State Building with 381 m height (without antenna) and 102 storeys built in 1931.

2.3 Behavior of Braced Frames

Like other high-rise systems the braced frames can be considered as a vertical cantilever truss which transfers the lateral loading through axial forces in its elements to the foundation. The columns act as the chords in resisting lateral loads, with tension and compression depending on loading direction. The diagonals serve as web members resisting the horizontal shear under axial forces. Under lateral loads, the resulting axial deformation of the columns tend to cause a flexural deformation of the frame with concavity downwind as shown in Figure 2.1a. On the other hand, the axial deformation of the diagonals cause a "shear" mode deformation with concavity upwind, a maximum slope at the base, and a zero slope at the top (see Figure 2.1b). Combination of flexural and shear modes results in a deflection shape shown in 2.1c in which the flexural deflection most often governs the deflection scene [39], [40].

The contribution of flexural and shear deformation components in overall deformation and storey drift could be found by virtual work drift analysis. This method is exact and can easily be summarized by tabulation. The results could be used in element size choice to control and optimize the drift [40].

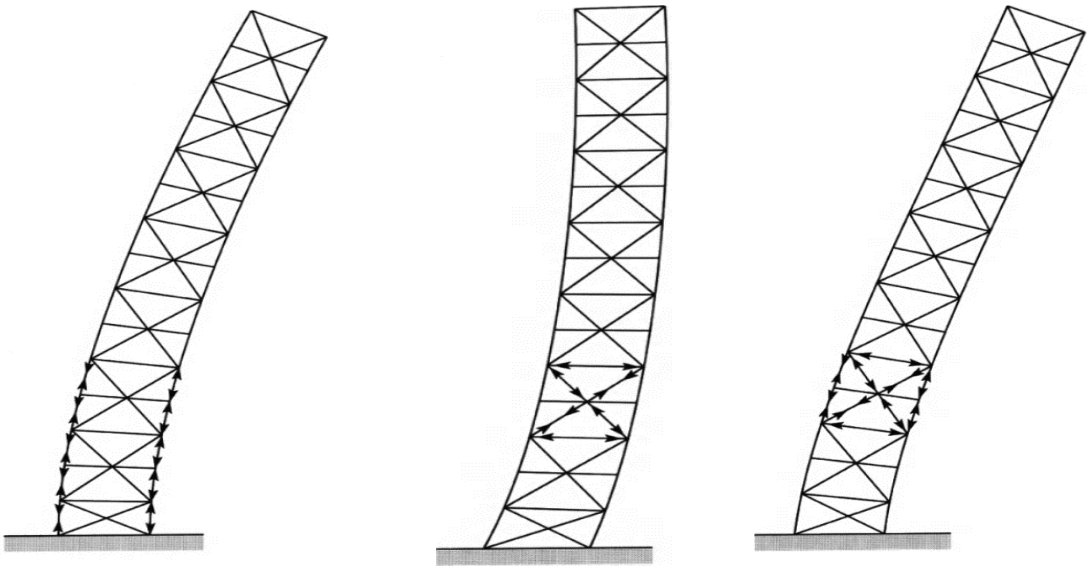

(a) (b) (c)

Figure 2.1: Braced frame behavior, (a): flexural deformation, (b): shear deformation, (c): combined configuration [39]

2.4 Rigid Frame Structures

Rigid frames, also called moment frame structures have normally simple configuration consisted of orthogonally or parallel arranged bents comprising columns and beams whose their connection is rigid. Rigid connections are those having sufficient stiffness which could resist moments and the angle between members is virtually unchanged under loading. Nondeformability of joints at the intersection of columns and girders provides the stiffness and strength of frame [39].

This structural system is economic up to 25 storeys, above this limit the drift control became costly [40].

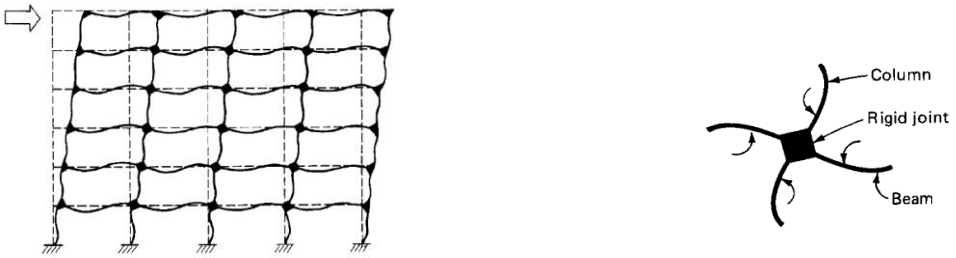

(a) (b)

Figure 2.2: (a) Rigid frame, (b) assumption made at structural node in analysis [41]

2.5 Rigid Frame Behavior

Lateral stiffness of rigid frames depend mainly on the bending resistance of the girders, the columns, and in high-rise buildings on the axial rigidity of the columns. Horizontal accumulated shear above each storey is resisted by columns. Storey columns respond to this shear with a double curvature which has a contraflexure point approximately at mid-storey-height. Girders have almost the same behavior, they bend in double curvature with cotraflexure point at midspan under moments applied to a joint from columns above and below. Bending of individual columns and beams results in the entire frame distortion which in turn results shear racking component of total deflection. This deflection mode hasa shear configuration with concavity upwind, a maximum inclination near the base, and a minimum inclination at the top [39].

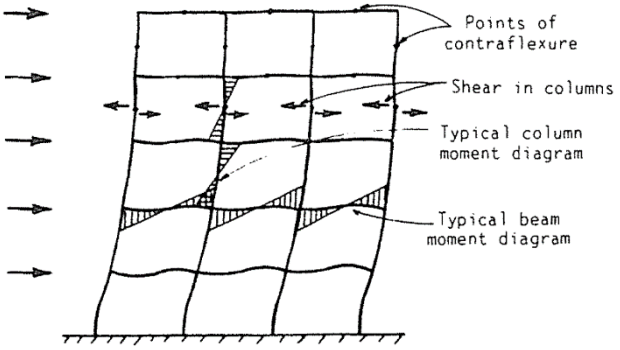

Figure 2.3: Response of rigid frame to lateral forces in shear mode [40]

Overturning moment of lateral loads are resisted by the couple resulting from the axial compression and tension forces in columns on opposite sides of the building. These axial forces cause extension and shortening of the columns which in turn leads in overall bending and associated horizontal displacement of structure. Contribution of Cantilever bending component known also as chord drift, to the total drift will usually not exceed 10 to 20 percent of total deflection [41].

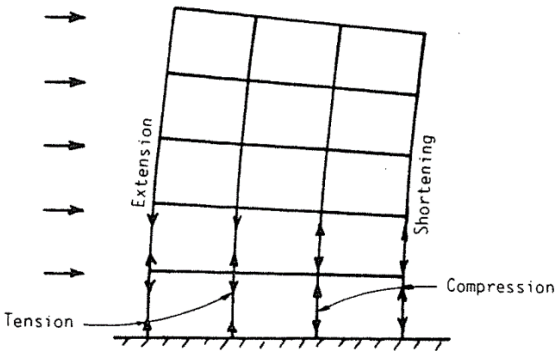

Figure 2.4: Forces and deformation under external moment in bending mode [40]

Resisting lateral loading through moment capacity of columns, increases the demand for larger profile sizes in comparison with corresponding fully braced simply connected frames. On the other hand in braced frames girders are designed for mid-span moment while girders in rigid frame are designed for the end-span moment. Consequently girders in rigid frames may be smaller than in corresponding braced frame [39].

2.6 Infilled-Frame Structures [26], [39]

These type of structures are consisted of normal rigid frame or braced frame systems in concrete or steel with infills of brickwork or concrete blockwork. These infill parts act not only as partition but also may serve structurally to brace the frame against lateral loading.

In nonearthquake regions where wind forces are not severe the frame could be designed only for gravity loading in which the required lateral stiffness is supplied with infill part. The masonry infilled concrete structures are one of the common structural systems which have been used in high-rise construction.

In regions with high to moderate earthquake hazard, using of masonry infills for bracing has severely restricted. In these regions it is more usual to design the frame for full horizontal and gravity loading and is assumed that infills do not participate as primary structural part. Experiences shows that after earthquake, diagonal cracks frequently occur in infills and implies that the neglecting of infills in structural behavior is not always true. The infills sometimes absorb significant bracing loads and, in doing so, modify the structure's mode of behavior and the forces in frame. More rational is to design the walls for lateral loads and the frame for its modified mode of behavior.

Another issue in areas with earthquake risk is that, walls might be shaken out of their frames transversely and be of little use as bracing or collapse completely out of plane when the earthquake excitation direction is normal to wall. Therefore additional provisions should be considered as, reinforcing the wall or anchoring and fixing it to the surrounding frame sufficiently to withstand their own transverse inertial forces.

2.6.1 Behavior of Infilled Frames

Infilled frame structure consists of relatively flexible and ductile frame with brittle and stiff masonry. The high in plane rigidity of masonry makes the system stiffer, while ductile frame chambers the masonry, after cracking, up to loads and displacements much larger than it could be achieved without frame. This makes the system stiff and though. The walls braces the frame with two actions first in-plane shear resistance and second by acting as diagonal bracing strut of frame under compression. These behaviors are shown in figure 2.5b [26].

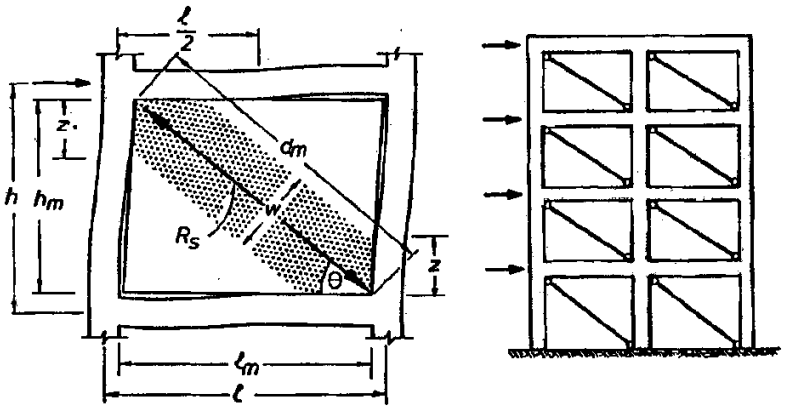

(a) (b)

Figure 2.5: (a) Deformation under shear load, (b) equivalent braced analogy [26]

There are different failure modes for masonry infilled frames, including [26]:

1. Tension failure of tension column at the windward side due to lateral horizontal loading
2. Sliding shear failure of the masonry generally close to mid-height of the panel (see figure 2.6).
3. Diagonal tensile cracking of the panel, but this mode dose not happens usually because higher horizontal forces could be carried by the next failure mode.
4. Compression failure of the diagonal strut.
5. Flexural or shear failure of the column.

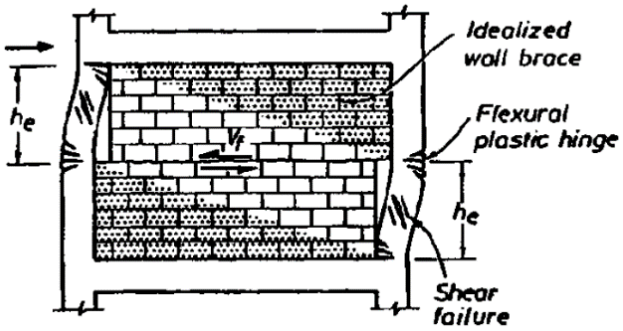

Figure 2.6: Sliding shear failure [26]

2.7 Shear Wall Structures

Structural systems that consist of assemblies of shear wall and lateral loads are resisted entirely by shear walls. They are unusually continuous down to the base and rigidly fixed in foundation which in this case they form a vertical cantilever. They have high inplane stiffness and strength. This form of structure is suitable up to 35 stories [41].

It is better to locate shear walls in a way that they attract gravity loading beside external moments, in so doing, the tensile stress caused by external moment could be suppressed by gravity loads. The term “shear wall” is in some ways confusing because the walls deflect predominantly in flexure. Shear walls may be planner, but often have also other shapes like L-, T-, I-, or U section. In this structural system walls are connected together with floor slabs or beams with negligible bending resistance, so that only horizontal interactive forces are transmitted [26].

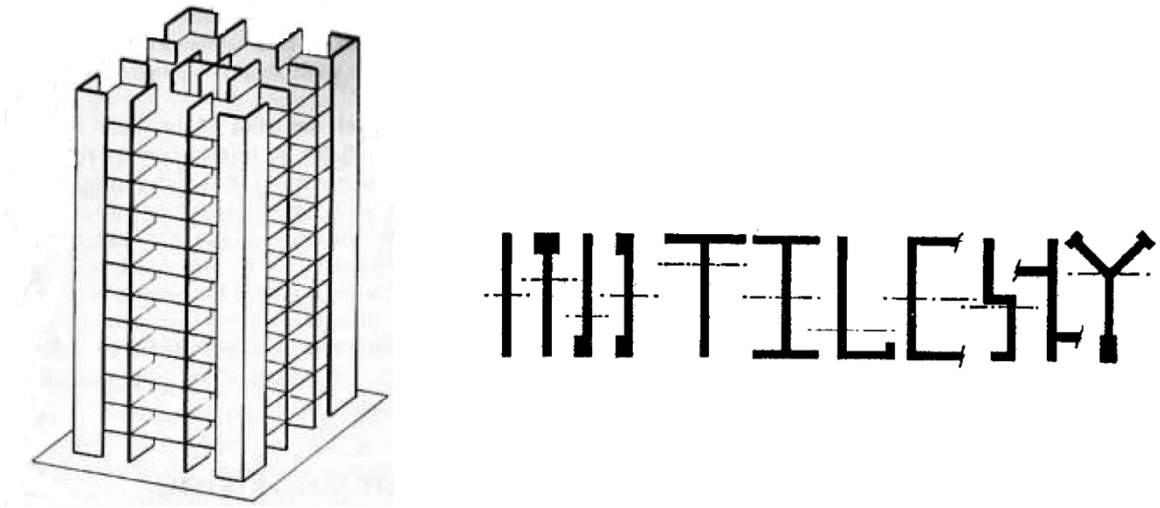

(a) (b)

Figure 2.7: (a) Shear wall structure [40], (b) common shear wall sections [26]

2.7.1 Behavior of Shear Wall Structures [40]

Shear walls undergo normally flexural deformation and behave like a vertical cantilever. Shear walls could be subdivided to proportionate and nonproportionate systems. When the ratios of the flexural rigidities of the walls remain constant throughout their height this system is a proportionate system. In proportionate system of walls there is no redistribution of shears and moments at the change levels. They are statically determinate and this allows their analysis to be made only with equilibrium equations.

Nonproportionate wall systems are those in which the ratios of wall flexural rigidities are not constant throughout the height. Redistributions occur at change levels, with

corresponding horizontal interactions between connecting members and the possibility of high local shear in the walls. They are statically indeterminate and therefore the analysis and behavior is more difficult and complex.

$$\frac{I_{1A}}{I_{2A}}=\frac{I_{1B}}{I_{2B}}=\frac{I_{1C}}{I_{2C}}$$

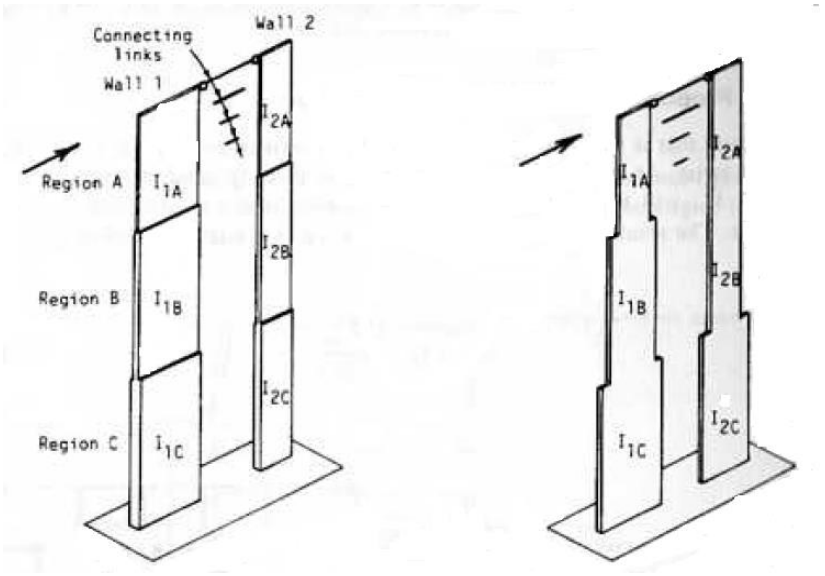

$$\frac{I_{1A}}{I_{2A}}\neq\frac{I_{1B}}{I_{2B}}\neq\frac{I_{1C}}{I_{2C}}$$

(a) (b)

Figure 2.8: (a) Proportionate wall system, (b) nonproportionate wall system [40]

Both of mentioned categories could be subdivided to twisting and nontwisting systems. A structure which is symmetric in plan about loading axis will not twist and external shear and moment will be distributed between walls in the ratio of their flexural rigidities.

Structures that are asymmetric in plan about axis of loading will generally twist as well as translate. In proportionate structures the center of twist and the centroid of the flexural rigidity coincide. Floor slabs in shear wall structures act as links which constrain the walls to have the same curvature in the uniform regions away from change levels. Therefore external moments in regions away from change levels is distributed between walls as the ratio of flexural rigidities of shear walls like the case as in proportionate walls. In the transition from above to below a change level, a redistribution of the wall moment happens to satisfy the change in the ratio of the wall rigidities. Only possible way in which the forces could be transferred between walls is connecting links. Therefore redistribution occur in couples consisted of horizontal forces which arises in links at successive levels around exchange level. Transferred moment is usually large enough which makes the interactive horizontal forces in links so large that the shear in a wall and the reverse shear in another wall may easily exceed the total external shear at that level.

This local effect on the wall due to moments transfer give rise to carryover effects above and below the change level, and disappear within one or two stories before

becoming negligible. The difference between nonproportionate twisting and nontwisting systems at change levels is that in twisting system resulting moment is a combination of the moment from flexural and flexural torsional rigidity effect of walls. In nontwisting system there is no flexural torsional effect.

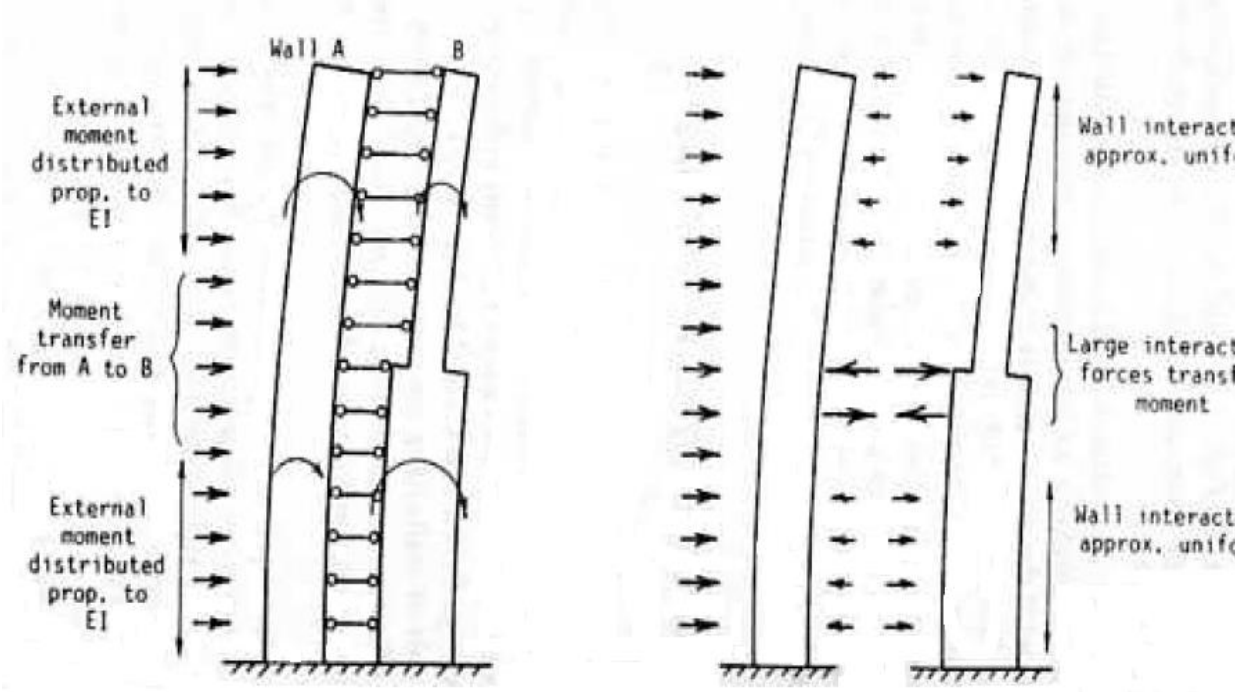

(a) (b)

Figure 2.9: (a) Allocation of moments between walls, (b) resulting interactions [40]

2.8 Coupled Shear Wall Structures

In Coupled shear wall structural system shear walls are connected with moment-resisting members. The presence of the moment-resisting connection like beams or floor slabs considerably increases the stiffness and efficiency of the wall systems, though coupling of walls through floor slabs and designing them in a way to resist moment is rarely done and is not effective as coupling beams [26].

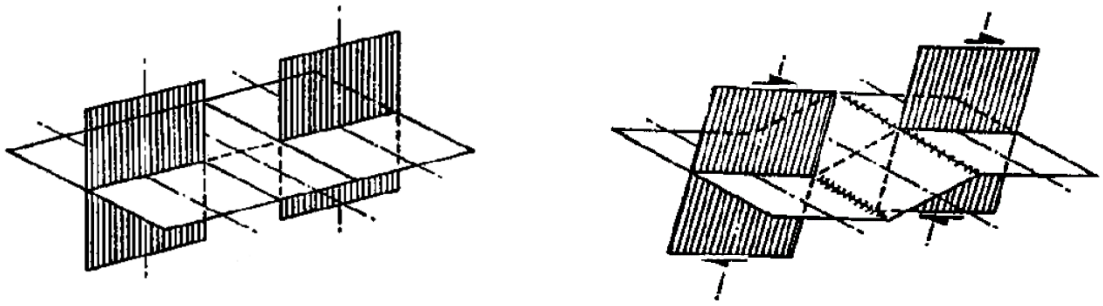

(a) (b)

Figure 2.10: (a) Coupling of walls solely by slabs; (b) developed yield lines under horizontal loading [26]

In case of coupling only with floor slab the interaction between walls and floor slab is supplied more with shear stresses and the behavior of connection is more like pinned connection. It is recommended that slab coupling should not be relied on as a significant source of energy dissipation in ductile coupled wall system. In this case coupling region should be strengthen with well confined slab reinforcement in relatively narrow band across the slab and the shear punching could be absorbed by placing a short rolled steel section in the floor slab between upper and lower reinforcement [26].

2.8.1 Behavior of Coupled Shear Wall Structures [11], [26], [40], [49], [51], [52]

In describing the coupled shear walls behavior two extreme cases will be considered. In First case coupling beams are considered pinned ended links that transmit only axial forces between walls and second case in which walls are connected by rigid beams to form a dowelled vertical cantilever with full composite action (see figure 2.11).

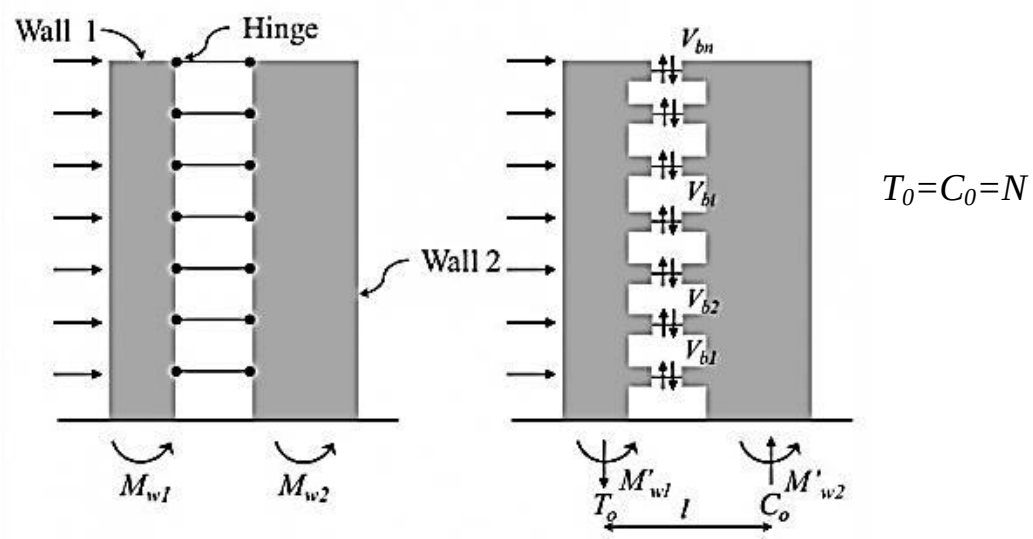

Figure 2.11: (a) Pin ended links; (b) moment resisting coupling [49]

In first case applied moment will be resisted by individual moments in the two walls, the magnitude of moments will be proportionate to wall flexural rigidities. The bending stresses are distributed linearly on the cross section of each wall, with maximum stresses on opposite edges (figure 2.12d).

In walls which are connected with rigid beams to form a dowelled vertical cantilever, external moment will be resisted by a single composite unit consisted of the two walls, bending about the centroidal axis of two walls. In this case the distribution of bending stress is linear across the composite unit, with maximum stresses occurring at the opposite extreme edges (figure 2.12c).

The practical situation of coupled walls connected with flexible beams will lie between two extreme cases mentioned before (figure 2.12b). The stiffer the coupling beams, the closer the behavior to fully composite cantilever.

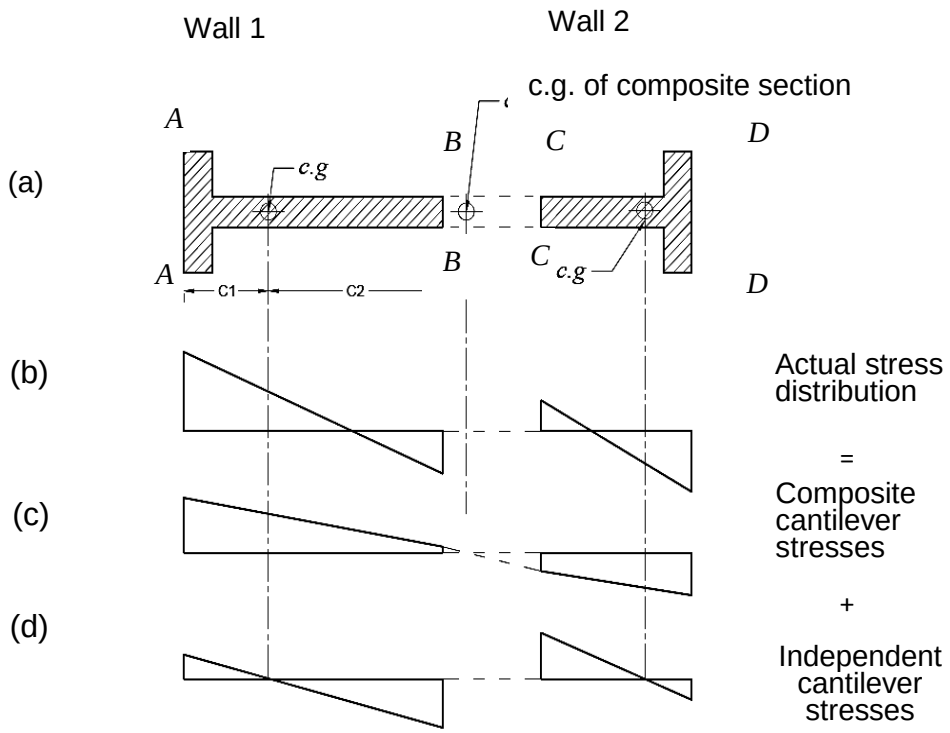

Figure 2.12: (b) True stress distribution on the wall based on superposition of stress distribution due to (c) composite and (d) independent action [52], [40]

As the walls deflect laterally, coupling beam ends rotate and displace vertically and consequently beams bents in double curvature and thus resists the free bending of walls. The bending action induces shear in coupling beams, which in turn exert resisting bending moments against lateral loading on each wall. This shear also causes an axial force in the walls, which is tensile in windward and compression in leeward wall. These axial forces also produce a couple which contributes in total resisting moment (see figure 2.11). As it is clear from figure 2.11(b), the external moment is resisted by the sum of three components as below

$$M = M'_{w1} + M'_{w2} + Nl \tag{2.3}$$

The last term NL represents the reverse moment caused by the bending of coupling beams, which resists the free bending of walls. This term in the case of linked walls is zero and reaches a maximum when couplings are infinitely rigid. The responsibility of these coupling beams is reducing the magnitude of wall moments by causing a proportion of external moment to be carried by axial forces in walls. The lever arm of resisting couple is relatively large (distance between centerline of walls) and a small axial stress can give rise to large moment of resistance. The maximum tensile stress

in concrete may then be greatly reduced and this makes easier to suppress the tensile stresses by gravity lading.

A free body diagram through the coupling beams halfway between the faces of two walls and the induced internal forces is shown in figure 2.13. Shear deflection of coupling beam causes localized cracking of the beam-to-wall joints, which decreases the angle the coupling beam must go through where it is connected to the walls. This localized effect is assumed with shifting the connection point from the face of the wall

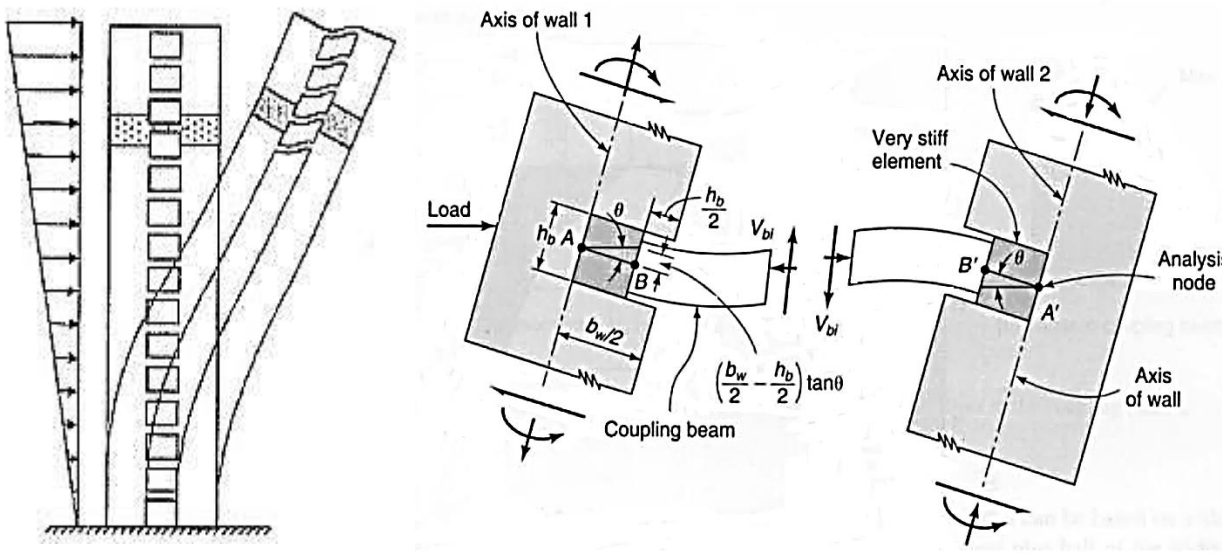

Figure 2.13: Effect of shear wall deflections in coupling beam and induced internal forces [49].

by approximately $h_b/2$ to the centerline. h_b is the height of beam. Therefore it will be assumed that the coupling beam is spanning from B to B'. Point B is assumed to be located at the half coupling beam height $0{,}5h_b$. These assumptions account for reduction of coupling beam stiffness where it is attached to the wall.

1.1.1 Analysis Methods of Coupled Shear Walls

Approximate closed form solutions are available for analyzing of shear walls which have simple systems and are subjected to symmetric loadings. These methods are appropriate for hand calculations in the preliminary design stage and give a sound insight to the structural behavior of coupled walls, which in turn helps in first approximation of member sizing. Nowadays, for complex systems which are not covered with approximate methods, computer aided calculations could be performed to get more accurate results.

2.8.1.1 The Continuous Medium Method (Laminar Analysis) [57]

In this method discrete coupling beams are changed with an equivalent continuous connecting medium between vertical elements, or in another word structure is simplified by assuming that all horizontal connecting elements are effectively smeared over the height of the building. This assumption is only applicable for a uniform system of connecting beams or floor slabs. This concept has been developed by Beck-Rosman and has been used in several studies. The idea of simulation originated with Chitty [.

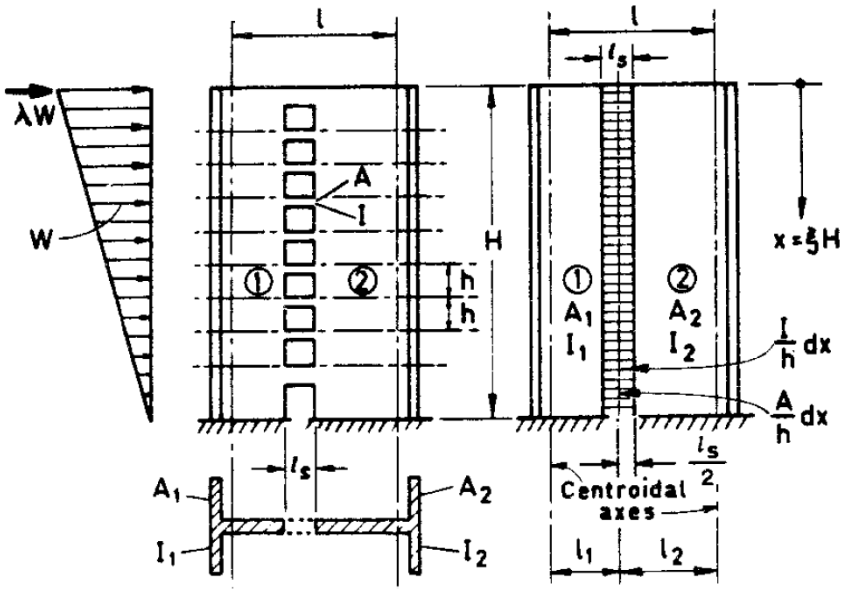

(a) (b)

Figure 2.14: (a) Coupled shear wall; (b) mathematical model [48]

In this method unknown parameters in highly statically indeterminate structures reduce to single differential equation and the flexibility of coupling beams is represented as a continuous flexible medium. First compatibility equations are written for beams. Solving these differential equations with their specific boundary conditions leads to conventional equations derived for different types of loading.

2.8.1.2 Frame Analogy Method

In this method walls and coupling beams are modeled as frames consisted of columns and beams, and the sectional properties of original members are assigned to new members, concentrated at their centerlines. In this model for realizing the original conditions and improving the accuracy of stiffness estimation it is necessary to take into account the rigid end zones. The length of the rigid link depends on geometric properties of beam and walls which this beam coupling them. The

recommended values in different research for this distance is from $L_{wall}/2$ to $(L_{wall}/2)$ - $(d/4)$, in which the d is the beam depth [53].

Rigid link also should be considered at the end of deep beams, because axial deformation is significantly high and it affects the shear transfer between coupled elements [55]. Figure 2.15 shows the different models of frame analogy.

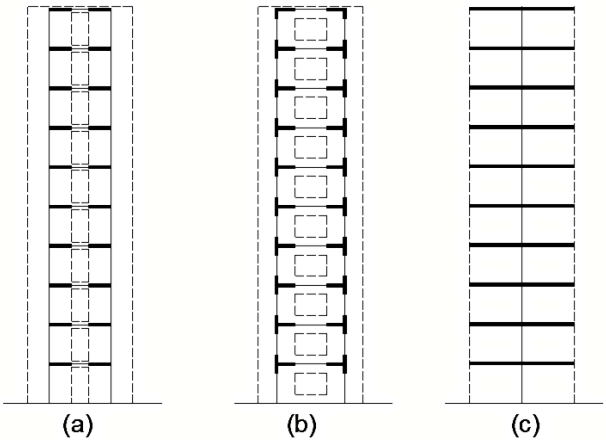

Figure 2.15: Different cases in frame analogy method; (a) model with shallow coupling beams; (b) model with deep coupling beams; (c) solid wall [55]

The modeled frame can be analyzed with hand calculations available for rigid frames or frame analysis program to obtain the internal forces.

2.8.1.3 Finite Element Method

The finite element method as a numerical solution removes many of limitations from the analysis of structures. Complete details of the stress pattern at the points where stress concentrations occur could be observed by using finer elements. Difficulties that could occur in case of irregular openings or complex support conditions in conventional methods are easily modeled with finite element method. For modeling purpose normally plate elements are used for shear walls and coupling beams could be modeled as beam elements in shallow beams and with plate elements as a part of wall in case of deep beam.

2.9 Wall-Frame Structures

Structures that the lateral loading effect is resisted by combination of shear walls and rigid frames are recognized as wall-frame structures or dual systems. Walls and frames have different deflection behaviors and they interact horizontally through floor slabs when they are laterally loaded. The effectiveness of wall-frame structure depends on the amount of interaction which is related to relative stiffness of the walls and frames and the height of the structures. In practical cases it is common to consider the frame as fully braced and design it only for gravity loading [47].

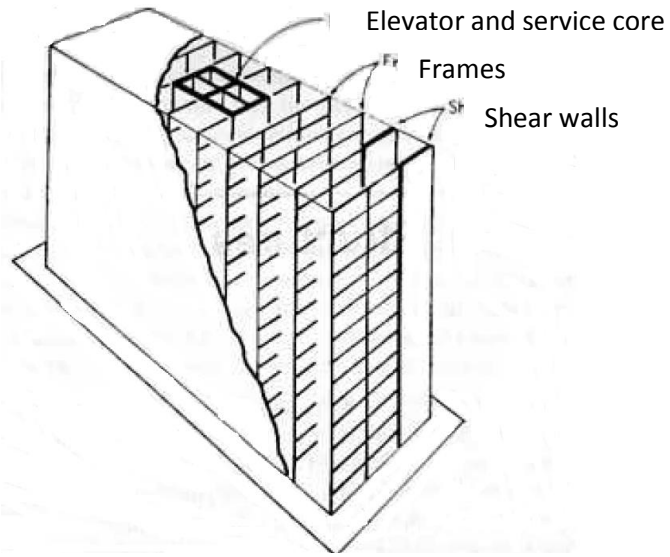

Figure 2.16: Representative wall-frame structure [40]

Dual systems combine the advantage of their constituent elements. Ductile frame in interaction with shear walls can dissipate a large amount of energy under seismic loading particularly in upper parts of building. Drift may be significantly less than if the walls alone were resisting the horizontal loading. As a result of large stiffness of walls development of storey mechanism involving column hinges and soft storey can be avoided. Action of dual system decreases the bending moments in walls or cores in comparison to the case that walls act alone. Columns may be taken into account as fully braced and the estimated shear in frames may be approximately uniform in many cases through the height [47].

2.9.1 Behavior of Wall-Frame Structures [11], [26], [40], [47], [48], [49]

In tall buildings shear walls act as vertical cantilevers and have a flexural deflection mode with concavity downwind and maximum slope at the top, in contrast frames deflects in shear mode with concavity upwind and a maximum slope at the base. This phenomenon occurs because the stiffness of shear wall cantilever is proportion to higher power of height but the stiffness of frame is directly proportion to its height.

When the walls and frames are connected through pin-ended links the deflection of the composite structure has flexural mode at the lower part and a shear profile at the upper part. Interaction forces in links in form of axial forces case the wall to restrain the frame near the base and frames to restrain the wall near the top. Figure 2.17 shows this phenomenon and interaction between wall and frame.

The effect of wall stiffness on load sharing between components of structure is considerable. With increased wall stiffness (i.e., wall length) the contribution of the walls in base moment attraction increases. At the upper parts walls attract less

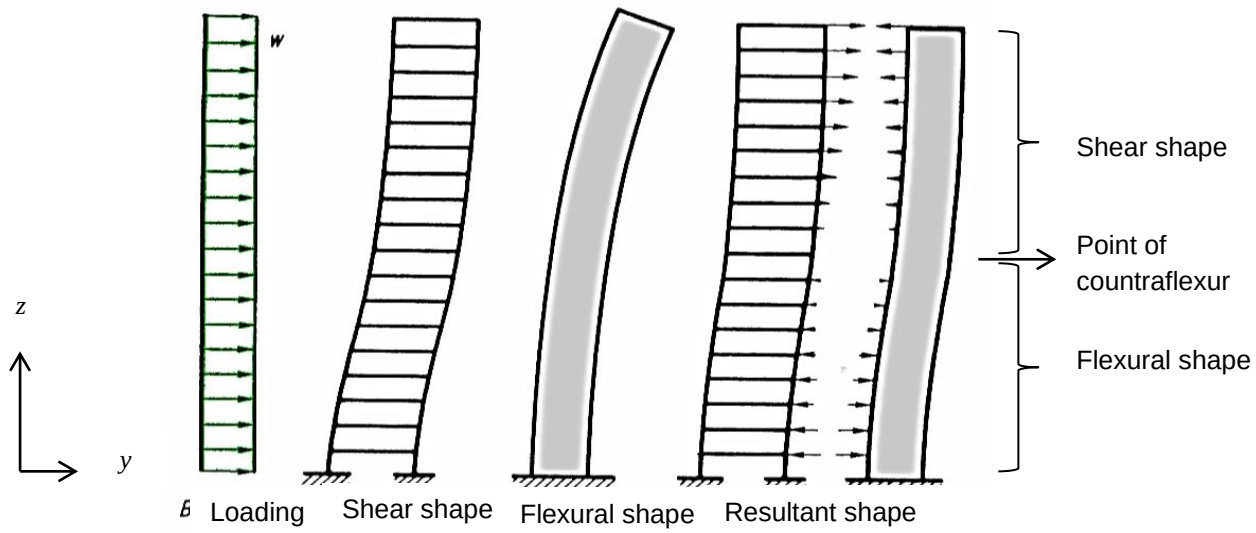

Figure 2.17: Deflection modes and interaction between wall and frame [11]

moments and become less effective. Flexible walls loose rapidly their contributions to horizontal load resistance with height. Above the point of inflexion, where $d^2y/dz^2=0$, the sign of moment changes and consequently the moment in the frame exceeds the external moment. Furthermore, in the upper regions where $d^3y/dz^3=0$, the shear in walls also reverse and so the shear in the frame exceeds the external shear.

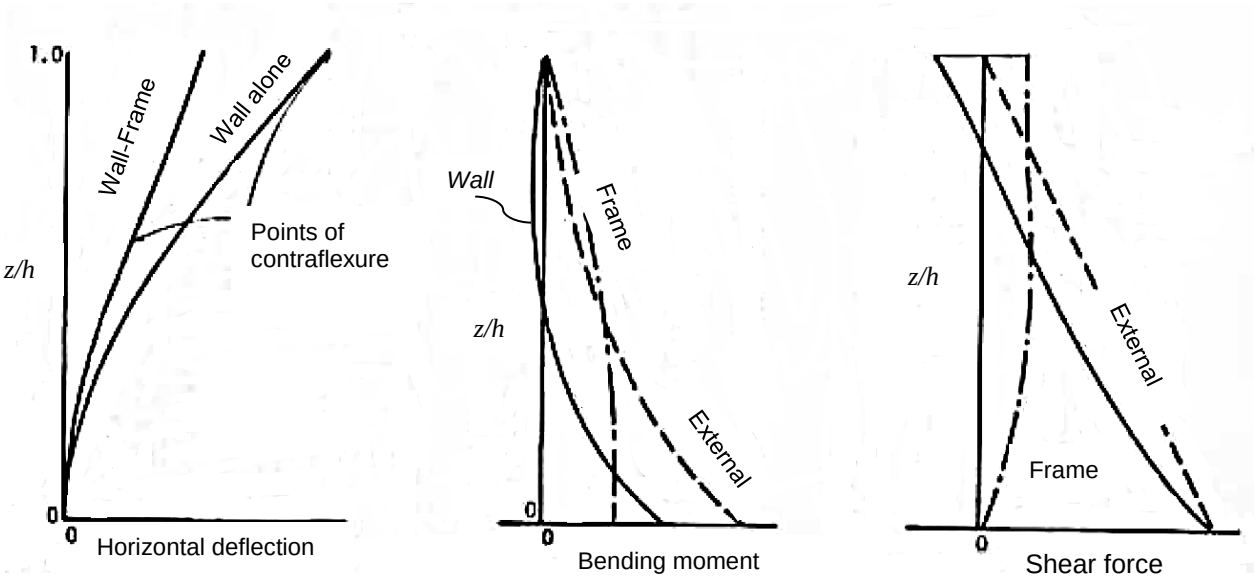

(a) (b) (c)

Figure 2.18: (a) Typical deflection of wall-frame system under horizontal static loading; (b) typical moment diagram of system; (c) typical shear diagram

With these considerations the walls could be curtailed above the countraflexure point because of economical or structural reasons, in doing so, the moment on the upper part of the frame is reduced, and if the walls are eliminated above the level where shear reverse in walls ($d^3y/dz^3=0$), both moments and shear in frame are reduced. In both cases curtailment of walls have little effect on the top displacement. These discussions are only true for static load cases; under seismic loading, load distribution mentioned earlier is different as a result of higher mode effect at the upper parts of structure.

Another characteristic of wall-frame structure is that, a concentrated interaction occurs at the top of the building (see figure 2.18 (c)) and this could be used in further stiffening of the structure by increasing the magnitude of this interaction. The interaction force could be increased by increasing the racking rigidity of the frame adjacent to the top of the wall. Higher shear rigidity could be achieved by increasing the second moment of inertias of beams and columns of the frame adjacent to the top of the wall, or by implanting a concrete diaphragm into the frame which leads a very high racking rigidity.

2.9.2 Analysis Methods of Wall-Frame Structures

The analysis methods of wall-frame structures are like coupled shear walls analysis methods. Analytical approximate solutions have been developed by Stafford Smith and Heidebrecht in which the continuous medium analogy is utilized. In this method connecting rigid links are substitute with a continuous medium smeared along the height of structure. Columns are assumed to be axially rigid and the property of walls and frames do not change over the height [58], [59].

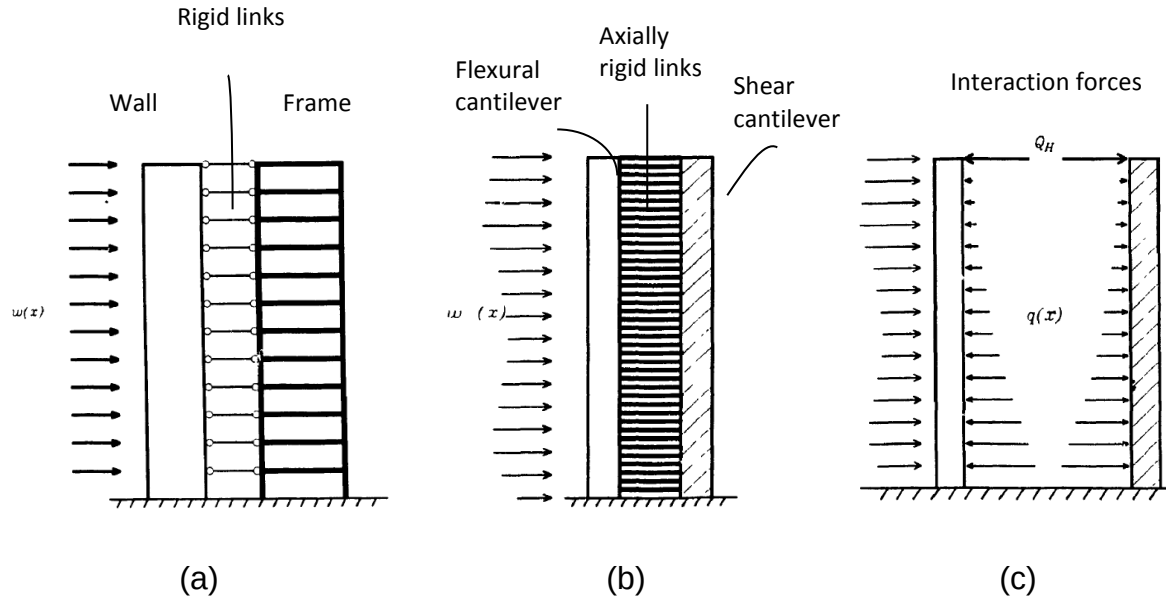

Figure 2.19: (a) Planner wall frame structure; (b) continuum analogy for wall frame structure; (c) free body diagram of wall and frame [59].

For derivation of internal forces, differential equations are written for equilibrium and solved to obtain a closed form solution for this problem. In later studies mentioned method has been extended with consideration of axial deformations of columns [59].

Another analysis method that could be used in modeling of wall-frame structures is wide column analogy. Shear walls are assumed as columns concentrated at their centerlines, in doing so, the rigid link beam span should be modified because of wall width. This method is studied by Nollet and Stafford Smith [60].

Discussed methods above are only suitable for plan-symmetric structures under symmetric loading which don't twist, and therefore could be analyzed as equivalent planar models. Structures those are asymmetric about the axis of loading twist about their shear center. Twisting structure also benefits from horizontal interaction between walls and frames, but their consideration in a general way is extremely complex because the amount of interaction is highly dependent on relative location of bents in the plan [40].

The last and the most accurate analysis method as mentioned earlier is finite element method with using full stiffness matrix of structure. Although this method also has its own tricks and using different elements, mesh sizes or model assumptions may give different results.

2.10 Tubular Structures [39], [40], [41], [61]

In these structures very stiff moment resisting frames which are arranged around the perimeter form a tube shape. The frames consist of closely spaced exterior columns and deep spandrel beams rigidly connected together, with the entire assemblage continuous along each facade and around the building corners. The philosophy of these systems has been to spread load-carrying materials around the external periphery of the building to maximize the flexural rigidity of cross section. In these systems gravity loading is shared between exterior frames and interior columns or structural walls and lateral loading is carried by external tube. These system works so that the perimeter frames aligned in the direction of loading serve as the "webs" and those, perpendicular to the loading direction as "flanges". Different types of Tubular structures which are developed during time involve a range of structural forms like: framed tube, tube in tube, bundled-tube, braced tube and composite tube systems.

2.10.1 Behavior of Tubular Structures

Framed tube structures consist only from periphery columns and deep beams around building. These systems are most used in rectangular shape plans. Flange-web action in these systems is complicated by the fact that flexibility of spandrel beams produces a shear lag. This phenomenon leads to uneven distribution of axial forces in columns. Axial stress is higher in corner columns than in the inner columns of both the flange and web panels. The principle interaction between the web and

the flange frame happens through the vertical displacement of corner columns. These type of structures are shown in figure 2.20.

Bundled-tube structures are those in which the shear lag effect is greatly reduced by introducing interior framed “web” panels across the entire width of the building. Since the end columns of interior webs will be mobilized directly by the webs, they will be more highly stressed.

The bundled tube uses a cellular concept. These bundle tubes may include belt trusses at levels where floor plans transition from large to small in order to interconnect or tie the tubular frames together [61]. Torsion from lateral or seismic loads is resisted by the closed-section form of the modulus. The concept of such structures is illustrated in figure 2.21.

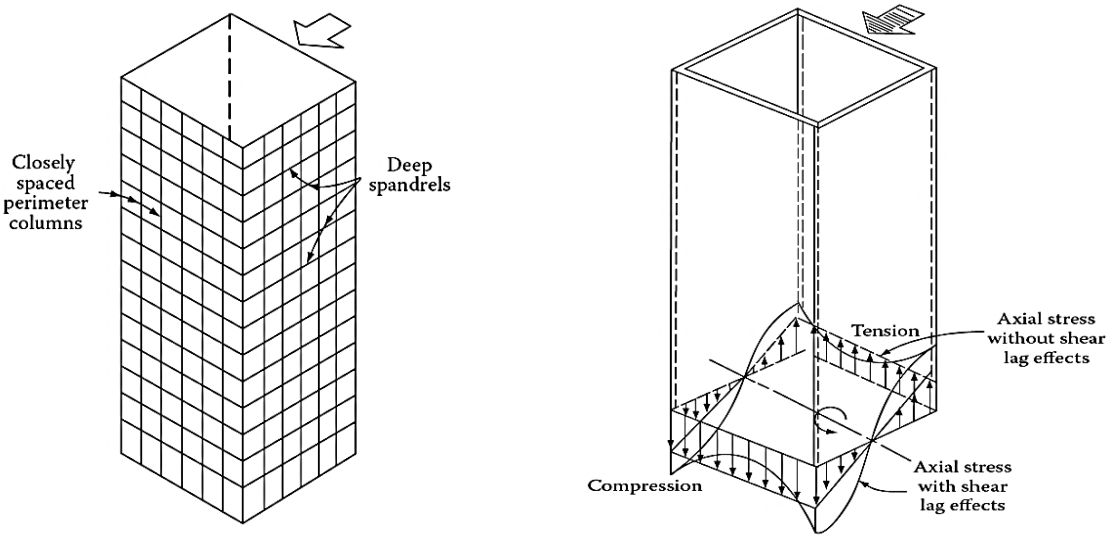

Figure 2.20: (a) Framed tube structure; (b) shear lag effect [39]

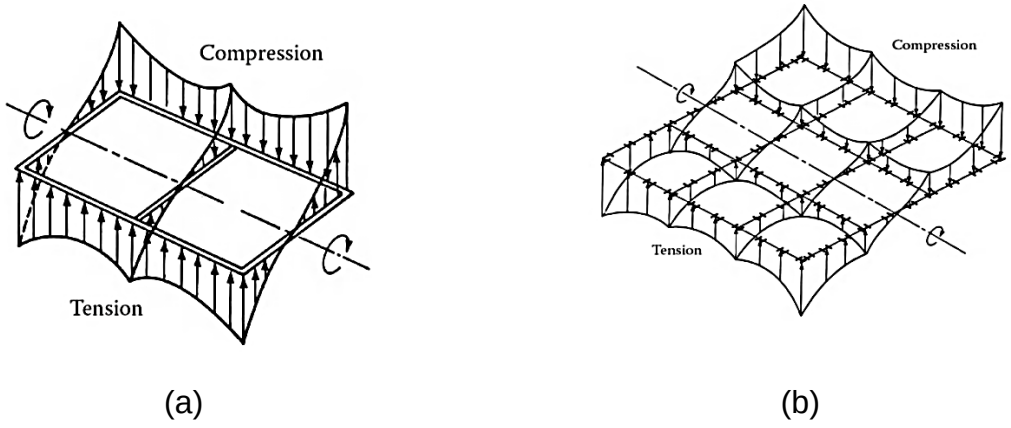

Figure 2.21: (a) Stress distribution in bundled tube with two cells; (b) multi-cell bundled tube stress distribution [39]

Braced-tube or trussed-tube structures are consisted of a minimum number of diagonals on each facade and making the diagonals intersect at the same point at the corner column. These diagonals brace the faces of the tube, in doing so, the exterior columns may then be more widely spaced. The diagonals are generally inclined at about 45 degree to the vertical. These diagonal elements usually exist on multiple-floor intervals. The structural system attempts to equalize axial load (reduce shear lag) attracted to columns when the overall structure is subjected to lateral loads. The use of diagonal elements in the tube significantly increases structural efficiency (less material using) since the behavior is governed by axial rather than bending behavior.

Tube in tube or hull-core structures are another variation of framed tube structures. This structural system consists of an outer framed tube, the “hull,” together with an internal core. The gravity and horizontal forces are shared between hull and core and the internal core could be in form of steel bracing or assembly of shear walls. . Partly, the outer framed tube and inner core interact horizontally, as the shear and flexural components of wall-frame structure, resulting increased lateral stiffness. The behavior of framed tube normally dominates because of its much greater structural depth.

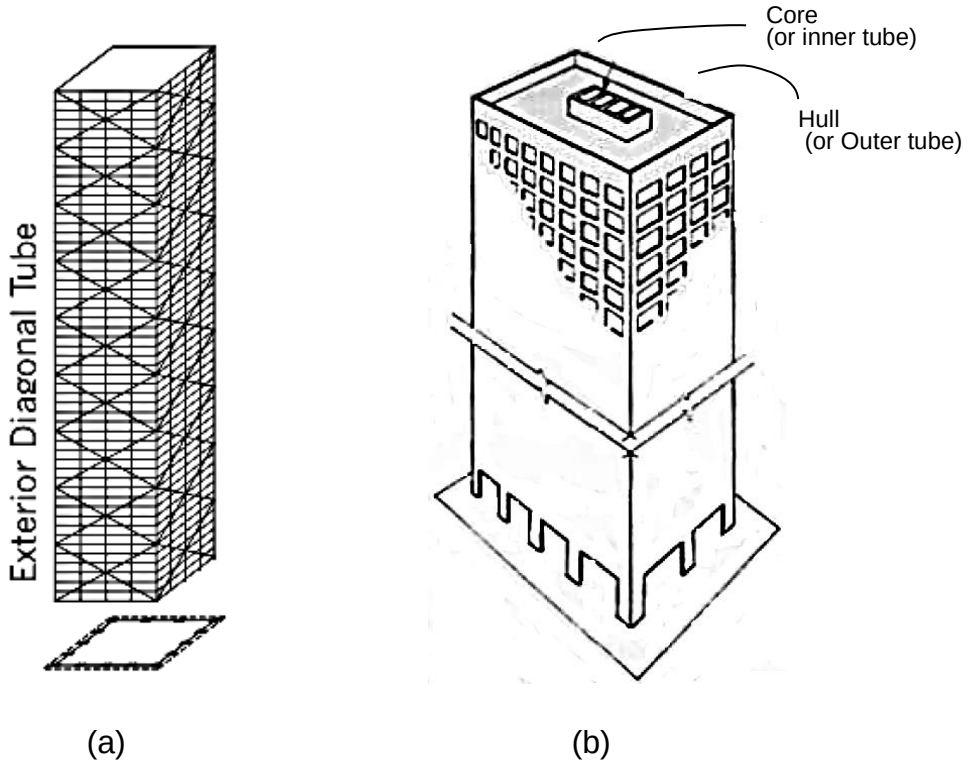

Figure 2.22: (a) Braced tube structure; (b) Tube in tube structure [61]

2.11 Core Structures

Concrete core structures usually consists of assembly of connected shear walls forming a box section containing openings for entrances of service shaft and they may be partially closed by beams or floor slabs. Cores with sufficient dimensions have enough moment of inertia to carry to whole lateral loading. The torsional stiffness of the core can be a main part of total torsional resistance of the building. They are normally located around stair cases or elevator shafts. The proportion of the height, length and the thickness of cores are usually in a range which classify them as thin-walled beam [40], [11].

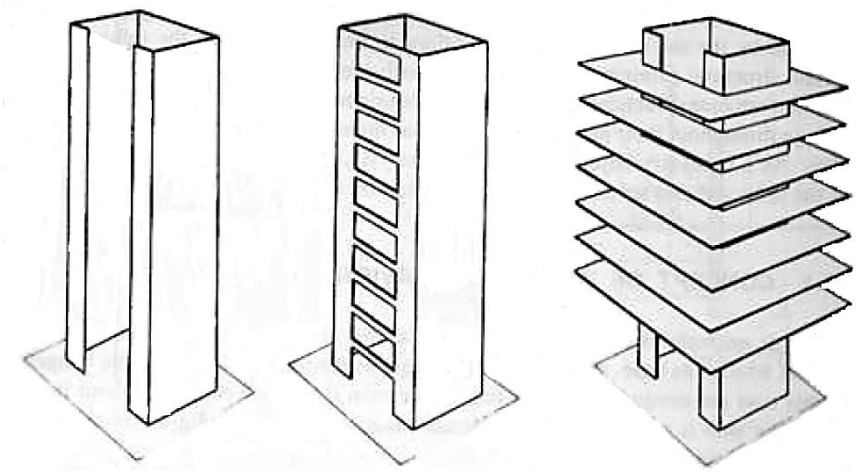

(a) (b) (c)

Figure 2.23: (a) Open section core; (b) core partially closed by beams; (c) core partially closed by floor slabs [40]

2.11.1 Behavior of Core Structures

When core structures are subjected to torque, as result of twisting, plane sections of the core warp. Because the core is normally fixed in foundation, this prevents the base section from warping and twisting induces vertical warping strains and stresses over the height of core walls. If the torsional stiffness of structure is supplied mostly through core, the vertical warping stresses at the base of the core could be in a range of magnitude which may compete with the bending stresses. This phenomenon is illustrated in figure2.27 (a). In this case the warping stresses should be taken into account in design [40].

The behavior of partially closed cores (see figure 2.24 (b)) lies between two extreme cases. First case is open section core (see figure 2.24 (a)) which is more flexible in torsion and has higher warping stresses at corners. The other limit state is a complete core section without opening, which normally is not used. Partial closure of

the core by coupling beams or slabs which lies between these two cases is frequently used. This coupling increases the torsional stiffness and restrains the core section from warping and reduces the warping stresses and core rotation. The connecting beams in this case are subjected to shear and bending which should be considered in their design [40].

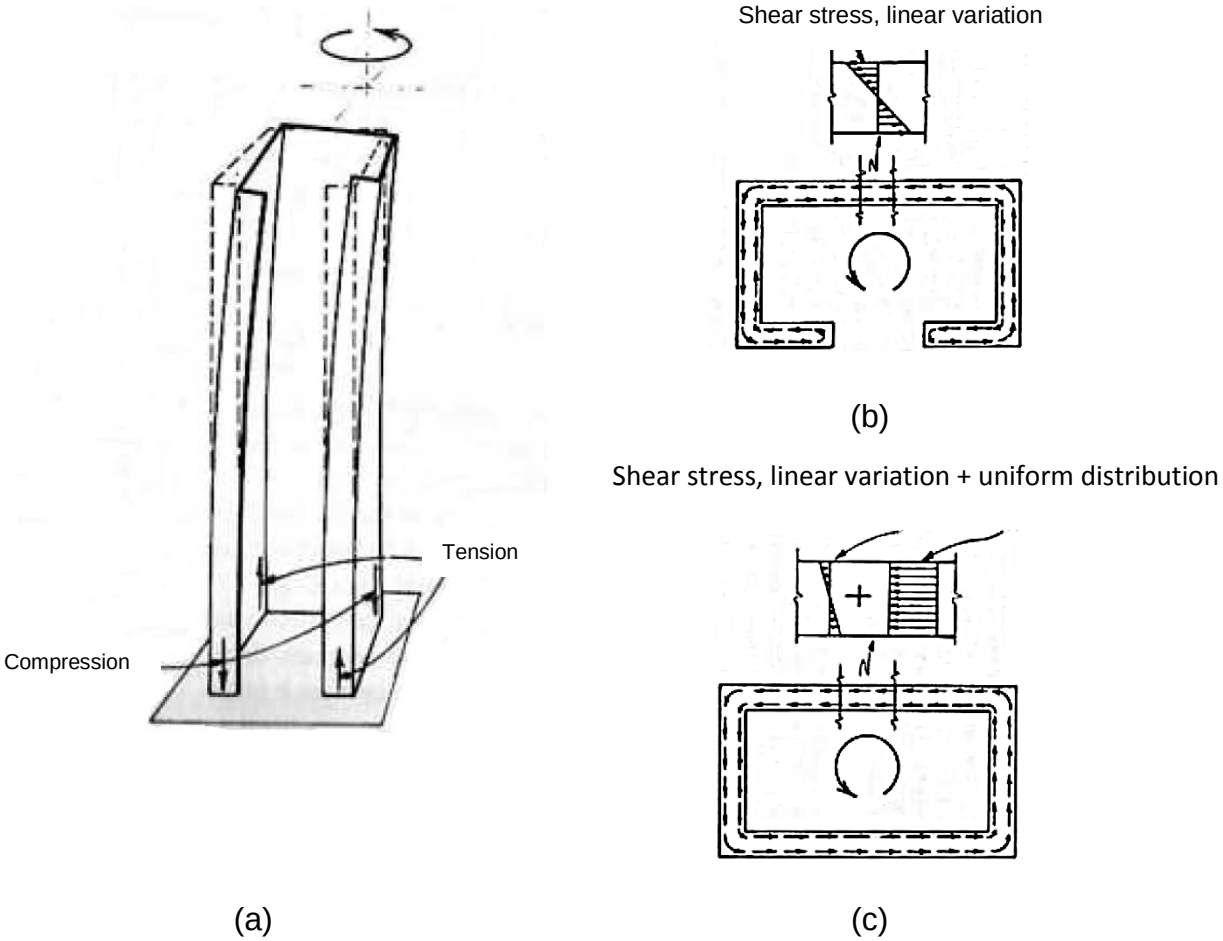

Figure 2.24: (a) Twisting of core under torque; (b) twisting shear Stress in open section; (c) shear stress in closed section [40]

The torsional resistance of core structures is provided by horizontal shear in the walls. As a part of this resistance, the warping shear which is associated with the inplane bending of walls. Other component is the shear resulting from plate twist action which causes circulating of shear stresses within the wall thickness (figure 2.24(b)) and, in closed- or partially closed-section core, from additional shear stress that unidirectionally circulate around the core (figure 2.24(c)) [63].

Warping torsion theory of thin-walled elements is relatively new in comparison to other modes of action. Vlasov is one of the persons which had a significant contribution to this theory and established the sectorial coordinate and bimoment

concept [62]. In other researches the close analogy between warping torsion theory in twisting and wall-frame theory in a planer mode is studied by Stafford Smith, Heidebrecht and Jesien [64], [65].

Important part of warping effect include the vertical stresses in the core walls, and in partially closed core, the shear and moments in beams. The principal warping action is resulted from bimoment. The magnitude of vertical stress distribution at a level depends on the magnitude of bimoment at that level. For a core with typical characteristics subjected to the uniformly distributed torque, the distribution of rotation, bimoment, shear in coupling beams and warping stress distribution are shown in figure 2.25. The bimoment curve (fig. 2.25 (d)) shows that the sense of warping stress distribution at the upper part of core is opposite in sense to that in lower part, while there is a level of contrawarping, in which at transition the bimoment and warping stress are zero [40].

In partially closed cores, when the core twists, the walls edges on opposite sides of an opening undergo vertical displacements in opposite direction and vertical plane rotations in the same direction. These displacements subject connecting beams to shear and bending. This vertical shear at the end of beams produces complementary horizontal shears in the core walls that circulate around the core. These shear stresses are like those that circulate in a closed section and results in a large increase in the effective torsional stiffness of core and decreases the core rotation and warping deformations and vertical stresses [40].

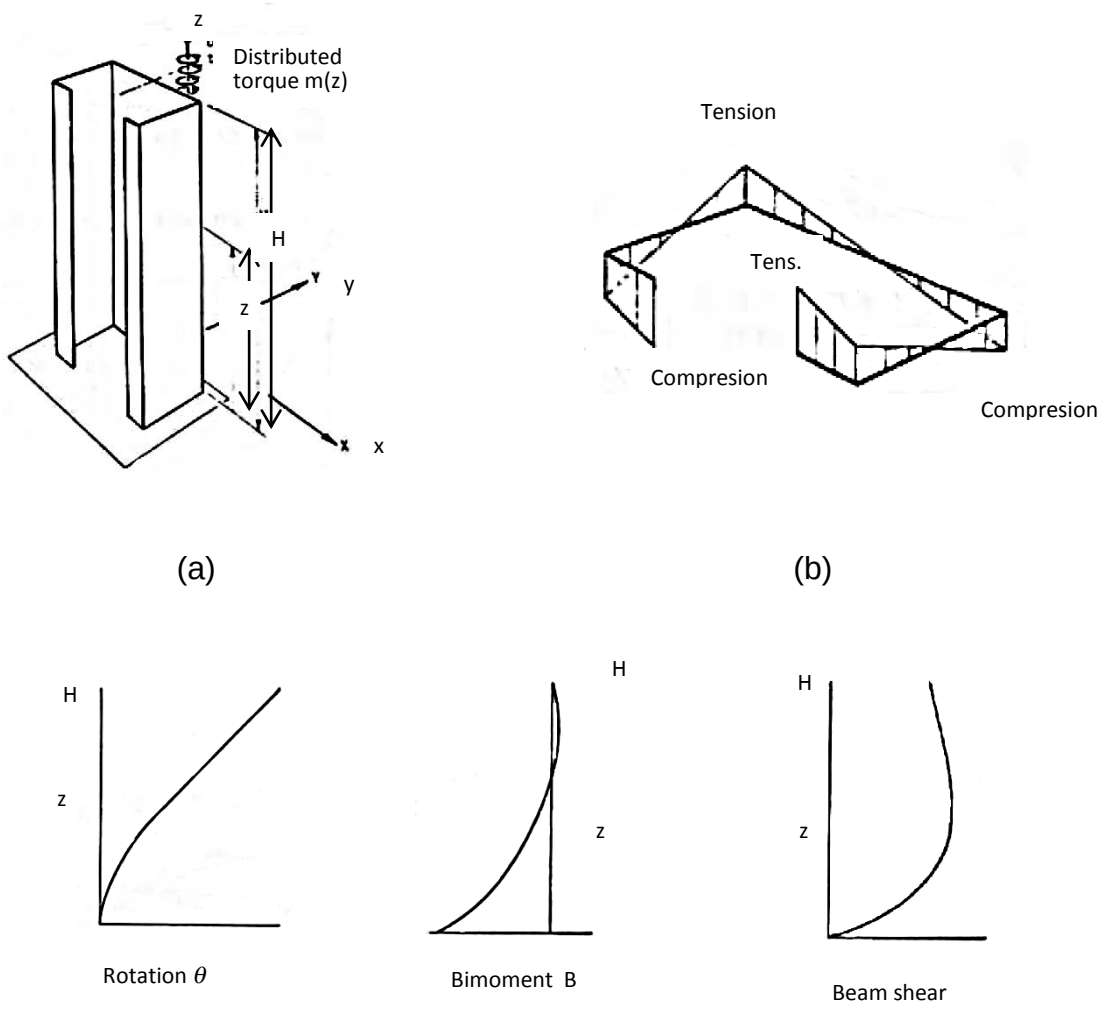

Figure 2.25: (a) Core under distributed torque; (b) stress distribution due to warping in core section; (c) rotation of core; (d) bimoment in core; (e) shear force in beams of partially closed core [40]

2.11.2 Methods of Analysis of Core Structures

Like coupled shear walls and wall-frame structures, closed form solutions are derived for simple cases with assuming the beams as a continuum media which acts only as a shear diaphragm. The flexural action of beam is converted to an equivalent

shear medium and is assumed that the original walls behave in shear and flexure and the diaphragm only in shear. The equivalent thickness of shear medium is extracted from flexural rigidity of beams and then is used in torsional stiffness of core. Then compatibility conditions are considered at the end of beams and from this differential equations of forces are derived. By solving these equations internal forces can be obtained [40].

One of the other methods for analyzing core structures is analogous frame method, in which core is modeled as braced frame with appropriate elements.

As third method, two-column analogy could be mentioned. In this method core is modeled with two columns placed on one of the core's principal bending axes, and located on opposite sides of the shear center. Multisection cores with changing locations of shear center can be analyzed by using of a transition mechanism. This model can be used for simple representation of a complex core [66].

The most concise model for analyzing of cores is single warping column model. This consists of a vertical assembly of column elements, in which every node have seven degree of freedom instead of six. The seven one is added to consider for warping. Multisectional cores can't be analyzed with this method, because there is no mechanism to represent the change of section [64].

The Last and the most effective method is the finite element method that does not require any knowledge of warping theory, nor does it require the calculation of the warping sectorial properties.

2.12 Core-Outrigger Systems [39], [40], [41]

In these systems concrete or steel main core is connected to the periphery columns by flexurally stiff horizontal cantilevers. The core may be located between columns centrally with outrigger trusses connecting on both sides, or it may be located on one side of building with outriggers extending to the building columns on the other side.

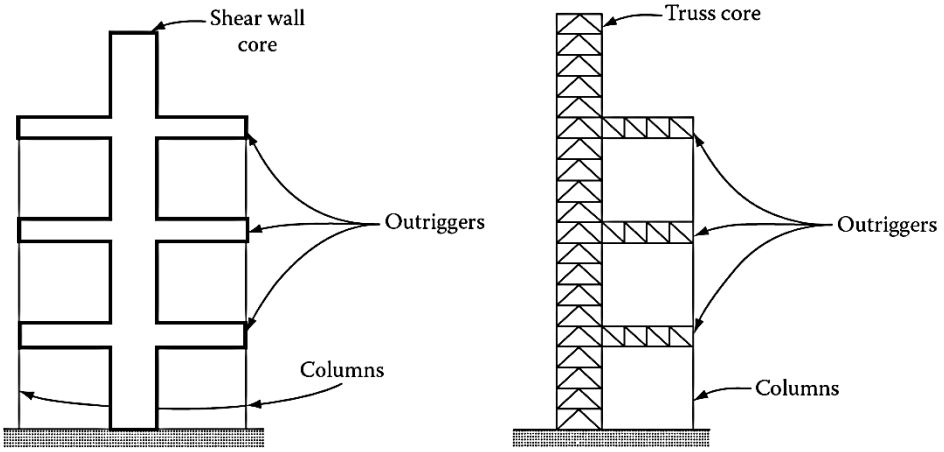

Figure 2.26: Core and outrigger system: (a) centrally located core; (b) offset core [39]

The feature of this system is the axial stiffness of the periphery columns is mobilized for increasing the resistance against overturning moments. Under lateral loads, the column-restrained outriggers resist the rotation of cores. This leads in less lateral deflections and moments in the core-outrigger system in comparison to free-standing core alone resisted the loading (figure 2.27). Connection of core and columns through stiff outrigger results in increased effective depth of the structure when it flexes as a vertical cantilever, by inducing tension in the windward and compression in the leeward columns.

To make the system more effective and to activate other periphery columns which are not located at the end of outrigger a deep spandrel girder or “belt” around the structure at the levels of outriggers is used, which is named occasionally “belt-braced” or “belt-truss” structure. This belt is at least one, and often three-to-four stories deep to make them stiff in flexure and shear. An outrigger with belt-truss is shown in figure 2.28.

As shown in figure 2.31 it is also possible in steel structures to extend diagonals through several floors to act as outriggers, or to use moment resistant connections in girders which connect the core to the exterior columns to act as outrigger.

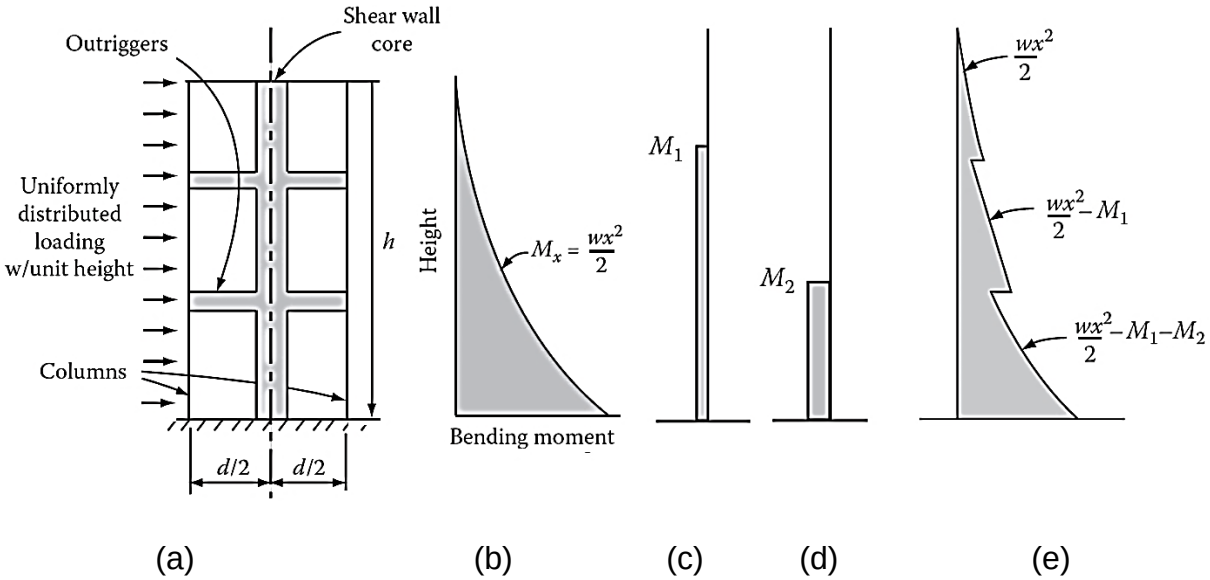

Figure 2.27: (a) Outrigger system under horizontal loading; (b) external moment diagram; (c) M_1 moment diagram caused by upper outrigger; (d) M_2 moment diagram caused by lower outrigger; (e) core resultant moment diagram [39]

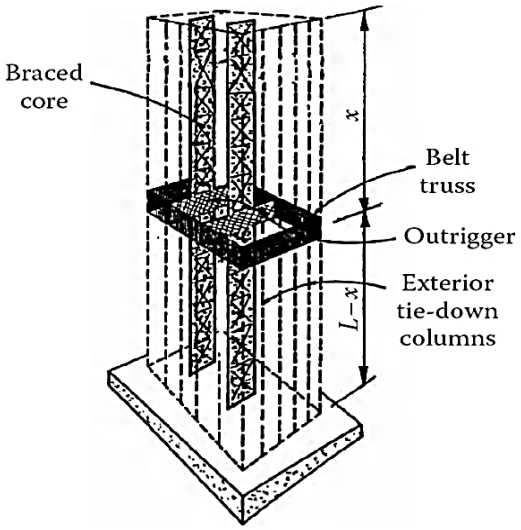

Figure 2.28: Belt truss system [39]

To minimize obstruction they could cause, they are located normally at plant levels. The outriggers increase the lateral stiffness of structure against horizontal loading, but they don't affect the shear resistance, which is carried mainly by the core.

The outrigger-braced structures are not proper to be analyzed with continuum methods and it should be considered as a discrete arrangement. Normally a compatibility condition is used in which the rotations of core at the outrigger levels are taken equal with corresponding outrigger. Rotations consist of two components,

first axial deformation of columns and the other by the outriggers bending under the action of column forces at their outboard ends.

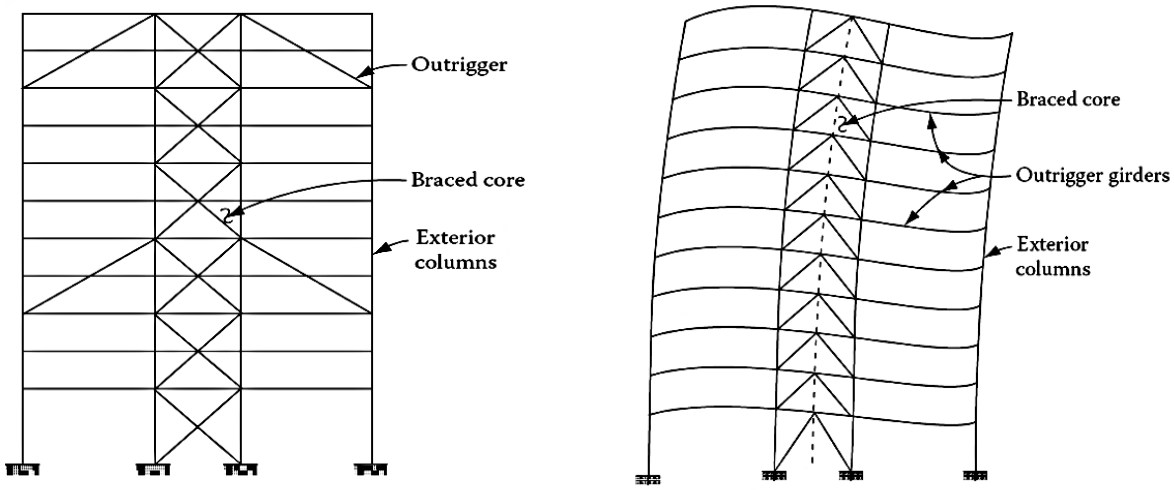

(a) (b)

Figure 2.29: (a) Extended diagonals as outrigger; (b) moment resistant connected girders acting as outrigger [39]

3 Gravity Loading

3.1 Loading Criteria

In civil engineering actions affecting structures are dependent on utilization, geography, topography and life cycle of structures. Magnitudes of these actions are determined probabilistic and normally the conditions with a high occurrence probability are considered. These actions are used with safety margins. These safety margins are considered with the use of safety factors. These factors increase the loads or decrease the strength. Structure under delivered loading should not undergo any global or local collapses, also the deformations under these loads should be in the range that the structure remains functional and it doesn't cause any damage to nonstructural parts or occupants shouldn't complain about structure vibration or movements. However, the last fact is true mostly for loads with low return period.
In investigated test building for determination of actions values, the suggested procedures of EN 1991-1, have been used and no specific national annex considered [1], [2], [3].

3.2 Dead Loads

Dead load of structure consists of self-weight of structure plus superimposed dead load coming from additional fixtures, pavement, mechanical installations and glass façade and its framing weight. The self-weight of structure is calculated automatically by Program and doesn't need to be considered in input data in our case study. Since in considered test building only a preliminary design is done and the feasibility of the given architectural design is checked, the superimposed dead load is determined on simple constructive assumptions according to EN 1991-1-1.
The weight of glass facade and its fixtures and framing is assumed smeared on floors because in this stage of design only horizontal load bearing system of structure, its stiffness and design is concerned. Obviously this load should be considered as a line load on the boundary element of floor system in the next design stages. This boundary element can be a beam or slab itself. In both case the local effect of this line load should be considered on structural elements.
Superimposed dead load in test building is considered to be 1.2 [kN/m^2] for internal partitions and pavement plus 0.6 [kN/m^2] for glass facade for stories above ground level. For underground levels glass load is omitted.

3.3 Live Loads

Provisions of EC1-1 for live load categorize the building based on its utilization. Table 6.1 of EC1-1 shows these utilization categories. Since the test building has an office utilization, category B is chosen from table. Values of actions have been extracted from table 6.2. In this table, two characteristic values are given. One for uniform distributed load which is shown by q_k and is considered for general effect

and Q_k which is a concentrated load for local effects. In calculations, q_k is assumed to be 2 [KN/m^2] for preliminary design. The effect of Q_k can be checked afterwards while slab is designing.

3.3.1 Live Load Reduction

Reduction factors have been considered due to EC1-1 section 6.3.1.2 for live loads, one for floors and another for columns and walls. These factors consider this fact for walls and column in multi-story buildings that all live load can't be present simultaneously in all stories. The same concept has been taken into account for floors based on this fact that all live load can't be present on all area of floor at the same time. This reduction factor for floors is given in [EC1-1] as:

$$\alpha_A = \frac{5}{7}\psi_0 + \frac{A_0}{A} \leq 1,0 \tag{3.1}$$

with the restriction for categories C and D: $\alpha_A \geq 0.6$

where

ψ_0 factor according to EN 1990 Annex A1 Table A1.1;

A_0 10,0 m^2;

A loaded area.

Another reduction factor for live loads is introduced in [EC1-1] section 6.3.1.2 for columns and walls. The total imposed loads from several storeys may be reduced by multiplying the reduction factor α_n :

$$\alpha_n = \frac{2 + (n-2)\psi_0}{n} \tag{3.2}$$

where

n number of stories (> 2) above the loaded structural elements from the same category;

ψ_0 factor according to EN 1990 Annex A1 Table A1.1.

For the first basement storey with considering 50 storey above and ψ_0 from table A1.1 of EN1990 equal to 0,7and α_n is calculated to 0,71.

4 Wind Loading

4.1 Design Consideration

Wind loads are one of the horizontal actions beside earthquake that affect the structures. The importance of wind loading could be clear with increasing the height

of the building. In low to medium rise buildings, up to 10 stories (Tall building page 21) the effect of wind is negligible against earthquake in most cases, but in high-rise building the effect of wind load can compete with earthquake depending on earthquake hazard level and region that building is setting up, and design could be governed by wind load. In design of tall buildings the surrounding area, terrain and the buildings nearby have a big influence on sway response of the structure.
The sway of building due to wind may not be recognized by the people passerby but, can concern people occupying top stories. The old high-rise buildings are less sensible to wind load due to their massive structural elements and heavy masonry partitions that gives them enough stiffness and strength. Modern construction techniques with light-weight materials that have less stiffness, mass and damping characteristics makes these buildings more sensible against wind loads and increase the number of requirements that should be checked about the structure and cladding of these buildings.
Some important criteria that may concern in designing for wind loads are [7]:

- Strength and stability.
- Structural elements and connections fatigue caused by dynamical effect of wind
- High lateral displacement that may crack internal partitions and damage external cladding,
- misalignment of mechanical and electronic systems, and possible permanent deformations of nonstructural elements like pipes, precise electronic devices, telecommunication systems, sensors and so on, that requires recalibration, regulation and fixing of these devices which is related with high costs.
- Discomfort to occupants due to frequency and high amplitude of sway.
- Possible buffeting that may increase the magnitude of wind velocities on neighboring buildings.
- Wind-induced discomfort in pedestrian areas caused by intense surface winds.
- Acoustical disturbances.
- Resonance of elevator hoist ropes vibration with building oscillations.

4.2 Definition, Nature and Classification of Wind

The horizontal motion of air in atmosphere is called wind, and for motion in vertical direction the term current is used. The currents have more importance in meteorology and whether prediction and of less concern in structural engineering, but the horizontal motion or wind causes pressure on structure which in turn with multiplying the projection of sweeping area of structure with this pressure gives the wind load acting on structure. The air motion near the ground is more affected by terrain, and the turbulence of wind is high. The zone of turbulence has a thickness of almost 400 m and is called surface boundary layer. After this layer the air motion is

not more affected with ground shape and the wind moves with a speed called gradient wind speed which is important from structural engineering aspect because the most high-rise building are built in this height interval. [5]
Winds can be categorized in three types [5], [7]:

- *Prevailing wind:* surface air motion toward the low-pressure equatorial zone.
- *Seasonal wind*: temperature difference between land and adjacent ocean in different seasons causes pressure difference leading seasonal wind.
- *Local wind*: which depends on daily temperature, pressure change and local terrain

Prevailing and seasonal wind mean velocity variation which occurs over months is called *fluctuation* and local wind variation that occurs every minute is called *gust.*
Another characteristic of wind is its turbulence, this specification of wind depend on low viscosity and velocity of wind. A velocity between 0,9 and 1,3 m/s makes air motion turbulent [vibration of buildings to wind and earthquake]. In structural engineering aspect wind velocity is assumed to have two components, mean velocity component varying proportionally with height and fluctuating or turbulent component which is not dependent on height. Figure 4.1 shows the mean wind and turbulent component or gust wind during time variation.

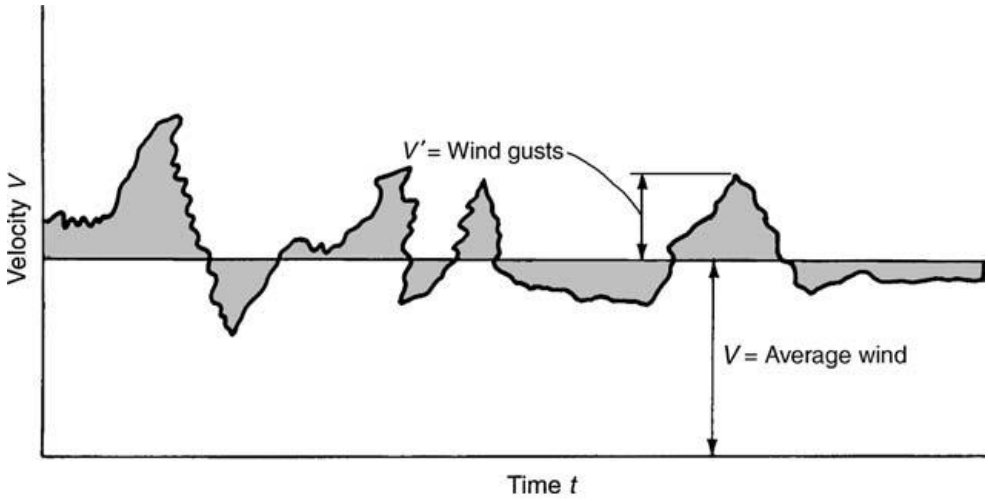

Figure 4.1: Variation of wind velocity with time [7]

As it can be seen later in Eq. (4.14) the wind pressure is proportional to square of mean wind velocity and fluctuates as well along the building height. The total pressure is sum of these two components. If we designate mean pressure with $\overline{\mathbf{P}}$ and fluctuating part with **P'** the total wind pressure will be the sum of these parts [7], [4]. Figure 4.2 illustrates this phenomenon.

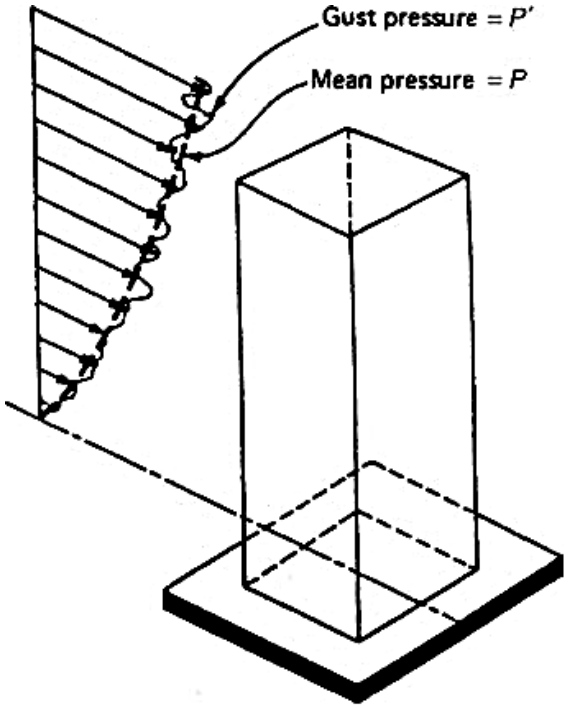

Figure 4.2: Representation of wind pressure composed from two components [7]

4.3 Variation of Wind Profile with Height

As we know from fluid mechanics at the boundary of streaming fluid a retarding in velocity occurs which comes from viscosity and friction of fluid with adjacent boundary. Exactly at the contacting surface the velocity is zero and with increasing of height the friction of fluid layers on each other decreases, which results in higher velocity. After a specific height, increasing of wind velocity proportional to height ceases, this height is called as *gradient height* and corresponding velocity as *gradient velocity*. At height approximately 500m the air motion is not more governed by ground friction and the prevailing and seasonal effects affect the air velocity [7].

4.4 Terrain Roughness Effect

Another factor influencing the wind profile is the exposure terrain which is reflected in table 4.1 of EC1-4. In this table different terrain categories are defined and values for minimum height z_{min} and roughness length z_0 are given. These values are used in calculation of terrain factor k_r. It can be seen with increasing terrain category-number the k_r coefficient which is defined as below results in higher velocities:

$$k_r = 0{,}19\left(\frac{z_0}{z_{0,\mathrm{II}}}\right)^{0{,}07} \tag{4.1}$$

$z_{0,\mathrm{II}}$ = 0,05 m (terrain category II, Table 4.1)

Terrain category	z_0 m	z_{min} m
0 Sea or coastal area exposed to the open sea	0,003	1
I Lakes or flat and horizontal area with negligible vegetation and without obstacles	0,01	1
II Area with low vegetation such as grass and isolated obstacles (trees, buildings) with separations of at least 20 obstacle heights	0,05	2
III Area with regular cover of vegetation or buildings or with isolated obstacles with separations of maximum 20 obstacle heights (such as villages, suburban terrain, permanent forest)	0,3	5
IV Area with regular cover of vegetation or buildings or with isolated obstacles with separations of maximum 20 obstacle heights (such as villages, suburban terrain, permanent forest)	1,0	10

Table 4.1: Terrain categories [1]

Terrain factor is used in calculation of roughness factor which considers the variation of mean wind velocity at the site of construction and is designated by $c_r(z)$. The value of this factor depends on height above the ground and is defined in EC1-4 as below with a logarithmic expression:

$$c_r(z) = k_r.\ln(\frac{z}{z_0}) \qquad \text{for} \qquad z_{min} \le z \le z_{max} \tag{4.2}$$

$$c_r(z) = c_r(z_{\min}) \qquad \text{for} \qquad z \le z_{min}$$

The k_r factor is defined before and z_{max} is to be taken as 200m. Wind profile varies exponentially from ground and in EC1-4 is defined in another way as a logarithmic function which is a function of $c_r(z)$ and k_r.

It has been assumed that such a high building normally is built in downtown that has enough building density surrounding and covers the description of category 4 in table 4.1. From table z_0 = 1 and z_{min} = 10 for category 4. From these values for considered terrain category we can calculate k_r as follow:

$$k_r = 0.19(1/0.05)^{0.07} = 0.2343 \tag{4.5}$$

From substitution of k_r value in Eq. (4.4) roughness factor $c_r(z)$ can be calculated:

$$c_r(z) = 0.2343\ \ln(z) \qquad \text{for} \qquad z_{min} \le z \le z_{max} \tag{4.6}$$

4.5 Mean Wind Velocity

The mean wind velocity is used in calculation of peak velocity pressure and is defined in section 4.3 of EC 1-4 as below:

$$v_m(z) = c_r(z) \cdot c_o(z) \cdot v_b \quad (4.7)$$

Where $c_r(z)$ is introduced earlier. $c_o(z)$ is the orography factor, taken as 1,0 unless in terrains like hills or cliffs, which in this case recommendations of appendix A.3 in EC1-4 should be considered.

v_b is the basic wind velocity calculated from section 4.2 of EC1-4 as below:

$$v_b = c_{dir} \cdot c_{season} \cdot v_{bo} \quad (4.8)$$

Where v_{bo} is the fundamental value of the basic wind velocity, c_{season} is the season factor and c_{dir} the directional factor. c_{dir} and c_{season} are taken as 1 unless in national annex other values are recommended. In EC1-4, v_{bo} is the fundamental value of the basic wind velocity and is defined as "the characteristic 10 minutes mean wind velocity, irrespective of wind direction and time of year, at 10 m above ground level in open country terrain with low vegetation such as grass and isolated obstacles with separations of at least 20 obstacle heights". By taking $c_{dir} = c_{season}$, we obtain:

$$v_b = v_{bo} \quad (4.9)$$

In investigated test building basic wind velocity is assumed as $v_b = v_{bo} = 37,4\ m/s$ and $c_r(z) = 0.2343 \ln(z)$, as calculated in (4.6), which by substitution in (4.7) we obtain:

$$v_m(z) = 0.2343 \cdot v_b \cdot \ln(z) \quad (4.10)$$

This equation shows that mean wind velocity varies logarithmic with height. It has been assumed that there is no such a high building as this investigated test building in the neighborhood thereby recommendations 4.3.4 and 4.3.5 of EC1-4 hasn't be considered.

4.6 Wind Turbulence

Wind turbulence intensity $I_v(z)$ is a factor which is used in calculation of peak velocity pressure and is defined in EC1-4 clause 4.4 as standard deviation of the turbulence divided by the mean wind velocity.

$$I_v(z) = \frac{\sigma_v}{v_m(z)} \quad \text{for} \quad z_{min} \le z \le z_{max} \quad (4.11)$$

Where σ_v is defined in EC1-4 as:

$$\sigma_v = k_r . v_b . k_l \tag{4.12}$$

k_l is turbulence factor recommended as 1, the other parameters are defined before. With substitution of values from given structure:

$$I_v(z) = \frac{0,2343 v_b}{0,2343 v_b . \ln(z)} = \frac{1}{\ln(z)} \tag{4.13}$$

4.7 Peak Velocity Pressure

Wind pressure in EC1-4 is defined in Eq. (4.8) which considers mean and short-term velocity fluctuations and is named as *peak velocity pressure*.

$$q_p(z) = \left[1 + 7 \cdot I_v(z)\right] \cdot \frac{1}{2} \rho \cdot v_m^2(z) = c_e(z) \cdot q_b \tag{4.14}$$

Where, ρ is the air density, $c_e(z)$ is the exposure factor which is defined in section 4.5 of EC1-4. The recommended value for air density is 1,25 kg/m^3. By substitution of air density if we need an SI pressure unit like KN/m^2 we should divide it by 1000. We calculate our pressure function by using wind turbulence, after substitution of values from Eq. (4) and (5), gives:

$$q_p(z) = \left(0,0342 Ln^2(z) \cdot v_b^2 + 0,239 Ln(z) v_b^2\right) \times 10^{-3} \tag{4.15}$$

4.8 Wind Pressure Acting On Building

Peak velocity pressure function is used for calculation of pressure acting on surface of structure along the building height. By multiplication of $c_{pe}(z)$ (pressure coefficient for external pressure) with $q_p(z)$, wind pressure w_e is obtained which afterwards is required for calculation of wind forces acting on the building. There is two kind of pressure coefficient, $c_{pe,10}(z)$, $c_{pe,1}(z)$. $c_{pe,10}(z)$ is used for design of overall load bearing system of structure and is define for loaded area of 10m^2. $C_{pe,1}$ is defined for loaded area of 1m^2 which is used in cladding design and local effects. After multiplying wind pressure with influence height of story slab we obtain line loads. We deliver these line forces on the edge of our floor slabs. Wind pressure w_e is defined in section 5.2 of EC1-4 as follow:

$$w_e = q_p(z_e) \, . \, c_{pe} \tag{4.16}$$

Where, z_e is the reference height for the external pressure described in Section 7 of EC1-4 for high-rise building. If $h > 2b$, the distribution of pressure is considered as in Figure 4.3.

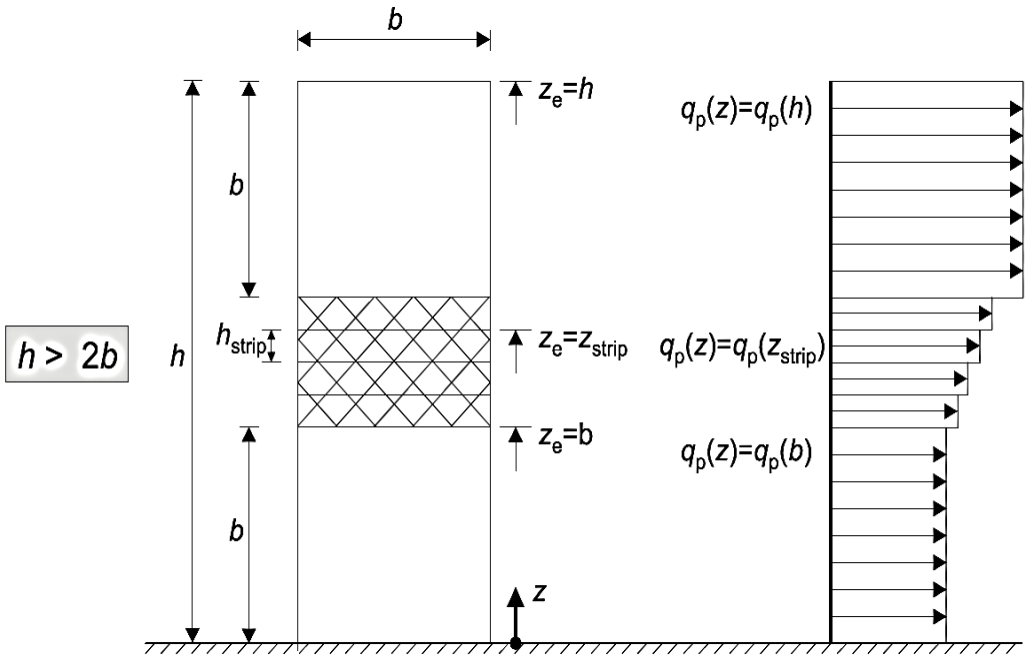

Figure 4.3: Assumption of EC1-4 for pressure distribution over height [1]

Height of investigated test building is h=160.35m, from building dimensions and with considering of wind blowing direction two cases can be taken into account as below:

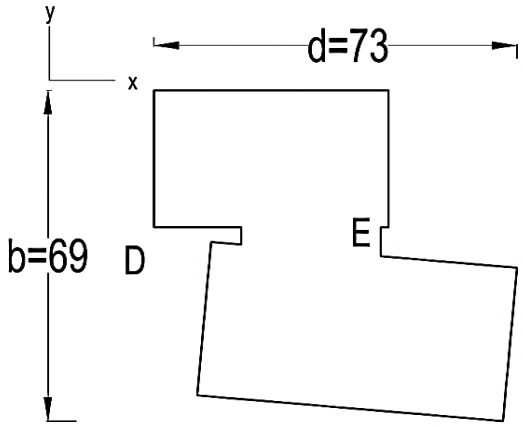

Figure 4.4: Pressure zones and dimensions in wind from both x and y directions

- For wind blowing in x direction:

$$e = Min\{b,\ 2h\} = Min\ \{69, 2\times 160.35\} = 69$$
$$d = 73,\ e = 69 < d,\ h/d = 2.196 < 5$$

External pressure coefficients for zones E, D is extracted from table 7.1 of EC1-4. The other zones on both sides of building parallel to wind direction have same pressure coefficients and areas. These pressures act in opposite direction on either

side of building and compensate the global effect of each other. Pressure zones A, B, C are important for local effect and cladding design. For other values of h/d which don't coincide with the given values of table 7.1 of EC1-4 a linear interpolation have been used.

	A	B	C	D	E
$C_{pe,10}$	-1.2	-0.8	-0.5	0.8	-0.56

Table 4.2: Pressure coefficients for wind blowing in x direction

- For wind blowing in y direction:

$$e = Min\{b,\ 2h\} = Min\{73,\ 2\times 160.35\} = 73$$

$$d = 69\ ,\ e = 73 < d = 69\ ,\ h/d = 2.31 <\ 5$$

The same procedure is done for y direction, but with this deference that in y direction there is no C pressure zone. Due to figure 7.5 of Ec1-4 when $e > d$, there is only two pressure zones A and B.

h/d values are almost same for both direction for this reason the $C_{pe,10}$ for y direction is taken the same as x direction:

	A	B	D	E
$C_{pe,10}$	-1.2	-0.8	0.8	-0.56

Table 4.3: Pressure coefficients for wind blowing in y direction

4.9 Structural Factor $c_s c_d$

Structural factor considers this fact that the peak wind pressures on the surface (c_s) and the effect of the vibrations of the structure due to turbulence (c_d) don't occur simultaneously [1]. $c_s c_d$ can be taken into account separately as a size factor (c_s) and a dynamic factor (c_d) but for this purpose it should be referred to national annex whether these two parameters should be treated separately or not.
Example test structure doesn't satisfy the requirements of 6.2 in [EC1-4] therefor structural factor should be calculated based on procedure mentioned in section 6.3 of [EC1-4] as below:

$$c_s c_d = \frac{1 + 2k_p . I_v(z_s)\sqrt{B^2 + R^2}}{1 + 7 . I_v(z_s)} \tag{4.17}$$

Where:

z_s reference height, see figure 4.6 ;

k_p peak factor, defined as the ratio of the maximum value of the fluctuating part of the response to its standard deviation;

I_v the turbulence intensity defined;

B^2 background factor, allowing for the lack of full correlation of the pressure on the structure surface;

R^2 the resonance response factor, allowing for turbulence in resonance with the vibration mode.

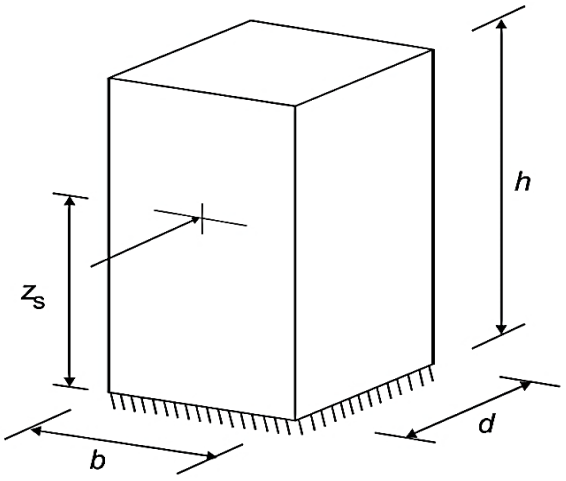

$z_s = 0.6h \geq z_{\min}$

Figure 4.5: Definition of reference height [1]

4.10 Background Factor

The background factor allows for the lack of full correlation of the pressure on the structure. The background factor B^2 could be calculated from annex B of [EC1-4] as below:

$$B^2 = \frac{1}{1+0,9\left(\frac{b+h}{L(z_s)}\right)^{0,63}} \tag{4.18}$$

where

b, h are the width and height of the structure, see figure 4.6;

$L(z_s)$ is the turbulent length scale at reference height.

$L(z_s)$ is defined as below [1]:

$$L(z_s) = L_t.\left(\frac{z_s}{z_t}\right)^{\alpha} \qquad \text{for} \qquad z \geq z_{\min} \;,\; z_t = 200 \tag{4.19}$$

and represents the average gust size for natural wind. This formula is valid for height up to 200 m as a reference height where is designated by Z_t and a reference length scale of $L_t = 300$ m. Parameter α is defined as $\alpha = 0,67 + 0,05\,Ln(z_0)$ where z_0 is the roughness length in meter and $z_{\min}$ is given in table 4.1 of [1].

Background factor is calculated for given building in both directions as below:

	b [m]	h [m]	z_0 [m]	$z_{\min}$ [m]	z_s [m]	α	$L(z_s)$ [m]	B^2
x direction	69	160,35	0,05	10	96,21	0,52	205,05	0,508
y direction	73	160,35	0,05	10	96,21	0,52	205,05	0,506

Table 4.4: Calculated background factor for both direction and related parameters

From results it is obvious that there is not a big difference between background factors in x and y direction because there is no big difference between dimensions of building in both directions.

4.11 Resonance Response Factor

Resonance response factor R^2 allows for turbulence in resonance with the consideration of vibration mode of the building and is expressed in [1] as:

$$R^2 = \frac{\pi^2}{2\delta}.S_L\left(Z_s, n_{1,x}\right).R_h\left(\eta_h\right).R_b\left(\eta_b\right) \tag{4.20}$$

Where:

δ is the total logarithmic decrement of damping;

S_L is the non-dimensional power spectral density function;

R_b, R_h are the aerodynamic admittance functions.

Two Eqs. (4.21) and (4.22) are given in [1] evaluating R_b, R_h for a fundamental mode shape as:

$$R_h = \frac{1}{\eta_h} - \frac{1}{2\eta_h^2}\left(1-e^{-2.\eta_h}\right) \qquad R_h = 1 \quad \text{for} \quad \eta_h = 0 \tag{4.21}$$

$$R_b = \frac{1}{\eta_b} - \frac{1}{2\eta_b^2}\left(1-e^{-2.\eta_b}\right) \qquad R_b = 1 \quad \text{for} \quad \eta_b = 0 \tag{4.22}$$

with

$$\eta_h = \frac{4.6h}{L\left(z_s\right)}.f_L\left(z_s, n_{1,x}\right) \quad \text{and} \quad \eta_b = \frac{4.6b}{L\left(z_s\right)}.f_L\left(z_s, n_{1,x}\right) \tag{4.23}$$

$f_L\left(z,n\right) = \frac{n.L\left(z\right)}{v_m\left(z\right)}$ is a non-dimensional frequency which is determined with n equal to natural frequency of structure in Hz, mean velocity $v_m\left(z\right)$ and the turbulence length scale $L\left(z\right)$ defined before. Non-dimensional power spectral density function $S_L\left(z,n\right)$, is defined in [1] as:

$$S_L\left(z,n\right) = \frac{n.S_v\left(z,n\right)}{\sigma_v^2} = \frac{6{,}8\,f_L\left(z,n\right)}{\left(1+10{,}2.f_L\left(z,n\right)\right)^{5/3}} \tag{4.24}$$

and shows wind distribution over frequencies. The parameters above have been calculated and are shown in table below:

	$f_L\left(z_s,n_1\right)$	$S_L\left(z_s,n_1\right)$	η_h	η_b	R_h	R_b
x direction	0.943	0.125	3.391	1.466	0.251	0.462
y direction	0.943	0.125	3.391	1.544	0.251	0.448

Table 4.5: Power spectral density function and related parameters

The logarithmic decrement of damping δ used in resonance response factor formula for fundamental bending mode is defined as below [1]:

$$\delta = \delta_s + \delta_a + \delta_d \tag{4.25}$$

where:

δ_s Logarithmic decrement of structural damping, values from table F.2 of [EC1-4];

δ_a Logarithmic decrement of aerodynamic damping for the fundamental mode;

δ_d logarithmic decrement of damping due to special devices (tuned mass dampers, sloshing tanks etc.).

δ_a for alongwind vibration can be determined as below [1]:

$$\delta_a = \frac{c_f . \rho . b . v_m(z_s)}{2 n_1 . m_e} \tag{4.26}$$

where

c_f is the force coefficient for wind action in the wind direction;

n_1 natural frequency of structure;

m_e equivalent mass per unit length of the fundamental mode shape defined in section (F.4) of [EC1-4];

ρ the air density;

b width of building;

$v_m(z_s)$ wind mean velocity defined befor.

This formula considers the modal deflection, for each height level constant. The expression is valid when there are no dissipative devices attached to the structure. Otherwise δ_a should be calculated with proper theoretical and experimental methods.

The force coefficient c_f for rectangular section with the wind blowing perpendicularly to the structural part is given as [1]:

$$c_f = c_{fo} . \psi_r . \psi_\lambda \tag{4.27}$$

where

c_{fo} is the force coefficient of rectangular sections with sharp corners and without free-end;

ψ_r is the reduction factor for square sections with rounded corners. ψ_r depends on Reynolds number, and could be found from figure 7.24 of [1];

ψ_λ is the end-effect factor for elements with free-end flow as defined in section 7.13 of [1].

The end-effect factor ψ_λ should be determined as a function of slenderness ratio λ, the effective slenderness λ is defined in table 7.16 of [1]. Values for this parameter can be extracted from the same table. ψ_λ is also dependent on solidity ratio φ where is given by Expression (7.28) of [1]. ψ_λ considers the reduced resistance of

the structure due to the wind flow around the end. Parameter ψ_r depends on corner radius and is equal to 1 when there is no rounded edge. Mentioned parameters have been determined and tabulated as below:

	c_{fo}	λ	φ	r	ψ_λ	ψ_r	c_f
x direction	2.183	3.24	1	0	3.24	1	1.421
y direction	2.11	3.075	1	0	0.623	1	1.367

Table 4.6: Force coefficients for x and y directions

Equivalent mass of structure is also needed to be determined for calculation of Eq. (4.26). The formula used for evaluating equivalent mass is described in [1] as below:

$$m_e = \frac{\int_0^{\ell} m(s).\Phi_1^2(s)\,ds}{\int_0^{\ell} \Phi_1^2(s)\,ds} \tag{4.28}$$

where:

m is the mass per unit length;

ℓ is the height or span of the structure or the structural element;

i = 1 is the mode number.

the total mass is derived from computer model of test structure and divided by height to give mass per unit length. The fundamental flexural mode $\Phi_1(z)$ of cantilever buildings could be evaluated by using Eq. (F.13) of [EC 1-4] which is expressed as:

$$\Phi_1(z) = (\frac{z}{h})^{\zeta} \tag{4.29}$$

Where:

ζ : is a parameter depends on structural system

In test building consisting of cores and peripheral columns ζ is equal to 1.

The fundamental frequency of structure can be evaluated approximately as below[1]:

$$n_1 = \frac{46}{h} \text{ [Hz]} \tag{4.30}$$

where h is the height of the multi-story building with a height over 50 m. Since a computer analysis has been made for the test structure the fundamental frequency from this analysis have been used. Eq. (F.2) gives the fundamental frequency equal to $n_1 = 0,287$ [Hz] and from computer analysis $n_1 = 0,184$ [Hz], for the rest of calculations the second value is used. Calculated values for δ_a in both directions are tabulated below:

	c_f	b [m]	ρ [kg/m^3]	$v_m(z_s)$ [m/s]	n_1 [Hz]	m_e [kg/m]	δ_a
x direction	1.421	69.3	1.25	40.02	0.184	1799671	0.00744
y direction	1.367	73	1.25	40.02	0.184	1799671	0.00753

Table 4.7: Values of δ_a in both directions

Since there is no damping device in our test structure the logarithmic decrement of damping δ_d is zero and logarithmic decrement of structural damping δ_s from [1] is equal to 0.1. From these parameters the logarithmic decrement of damping δ in both directions is calculated as below:

	δ_a	δ_s	δ_d	δ
x direction	0.007144	0.1	0	0.1074
y direction	0.00753	0.1	0	0.1075

Table 4.8: Logarithmic decrement of damping

After obtaining required parameters now the resonance response factor could be calculated. From Eq. (4.20) we have:

	R^2
x direction	0.666
y direction	0.644

Table 4.9: Resonance response factor values in both directions

4.12 Peak Factor

The peak factor k_p, is the ratio of the maximum value of the oscillating part of the response to its standard deviation, and is given in Expression (4.31) [1] . The variation of k_p against $\nu.T$ is shown in Figure 4.7.

$$k_p = \sqrt{2Ln(\nu.T)} + \frac{0.6}{\sqrt{2Ln(\nu.T)}} \tag{4.31}$$

where:

ν is the up-crossing frequency given as below

T is the averaging time for the mean wind velocity, T = 600 seconds.

Up-crossing frequency should be obtained from expression (B.5) of [EC1-4] as:

$$\nu = n_{1,x}\sqrt{\frac{R^2}{B^2 + R^2}} \quad ; \quad \nu \geq 0.08Hz \tag{4.32}$$

ν is natural frequency of structure, and other parameters are defined before.

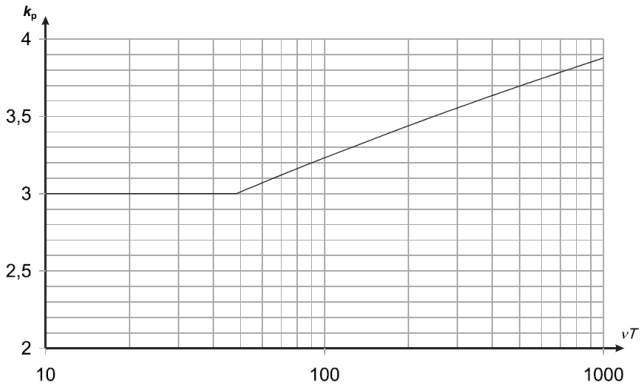

Figure 4.6: Peak factor [1]

The peak factor is calculated for both directions:

	ν	k_p
x direction	0.139	3.175
y direction	0.138	3.173

Lastly the structural factor can be determined from Eq 6.1 as:

	B^2	R^2	$I_v(z_s)$	k_p	$c_s c_d$
x direction	0.508	0.668	0.219	3.175	0.990
y direction	0.506	0.647	0.219	3.173	0.984

Calculating of structural factor is an iterative procedure since we don't know the exact mass of the structure at the first stages of design and it is calculated based on assumptions. After some cycle of designing the values of structural factor and structural elements dimensions converges to their final values, alternatively structural factor can be taken as 1 that in some cases depending on dynamical characteristics could be conservative.

4.13 Wind Forces

Blowing wind with a specific velocity causes pressure on surfaces which in turn results in force acting on surface. Due to EC1-4 part 5.3, wind forces can be calculated in two ways:

- Using force coefficient c_f.
- Using surface pressure w_e.

4.13.1 Wind Forces Using Force Coefficient

The wind force acting on the structure can be obtained directly using force coefficient from [EC1-4] as below:

$$F_w = c_s c_d . \sum c_f . q_p(z_e) . A_{ref} \tag{4.34}$$

This formula gives the whole wind force acting on structure and is not convenient for computer modeling because the distribution of wind force on the structural elements over height is lost. If we want to have the force distribution over height the force coefficient should be calculated for every story which in an irregular structure could be cumbersome. With this formula calculation of overturning moment, design forces and moments at the base is easier, and there is no need to calculate wind suction force at the leeward side of structure.

In this equation pressure at height z_e for each part due to figure 4.8 should be found.

Height z_e is chosen in a way that the whole height of pertinent story is covered at the end of each part. For this reason two parts at the beginning and end are not equal, this is done for simplicity of calculation and load distribution. This difference doesn't affect the result in considered test building and is negligible because we have almost the same dimensions in both directions. The pressure profile and height classification has been considered same in x and y directions. The calculated parameters and wind forces can be seen in table 4.10

	z [m]	$q_p(z)$ [KN/m^2]	$c_s c_d . c_f$	A [m^2]	F [KN]	F_{total} [KN]
x direction						
	69,3	2,29	1,407	4802,49	15450,69	
	89,1	2,48	1.407	1372,14	4780,81	
	160,35	2,94	1.407	4937,63	20450,16	
						40681,66
y direction						
	69,3	2,29	1,344	5058,9	15546,86	
	89,1	2,48	1,344	1445,4	4810,56	
	160,35	2,94	1,344	5201,25	20577,45	
						40934,87

Table 4.10: Wind forces using force coefficient

4.13.2 Wind Forces Using Surface Pressure

Resultant of wind forces acting on structure F_w is the vectorial sum of three components: external forces $F_{w,e}$, internal forces $F_{w,i}$ and friction forces F_{fr} which acts on structure and could be calculated by using formulas in section 5.3 of [EC1-4].
External forces:

$$F_{w,e} = c_s c_d . \sum w_e . A_{ref} \tag{4.33}$$

internal forces:

$$F_{w,i} = \sum w_i . A_{ref} \tag{4.34}$$

friction forces:

$$F_{fr} = c_{fr} . q_p(z_e) . A_{fr} \tag{4.35}$$

where:

w_e external pressure on the individual surface at height z_e, given in section 5 of

w_i internal pressure on the individual surface at height z_i, given in section 5 of [1]

A_{ref} reference area of the individual surface

c_{fr} friction coefficient derived from section 7.5 of [1]

A_{fr} area of external surface parallel to the wind, given in section 7.5 of [1]

Friction forces acts on surfaces parallel to wind direction, and could be neglected when the sum of the surfaces parallel with or at a small angle to the wind direction is equal to or less than 4 times the total area of all external surfaces perpendicular to the wind (windward and leeward) [1]. In test building this condition is satisfied and no friction forces have been considered.
Internal forces normally should be taken into account when internal pressure could change suddenly or the magnitude of forces related to these pressures are in the order that they could affect our internal partition walls or load bearing system. Common cases that these forces should be considered are normally industrial halls with large roofs or halls in which partition walls have large surface and wind pressure-changes could result in large forces on these walls. For internal forces existence of openings which the wind can blow throw and cause pressure difference is important. These openings can be in the form of doors and windows when they are open, or air conditioning channels and etc. In high-rise buildings normally the stories are completely separated from each other and no pressure-changes could be transmitted. Internal pressure has no global effect on building and in overall design of horizontal load bearing systems could be neglected.
Wind forces and pressure distribution over height is calculated for linearized strips define in section 7.2.2 of [EC1-4], table 4.11 shows these values. Pressure profile and linearization for each part in investigated given building has been illustrated in figure 4.8.

z [m]	$q_p(z)$ [KN/^{2}]	$c_s c_d$	$c_{pe,10}$ Windward	$c_{pe,10}$ Leeward	w_e Windward [KN/m2]	w_e Leeward [KN/m2]	A [m^2]	F Windward [KN]	F Leeward [KN]
x direction									
69,3	2,29	0,990	0,80	-0,56	1,829	-1,280	4802	8697,19	6088,03
89,1	2,48	0,990	0,80	-0,56	1,981	-1,387	1372	2691,11	1883,78
160	2,94	0,990	0,80	-0,56	2,355	-1,648	4937	11511,39	8057,97
								22899,70	16029,7
								$F_{total,x}$	38929,48
y direction									
69,3	2,29	0,984	0,8	-0,56	1,829	-1,280	5059	9106,02	6374,21
89,1	2,48	0,984	0,8	-0,56	1,981	-1,387	1445	2817,62	1972,33
160	2,94	0,984	0,8	-0,56	2,355	-1,648	5201	12052,50	8436,75
								23976,14	16783,3
								$F_{total,y}$	40759,44

Table 4.11: Wind forces using surface pressure coefficient

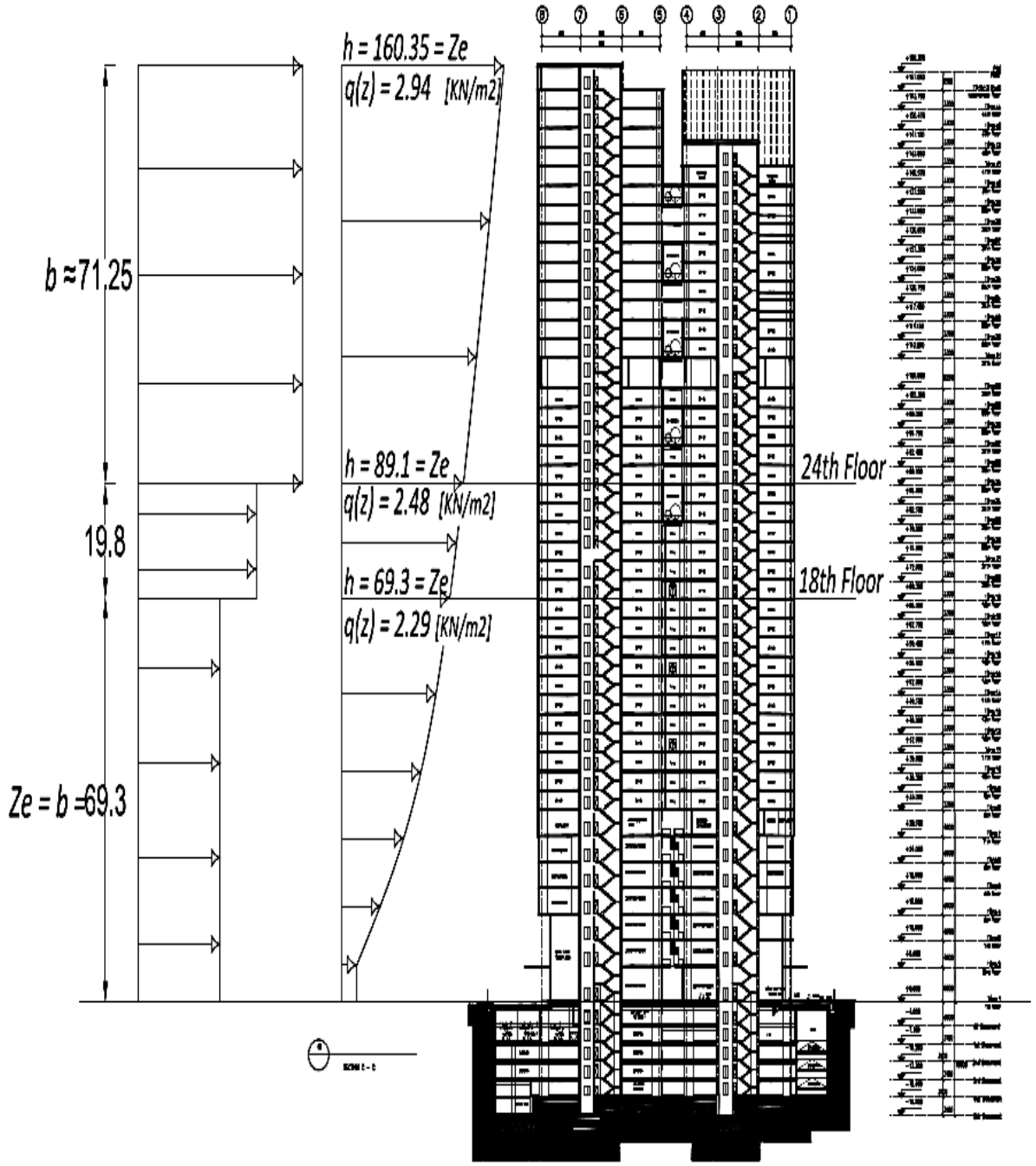

Figure 4.7: Wind Pressure profile and its classification on test building due to [EC1-4] provisions

4.13.3 Comparison of Two Methods for Wind Forces

Calculated values for wind forces based on two methods given in [EC 1-4] have been shown in table 4.10, 4.11. The difference between values of two methods in x direction is about 104 [KN] which mean force coefficient method gives a difference of only 0.3% more than the value calculated from surface pressure method. In y direction we have a difference about 1378 [KN] which in this case the difference is about 3.4% and surface pressure method gives a greater value. In both cases the difference is negligible and could be said that both methods give the same result but

for computer modeling as mentioned before the surface pressure method is more convenient because not only the global effects but also the local effect like cladding design forces can be calculated more easily. In our computer model the later method have been used.

4.14 Vortex Shedding

In civil engineering the flow of wind is simplified and assumed two-dimensional (lift force and yawing moment are of little significance) as shown in figure 4.8. This simplified wind is composed of along wind and transverse wind. The along wind is term used to show the drag forces and building behavior in the direction of wind blow and cross wind is the expression used to refer to wind in direction perpendicular or transverse to the along wind.

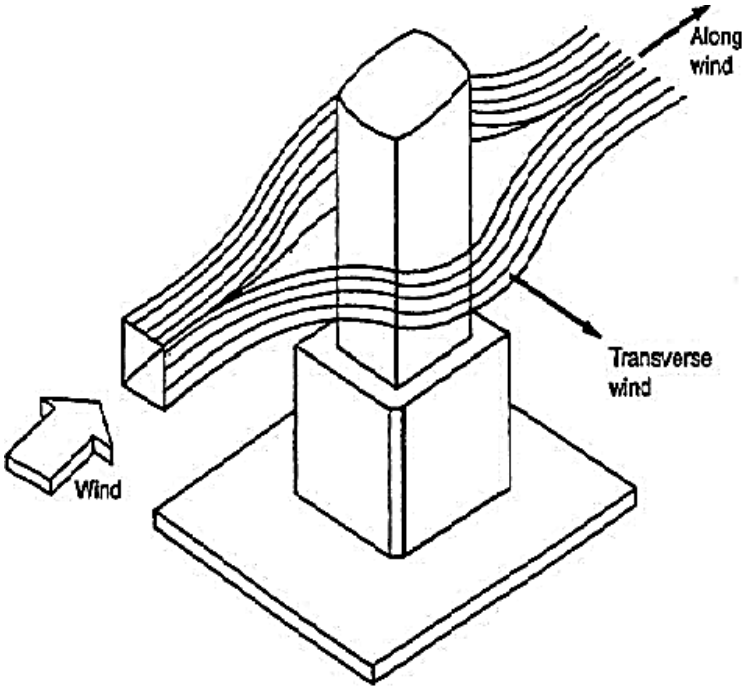

Figure 4.8: Wind streamlines and directions of along-wind and crosswind [7]

Vortex shedding is an oscillating flow that occurs when a fluid flow passes a body and parallel up-flow streamlines are displaced on either side of the building, this distortion in streamlines begins on the sides of body and results to form vortices which sheds periodically from either side to the downstream which is called the wake and depends on the shape, size and the velocity of fluid. Vortices forming are completed at the back of body causing low-pressure zones which in turn causes impulses in both directions.
At low velocities, since the shedding occurs at the same time on the both sides of the building no vibration happens. At the higher speeds, vortices are shed first from one side then from the other side alternatively. This causes impulses in both directions, the transverse impulse is applied to the left and then right alternatively [7] [8].

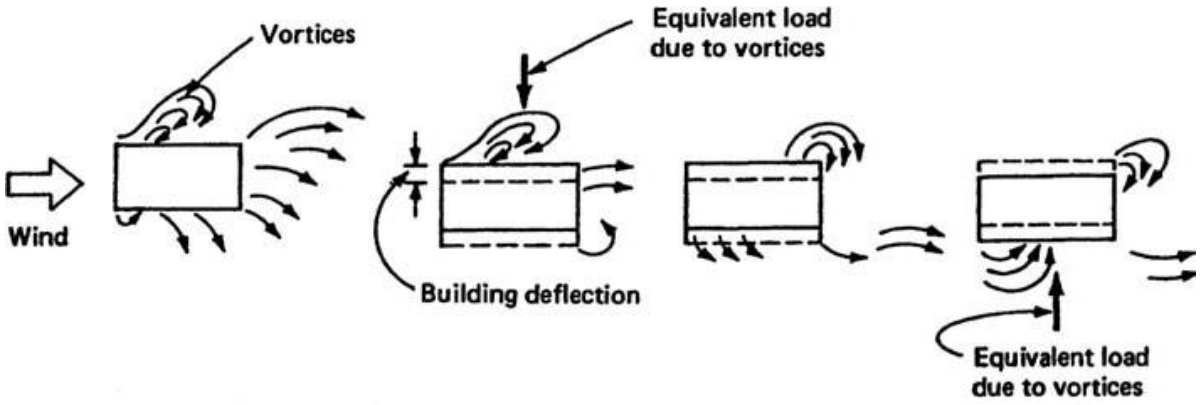

Figure 4.9: Forming and shedding of vortices and equivalent loads [7]

The frequency of along-wind impulse is twice as the crosswind impulse frequency [7]. If the frequency of vortex shedding matches the resonance frequency of the structure, the structure can begin to resonate, vibrating with harmonic oscillations driven by the energy of the flow [9]. This condition happens when the wind velocity is identical with critical wind velocity. The critical wind velocity is a frequent wind velocity for this reason the fatigue should be controlled in elements that could oscillate under vortex shedding.
The vortex shedding effect is not to be checked for structure when [1]:

$$v_{crit,i} > 1,25\, v_m \tag{4.36}$$

where:

$v_{crit,i}$ critical wind velocity for mode *i*;

v_m mean wind velocity at the cross section where vortex shedding occurs

The critical wind velocity for bending vibration mode *i* is expressed in [1] as the wind velocity at which the frequency of vortex shedding is identical with the natural frequency of the structure. This equation is shown below:

$$v_{crit,i} = \frac{b \,.\, n_{i,y}}{St} \tag{4.37}$$

b reference width of the cross-section at which resonant vortex shedding occurs and where the modal deflection is maximum for the structure or structural part considered

$n_{i,y}$ natural frequency of the considered flexural mode *i* of cross-wind vibration

St Strouhal number as defined in E.1.3.2 of [EC 1-4] and could be taken from table E.1

From table E.1 of [EC 1-4] and building dimensions the Strouhal number is determined to St = 0.12. By substituting in equation (E.2) gives:

$$v_{crit,i} = 106,25 \quad m/s \; > \; 1,25\, v_m = 55,62\, m/s \tag{4.38}$$

From these values it is obvious that vortex shedding is not relevant for this structure.

4.15 Galloping Effect

Galloping is a form of aeroelastic instability caused by negative aerodynamic damping in the cross wind direction and is a self-induced vibration of a flexible structure in cross wind bending mode [1], [9]. Non circular cross sections are prone to galloping. Ice on structural elements in cold seasons of year can cause galloping effect especially on electrical wires. Most aeroelastic instabilities occur at special wind velocities and induce dynamical motions. Galloping oscillation starts at a wind velocity equal to v_{CG} given in Annex (E) of [EC 1-4].

$$v_{CG} = 2\frac{Sc}{a_G}.n_{1.y}.b \tag{4.39}$$

where

Sc Scruton number as defined in E.1.3.3 (1) of [EC 1-4]

$n_{1.y}$ cross-wind fundamental frequency of the structure

b width as defined in Table E.7 of [EC 1-4]

a_G the factor of galloping instability from Table E.7 of [EC 1-4]

If $v_{CG} > 1,25\, v_m$ there is no need to consider the galloping effect on structure. Table 4.12 shows calculated values for galloping critical velocity and comparison with mean velocity.

δ_s	$m_{i,e}$ [kg/m]	ρ [kg/m3]	b [m]	Sc	a_G	$n_{1.y}$ [Hz]	v_{CG} [m/s]	$1,25\, v_m$ [m/s]
0,1	1799671	1,25	69	60,48	1,17	0,184	1312,58	55,63

Table 4.12: Galloping effect parameters

From table it is clear that Galloping effect is not to be considered.

4.16 Along Wind Response and Serviceability Control

Normally perception of building dynamic excitations in earthquake situations by the occupants is not a serviceability issue; insofar occupants are thankful to have survived the trauma and are less prone to complain about motion perception.
However, this issue is completely different in wind peak dynamic response of building, because windstorm return period is much less than earthquake and it can occur more frequently and is not traumatic as earthquake. Consequently, it should be checked whether the building is prone to wind-induced problems related to the comfort of the occupants.
When the response of structure to the wind action in serviceability limit state is considered, both along-wind and crosswind response should be checked. Normally the along-wind response is related to buffeting effects caused by turbulence and crosswind response is caused basically due to alternate-side vortex shedding.
In buildings which are slender about both axes, such that the geometric ratio $\sqrt{(b.d/h)}$ is less than one third, where b and d are the along-wind plan dimensions and h is building height, the crosswind response may be more important than along-wind, because the acceleration of crosswind response can exceed the along-wind response [7].
The peak acceleration is the most important criterion for building occupants comfort and it is important to be able to determine the acceleration related to peak response in both directions. Annex B and C of [Ec 1-4] gives a method for determining along-wind acceleration but there is no provided procedure for estimating of crosswind response peak acceleration. However, for this purpose the section 1.4.3 of (NBCC) code (National Building Code of Canada) can be used which provides such a procedure.

4.17 Maximum Along-Wind Acceleration

The maximum characteristic acceleration under wind action is defined in annex B of [EC 1-4] as multiplication of the standard deviation of the characteristic along-wind acceleration by the peak factor using the natural frequency as upcrossing frequency.
Due to section B.4(2) of [EC 1-4] the standard deviation $\delta_{a,x}$ of the characteristic along-wind acceleration of the structural point at height z should be determined using:

$$\delta_{a,x} = \frac{c_f . \rho . b . I_v(z_s) . v_m^2(z_s)}{m_{1,x}} . R . K_x . \Phi_{1,x}(z) \qquad (4.40)$$

where

c_f force coefficient

ρ air density

b the width of the structure, defined in Figure 6.1 of [EC 1-4]

$I_v(z_s)$ turbulence intensity at the height $z = z_s$

$v_m^2(z_s)$ mean wind velocity for $z = z_s$

z_s reference height, given in Figure 6.1 of [EC 1-4]

R square root of resonant response calculated before

K_x non-dimensional coefficient, given below

$m_{1,x}$ along wind fundamental equivalent mass, in section F.4 (1) of [EC 1-4]

$\Phi_{1,x}(z)$ is the fundamental along wind modal shape

K_x is expressed in annex B of [EC 1-4] as below:

$$K_x = \frac{(2\zeta+1)\left\{(\zeta+1)\left[Ln\left(\frac{z_s}{z_0}\right)+0.5\right]-1\right\}}{(\zeta+1)^2 Ln\left(\frac{z_s}{z_0}\right)} \quad (4.41)$$

where:

z_0 roughness length discussed before

ζ exponent of the mode shape from Annex F of [EC 1-4]

In our test building z_s is equal to 96.21m, z_0 as defined earlier is equal to 1m and ζ from section F.3 of [EC 1-4] for structures with core and peripheral columns is equal to 1. Calculated values and parameters for along-wind acceleration is shown in table x:

	K_x	k_p	$\delta_{a,x}$	a_x
x direction	1,5	3,175	0,0294	0,0933
y direction	1,5	3,173	0,0293	0,0929

Table 4.13: Parameters of standard deviation of the characteristic along-wind acceleration

A commonly used criterion is to limit the acceleration of a building's upper floors to less than 2.0% of gravity (20 mg) for a 10-year return period. The building motions associated with this acceleration are believed to not seriously affect the comfort and equanimity of the building's occupants. From result above for along wind acceleration it is obvious that the criterion is satisfied. Since for cross wind acceleration there is no provisions in EC1-4 it hasn't been checked.

5 Earthquake Loading

5.1 Seismic Actions

Periodical activities or dynamical motions inside or around the structure normally cause oscillations in structure. These vibrations are related with dynamical loads which arise in structural members. In civil engineering occurring dynamic loads, could be classified based on different point of views. One of these criteria is to characterize dynamic loads due to their time dependent behavior. They could be subdivided to: harmonic loads, periodic loads, transient loads and impulsive loads [9]. Earthquake is one of the natural phenomena which causes dynamic loads on structures and is categorized in transient load group.

5.2 Earthquake

Movement of the tectonic plates at the outer layer of earth relative to each other leads to an accumulation of strain energy. This energy is the elastic energy that is stored due to the straining of rocks, as for elastic materials. When the strain reaches its limiting value along a weak region or at existing faults or at plate boundaries, a sudden movement or slip occurs releasing the energy. This action generates elastic waves, which propagate through the elastic medium, and eventually reach the surface of the earth. Most earthquakes are produced due to slips at the faults or at the plate boundaries [23].
An earthquake is a sudden and transient movement of the earth's surface. This surface seismic motion has an acceleration which is transmitted through foundation to the structure body. Masses in the structure undergo an acceleration equal to ground acceleration which induces inertial forces equal to mass multiplied by acceleration.

Structure response to acceleration induced by earthquake is normally a dynamical nonlinear response. However, most practical earthquake design codes are based on linear analysis procedures [29].

Seismic horizontal action is assumed to have two orthogonal independent components which are represented by the same response spectrum.

5.3 Seismic Requirements

Earthquake engineering could be considered as design of seismic capacity of structure with the expected seismic demand to which they may be subjected. Due to (EN 1998-1, cl 2.1) these requirements should be met:

No collapse requirement:
This requirement declares that structure should not undergo any local or global collapse under design seismic action. Structure should maintain its integrity and residual load bearing capacity after the earthquake. This requirement is corresponding with ultimate limit states.
Damage limitation requirement:
The structure should be designed to withstand a seismic action having a higher probability of occurrence than the design seismic action, without any damage and the associated limitations of use. This requirement is checked under damage limitation states.

5.4 Ground Types

One of the important factors that affect the earthquake wave propagation and the value of ground peak acceleration or spectral acceleration and dynamical parameters is ground type. Euro code 8 classifies grounds in 7 types as A, B, C, D, E, S1 and S2; this classification is based on stratigraphic profiles and parameters like average shear wave velocity in first 30 m depth, Standard penetration test result (Nspt) for 30 cm penetration, and undrained shear strength of soil (cu). The classification can be done also by additional consideration of deep geology on the seismic action.

5.5 Importance Factors and Classes of Structures

Depending on the consequences of collapse for human life, public safety and civil protection in the immediate post-earthquake period, and on the social and economic consequences of collapse, 4 importance classes is mentioned in EN 1998-1as below. This factor is used for determination of design ground acceleration with a return period different from reference period.

Importance class	Buildings	γ_I
I	Buildings of minor importance for public safety, e.g. agricultural buildings, etc.	0.8
II	Ordinary buildings, not belonging to the other categories.	1
III	Buildings whose seismic resistance is of importance in view of the consequences associated with a collapse, e.g. schools, assembly halls, cultural institutions etc.	1.2
IV	Buildings whose integrity during earthquakes is of vital importance for civil protection, e.g. hospitals, fire stations, power plants, etc.	1.4

Table 5.1: Importance classes and importance factors [15]

5.6 Response Spectrum

The response of wide range of structures to a particular seismic action can be summarized using a response spectrum. A response spectrum is a plot of the peak response (acceleration, velocity or displacement) of a series of oscillators with single degree of freedom (SDOF) and varying natural frequency that are excited into motion by the same base vibration or impulse. This procedure can be done for different damping ratios to cover wide range of structures. The plotted result can then be used to pick off the response of any linear system, given its natural frequency of oscillation.

In another word, the response spectrum shows the peak response of an SDOF structure to a specific earthquake, as a function of natural period and damping ratio of structure.

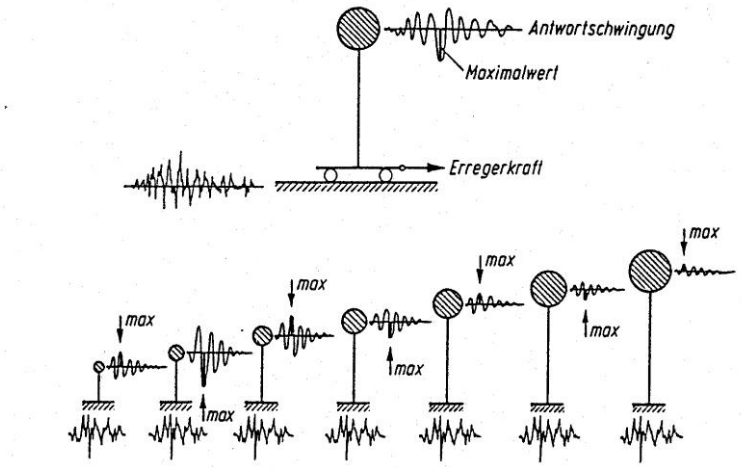

Figure 5.1: Response spectrum determination concept [30]

An important advantage of the response spectrum approach is that earthquakes that look different when represented in the time domain may actually have similar frequency contents, and result in broadly similar response spectra. For this reason the response spectrum is a useful design tool for dealing with a further earthquake whose exact nature is unknown [29].

Disadvantages of this method are, first, the peak spectral values occur with time offsets and there is no information about their angular phase shift and, second, the response spectra derived from Duhamel's integral is restricted to linear systems because it is based on principle of superposition [16] [9].

5.6.1 Elastic Response Spectrum in Euro Code 8

In EN 1998 the motion of particular point under seismic action on surface could be represented with an elastic response spectrum. For both requirements of EN1998-1 mentioned in 3.2 the shape of elastic response spectrum is taken as being the same.

Due to [EN1998-1, cl. 3.2.2.1(5)] when seismic actions are generated by widely differing sources, more than one shape of spectra could be considered to enable the design seismic action to be adequately represented, different values of a_g will normally be required for each type of spectrum and earthquake. Horizontal elastic response spectrum $S_e(T)$ due to [EN1998-1, 3.2.2.2] is defined by following expressions for earthquake action:

$$0 \le T \le T_B \ : \ S_e(T) = a_g \ . S \ . \left[1 + \frac{T}{T_B} \ . \ (\eta \ . \ 2{,}5 - 1) \right] \tag{5.5}$$

$$T_B \ \le T \le T_C : \ S_e(T) = a_g \ . S \ . \eta \ . \ 2{,}5 \tag{5.6}$$

$$T_C \le T \le T_D : \ S_e(T) = a_g \ . S \ . \eta \ . \ 2{,}5 \left[\frac{T_C}{T} \right] \tag{5.7}$$

$$T_D \le T \le 4s : \ S_e(T) = a_g \ . S \ . \eta \ . \ 2{,}5 \left[\frac{T_C T_D}{T^2} \right] \tag{5.8}$$

Where

$S_e(T)$	elastic response spectrum
T	vibration period of a linear single-degree-of-freedom system
a_g	design ground acceleration on type A ground
T_B	lower limit of the period of the constant spectral acceleration branch
T_C	upper limit of the period of the constant spectral acceleration branch
T_D	value defining the beginning of the constant displacement response range
S	soil factor
η	damping correction factor with a reference value of η = 1 for 5% viscous damping

The value of the damping correction factor η is given by the expression:

$$\eta = \sqrt{10 / (5 + \xi)} \ge 0{,}55$$

where ξ is the viscous damping ratio of the structure, in percentage. Usually ξ is taken as 5% for normal concrete structures.

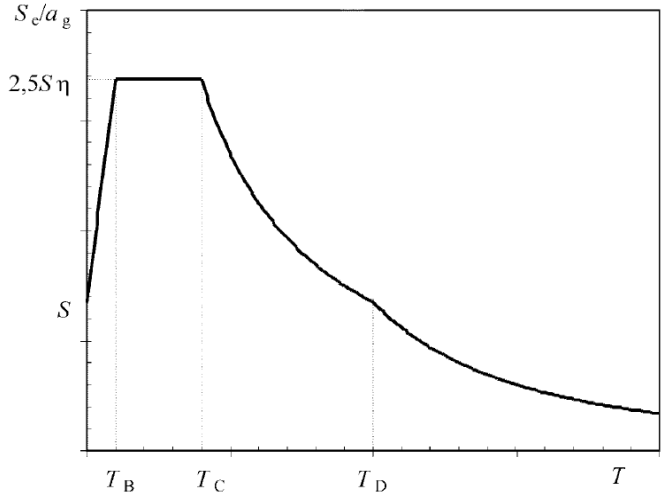

Figure 5.2: Shape of the elastic response spectrum [15]

The values of the periods T_B, T_C, T_D and of the soil factor S describing the shape of the elastic response spectrum depend on the ground type.

There are two types of spectra in Euro code 8: type 1and Type 2. If the earthquakes have a surface-wave magnitude, $M_s \leq 5.5$ it is recommended to use spectrum type 2, and if $M_s \geq 5.5$ type 1 should be used. Figure 3.3 and Figure 3.4 show the shapes of recommended Type 1 and Type 2 spectra, respectively, normalized by a_g, for 5% damping.

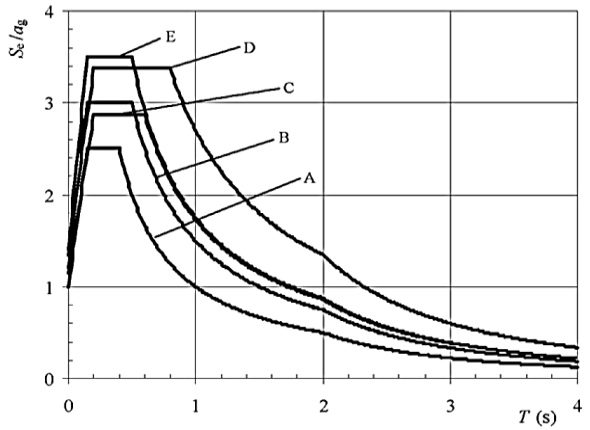

Figure 5.3: Type 1 elastic response spectra [15]

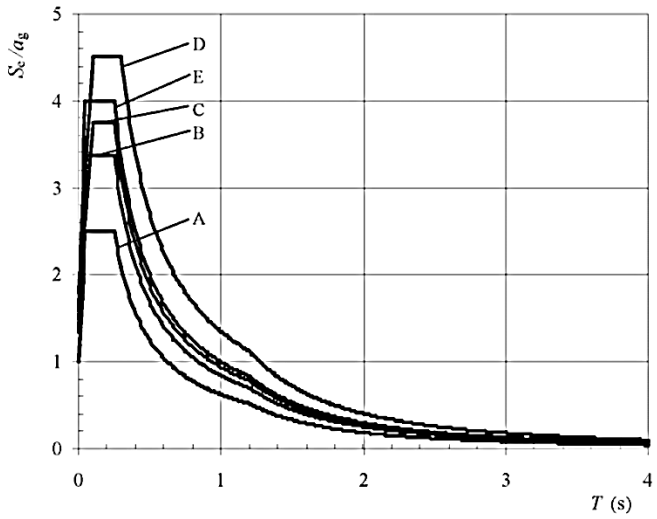

Figure 5.4: Type 2 elastic response spectra [15]

Euro code 8 considers also two types of vertical elastic response spectra for evaluation of earthquake action in vertical direction. These spectrums are given in section 3.2.2.3 of EN1998-1. If a_{vg} is greater than 0.25g (2.5 m/s^2) the vertical component of the earthquake action, as defined in 3.2.2.3 of EN 1998-1, should be considered in the cases listed below:

- for horizontal or nearly horizontal structural members spanning 20 m or more;
- for horizontal or nearly horizontal cantilevers longer than 5 m;
- for horizontal or nearly horizontal pre-stressed members;
- for beams supporting columns;
- in base-isolated structures.

5.6.2 Design Spectrum

Designing structures to remain elastic in large seismic actions seems to be uneconomic in most cases, as the force demand will be large. The ability of structures to dissipate energy in inelastic range permits their design for smaller seismic forces than is needed in elastic linear analysis. This energy dissipation occurs due to ductility of materials and developing large deformations beyond elastic range.

To make use of ductility requires non-linear response of structure, meaning that the linear methods introduced above cannot be used. To avoid this conflict a ductility-modified response spectrum is adopted by reducing the elastic response spectrum with a behaviour factor q, henceforth called a "design spectrum".

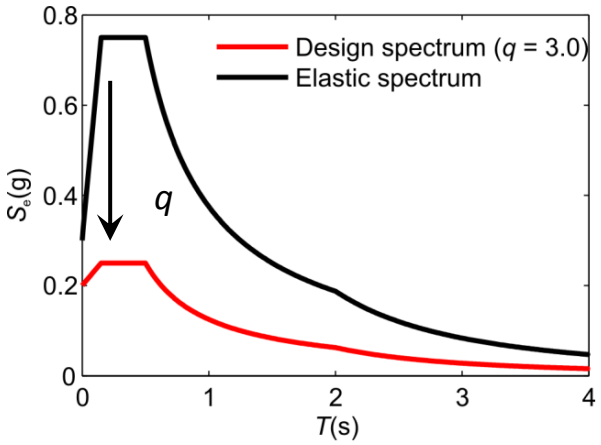

Figure 5.5: Elastic and design response spectrum [28]

Design spectrum for horizontal components of seismic action, $S_d(T)$ is expressed as below in Euro code 8:

$$0 \le T \le T_B : \; S_d(T) = a_g \,.\, S \,.\left[\frac{2}{3} + \frac{T}{T_B} \,.\, (\frac{2,5}{q} - \frac{2}{3})\right] \tag{5.9}$$

$$T_B \le T \le T_C : \; S_d(T) = a_g \,.\, S \,.\, \frac{2,5}{q} \tag{5.10}$$

$$T_C \le T \le T_D : \; S_d(T) \begin{cases} = a_g \,.\, S \,.\, \dfrac{2,5}{q} \,.\left[\dfrac{T_C}{T}\right] \\ \ge \beta . a_g \end{cases} \tag{5.11}$$

$$T_D \le T : \; S_d(T) \begin{cases} = a_g \,.\, S \,.\, \dfrac{2,5}{q}\left[\dfrac{T_C T_D}{T^2}\right] \\ \ge \beta \,.\, a_g \end{cases} \tag{5.12}$$

Where the parameters definition is as below:

$S_d(T)$	design spectrum;
q	behaviour factor;
β	lower bound factor for the horizontal design spectrum. The recommended value for β is 0,2.

For vertical components of earthquake action the design response spectrum is defined as above equations only a_g should be replaced by a_{vg} and S taken as 1.

5.7 Methods of Structural Analysis

Different methods of analysis for seismic actions are developed in recent decays. Euro coed 8 introduces and covers some of the most important methods. Basically

these methods could be used for all dynamical loads like machinery dynamic loads in industrial or residential facilities, wind, water wave, impulse and earthquake excitation loads. On a worldwide scale, current principal task of dynamical analysis is to consider the earthquake action. For this purpose a few computer programs are developed which could be used easily.

Following methods are available for dynamical analysis:

- lateral force method of analysis or Equivalent static analysis,
- modal response spectrum analysis,
- time history modal analysis,
- direct-integration time history analysis,
- non-linear static analysis.

5.7.1 Modal Response Spectrum Analysis

Modal analysis, or the mode-superposition method, is a linear dynamic-response procedure which determines and superimposes free-vibration mode shapes to obtain displacement patterns. Mode shapes display the configurations into which a structure will naturally deform. Lateral deflection patterns are typically, of primary concern.

A structure with N degrees of freedom has N corresponding mode shapes. Each mode shape is an independent and normalized displacement pattern which is superimposed in modal analysis to create the final displacement pattern, as shown in Figure 5.6 [17].

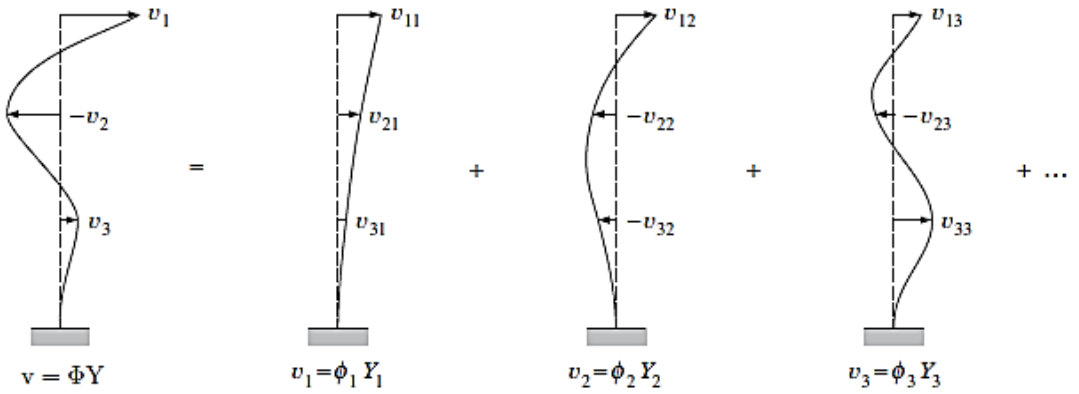

Figure 5.6: Representing deflections as sum of modal components [17].

For a multi degree of freedom (MDOF) system first the equation of motion is written for lumped masses at storey levels in building. This set of equations is then transformed to a matrix form as below (for the given formulas in this section and their derivations could be referred to [9] [16] [17] [18] [19] [29]):

$$\mathbf{m}\ddot{\mathbf{u}}(t) + \mathbf{c}\dot{\mathbf{u}}(t) + \mathbf{k}\mathbf{u}(t) = \mathbf{p}(t) \tag{5.14}$$

Where

$\mathbf{m}$	is the mass matrix (diagonal matrix);
$\mathbf{c}$	damping matrix;

$\mathbf{k}$ stiffness matrix (symmetric about main diagonal);

$\mathbf{p}(t)$ loading vector;

$\mathbf{u}(t)$, $\dot{\mathbf{u}}(t)$, $\ddot{\mathbf{u}}(t)$ displacement, velocity and acceleration vectors, respectively.

An N-DOF system can oscillate in n different modes, each having a unique shape and occurring at particular natural frequency (or period). These modal shapes are system properties and independent from external loading pattern. To calculate natural frequencies of associated mode shapes of system it is helpful to consider the free undamped oscillation problem as below:

$$\mathbf{m}\ddot{\mathbf{u}}(t) + \mathbf{k}\,\mathbf{u}(t) = 0 \tag{5.15}$$

This equation has a solution in trigonometric function form:

$$\mathbf{u}(t) = \phi_n(A_n \cos\omega_n t + B_n \sin\omega_n t) \tag{5.16}$$

Where

ϕ_n is the mode shapes;

A_n, B_n are constants;

ω_n is circular natural frequency.

Substituting Eq. (5.16) in Eq. (5.15) gives:

$$(\mathbf{k} - \omega_n{}^2\mathbf{m})\phi_n = 0 \tag{5.17}$$

Solution of Eq. (5.17) gives n circular natural frequencies $\omega_1, \omega_2, ..., \omega_i, ..., \omega_n$ each associated with mode shape ϕ_i. After determining the natural frequencies and mode shapes the response of structure to the applied load is analyzed. Eq. (5.14) involves n coupled equations in terms of n degrees of freedom. To solve this equation the principle of modal superposition is used, which states that any set of displacement can be expressed as a linear combination of modal shapes:

$$\mathbf{u} = \phi_1 Y_1 + \phi_2 Y_2 + \phi_3 Y_3 + ... + \phi_n Y_n = \sum_{i=1}^{n} \phi_i Y_i \tag{5.18}$$

Y_i are called normal coordinates or generalized coordinates, which are the oscillation amplitude of corresponding eigenmodes. Transformation of equations of motions into a set of the modal displacements rather than the original degrees of freedom is feasible by using Eq. (5.18). After a few mathematical operations on Eq. (5.14) and using Eq. (5.17) gives:

$$\mathbf{M}\ddot{\mathbf{Y}} + \mathbf{C}\dot{\mathbf{Y}} + \mathbf{K}\mathbf{Y} = \mathbf{P}(t) \tag{5.19}$$

Where

$\mathbf{Y}$ is generalized coordinate vector;

$\mathbf{M}$ is generalized mass;

$\mathbf{C}$ is generalized damping;

$\mathbf{K}$ is generalized stiffness;

$\mathbf{P}(t)$ is generalized load.

From orthogonality property of the modes, it turns out that $\mathbf{M}$, $\mathbf{C}$ and $\mathbf{K}$ are diagonal matrices, so that the n equations in Eq. (5.19) are uncoupled, i.e. each mode acts as an SDOF system and is independent of other modes. Each line of Eq. (5.19) in uncoupled form, with replacing of general load pattern with ground excitation acceleration could be written as below:

$$M\ddot{Y} + C\dot{Y} + KY = \alpha_i \ddot{u}_g(t) \tag{5.20}$$

and by analogy to a damped SDOF system:

$$\ddot{Y}_i + 2\xi\omega_i\dot{Y}_i + \omega_i^2 Y_i = \frac{\alpha_i}{M_i}\ddot{u}_g(t) \tag{5.21}$$

where

$$\alpha_i = \sum_{j=1}^{n} m_j \phi_{ij} \tag{5.22}$$

$$M_i = \sum_{j=1}^{n} m_j \phi_{ij}^2 \tag{5.23}$$

Here i and j refer to mode shapes and degrees of freedom in structure respectively. M_i is modal mass and α_i an earthquake excitation factor which represent the extent to which the earthquake tends to excite response in mode i. Since Eq. (5.21) can be solved to give Y_i as a time function for each mode, it is more rational to use the response spectrum method. For each mode we can read the spectral acceleration, S_{ei}, corresponding to that mode's natural period and damping. This is the peak response of an SDOF system to the ground acceleration $\ddot{u}_g(t)$ with period T_i. Breaking a MDOF system into separate modes results in ground acceleration being scaled by factor α_i / M_i. Structural response will also be scaled by the same amount while the system is linear, from this it is obvious that the acceleration amplitude in mode i is $(\alpha_i / M_i).S_{ei}$ and the maximum acceleration of DOF j in mode i is:

$$\ddot{u}_{ij}(\max) = \frac{\alpha_i}{M_i} S_{ei}\phi_{ij} \tag{5.24}$$

Similarly for displacements:

$$y_{ij}(\max) = \frac{\alpha_i}{M_i\omega_i^2} S_{ei}\phi_{ij} \tag{5.25}$$

Horizontal force on mass j in mode i could be found with multiplying acceleration by mass:

$$F_{ij}(\max) = \frac{\alpha_i}{M_i} S_{ei} \phi_{ij} m_j \tag{5.26}$$

and total horizontal force or base shear in mode i could be calculated by summing all story forces to give:

$$F_{bi}(\max) = \frac{\alpha_i^2}{M_i} S_{ei} \tag{5.27}$$

The ratio (α_i^2 / M_i) is called *effective modal mass.* It is the amount of mass participating in structural response in a specific mode. To determine the overall response of structure, Eq. (5.24) to Eq. (5.26) should be applied to each mode and then the results should be combined. There are as many modes as there are degrees of freedom; therefore combination of modes could be a long process which using of computer aided structural analysis seems to be inevitable.

The response of all vibration modes contributing significantly to the global response should be considered. This requirement seems to be satisfied due to EC8, when so many modes has been taken into account that the sum of effective modal masses is at least 90 percent of total structural mass, or all modes with an effective modal mass greater than 5 percent have been included.

Disadvantage of this method is that the peak values of each mode occur with a time offset and there is no information about their phase relationship therefore combination formulas used for superposition of modes delivers only probable peak value of total investigated quantity. Figure 5.7 shows this phenomenon.

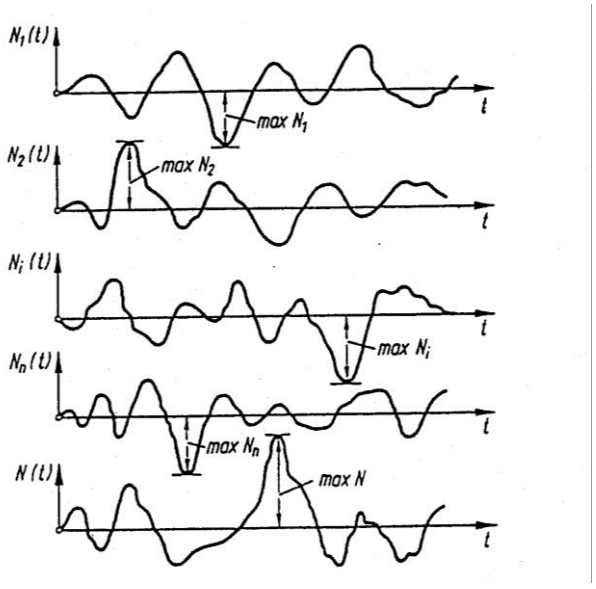

Figure 5.7: Superposition of modes and phase shift between them [30]

5.7.2 Combination of Modes

Response spectrum modal analysis gives only the peak value of each mode, and it's unlikely that these peaks occur at the same point in time. Simple combination rules are available to give an estimate of the total response. Different combination rules are available in literatures which only two combination methods SRSS and CQC are introduced by EC8. Some of other methods are: GMC, Absolute sum, NRC ten percent and NRC double sum method.

5.7.2.1 SRSS Method

If the difference in natural period between any two modes is less than 10 percent of longer mode or in another word if periods T_i and T_j satisfy (with $T_j \leq T_i$) the condition $T_j \leq 0,9T_i$ then these modes may be taken as independent of each other and the following formula could be used [15]:

$$N = \sqrt{\sum_{i=1}^{n} N_i^2} \tag{5.28}$$

Where

N is the seismic action effect under consideration (force, displacement, etc.);

N_i is the value of this seismic action effect due to the vibration mode i.

Square Root of Sum of Squares or abbreviated SRSS method does not take into account any coupling of the modes and modal damping does not affect the results. If the natural frequencies of different modes are too close together and above mentioned condition could not be satisfied, the results of this method could differ considerably from time history method and is not more reliable, in this case other combination methods should be used.

5.7.2.2 CQC Method

If the independency of modes mentioned in SRSS method is not satisfied the *Complete Quadratic Combination* technique for calculating the periodic response could be used. This method is described in [33] and is the default method of modal combination.

The CQC method considers the statistical coupling between closely-spaced modes caused by modal damping and calculates a correlation coefficient between two modes. Coupling between closely-spaced modes increases if the modal damping increases. This method degenerates to the SRSS method if the damping is equal to zero for all modes [31].

In [33] suggested formula for estimating the total response is expressed as:

$$N = \sqrt{\sum_{i=1}^{n}\sum_{j=1}^{n} N_i \rho_{ij} N_j} \tag{5.29}$$

Where N_i and N_j are the peak responses in the i th and n th modes and ρ_{ij} the correlation coefficient for these two modes; ρ_{ij} varies between 0 and 1 and ρ_{ij} = 1 for $i = n$. If there is adequate difference between earthquake duration and fundamental frequency and also if the spectrum is enough smooth the term for correlation factor ρ_{ij} could be written as:

$$\rho_{ij} = \frac{8\sqrt{\xi_i \xi_j \left(\xi_i + r\xi_j\right) r^{3/2}}}{\left(1-r^2\right)^2 + 4\xi_i \xi_j r\left(1+r^2\right) + 4\left(\xi_i^2 + \xi_j^2\right) r^2} \tag{5.29}$$

With

$r = \omega_j / \omega_i$

ξ_i , ξ_j = modal damping ratios of modes i and j

For equal modal damping $\xi_i = \xi_j = \xi$ this equation simplifies to:

$$\rho_{ij} = \frac{8\xi^2 \left(1+r\right) r^{3/2}}{\left(1-r^2\right)^2 + 4\xi^2 r\left(1+r\right)^2} \tag{5.30}$$

For structures with well-separated natural frequencies the coefficient ρ_{ij} vanishes.

5.8 Accidental Torsional Effects

In most seismic codes accidental torsional effects are taken into account by considering an additional torsional moments about the vertical axis which should be added to dynamic analysis result. A few reasons for the inclusion of accidental torsion are as follow [31], [15]:

- Torsional ground motion possibly subjecting the structure to rotation about the vertical axis.
- Spatial variation of the seismic motion.
- Uneven distribution of live-load mass during lateral loading.
- Variation between computed and actual values of structural properties.

In order to account for this effect due to Eurocode 8, as first step the calculated center of mass at each floor *i* shall be considered as being displaced from its location in each direction by an eccentricity equal to 5% of floor dimension perpendicular to the direction of seismic action.

$$e_{ai} = \pm 0,05 L_i \tag{5.36}$$

where

e_{ai} is the accidental eccentricity of storey mass i , applied in the same direction at all floors;

L_i the floor-dimension perpendicular to the direction of the seismic action.

At the second step torsional moment is calculated as:

$$M_{ai} = e_{ai} . F_i \tag{5.37}$$

where

M_{ai} is the torsional moment applied at storey i about its vertical axis;

e_{ai} accidental eccentricity of storey mass i as defined before

F_i horizontal force acting on storey i, derived from structural analysis

In a spatial structural model, the accidental torsional effects is determined as the envelope of the effects resulting from the application of static loadings, consisting of sets of torsional moments M_{ai} about the vertical axis of each storey *i* [15]. It should be noted that floor diaphragms must be rigid, otherwise torsional effects are not substantial.

6 Modeling and Analysis

6.1 Structural Model

A three-dimensional finite element model is used. The program ETABS is used for analysis and modeling purposes (CSI 2013. ETABS, Integrated Building Design Software, Computers & Structures Inc. Berkeley). The origin of coordinate system is considered at the corner of basement periphery walls which is shown in figure 6.1. Building has been modeled in two stages. First a preliminary model was made from given architectural design based on preliminary structural system described in section 2.2. Analyses were performed to obtain forces and displacements to compare with Euro codes requirements. Since this model did not satisfied the displacement, drift and strength requirements, structural system have been improved with adding beams in y direction. Improved structural system is described in next section.

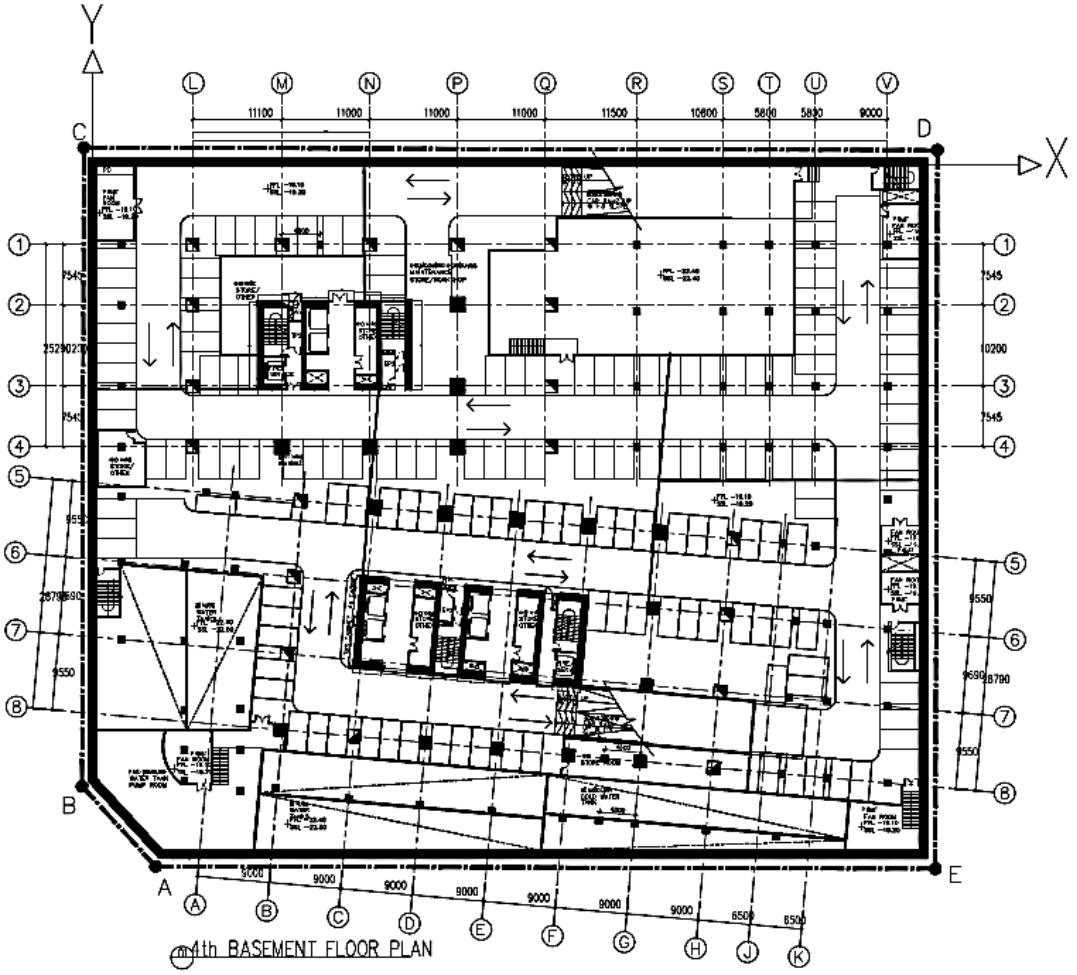

Figure 6.1: Model coordinate system

The primary specifications of structural model are as follow:

- Floor slabs are modeled as thin-shell elements. For in-plane behavior rigid diaphragm property is assigned. With this assignment floor slab experience only rigid body motion in plane of slab and lateral forces is distributed due to these in-plane translational and rotational displacements. Out of plane forces are determined as normal for design purpose.
- Columns are modeled as line elements. In preliminary model they have been modeled as pinned and in the improved model as fixed elements in frames.
- Shear walls and basement periphery walls are modeled as thin-shell elements. Walls are generally not designed for out of plane bending to avoid excessive longitudinal reinforcement. For this purpose, the stiffness of shear walls is modified in a way that they don't attract forces in direction perpendicular to their plane. To reach this aim, their stiffness perpendicular to their plane is multiplied by 0.01.
- Beams in improved model are modeled as line elements by assigning their corresponding T-shape for internal beams and L shape for edge beams. Effective widths of beams are calculated according to (EN1992-1-1, cl.5.3.2.1).
- All elements are asumed fully fixed in foundation.
- Rigid offset for the interconnecting beams and columns elements are not taken into account.
- Masses and moments of inertia of each floor are lumped at centers of masses (EN 1998-1, cl 4.3.1(4)).
- Glass facade is not considered in this model.
- The accidental torsional effects are taken into account; this moment acts about the vertical axes and is equal to horizontal seismic action multiplied by accidental eccentricity (EN 1998, cl 4.3.3.3.3). This eccentricity is equal to 0.05 of the floor-dimension perpendicular to the direction of the seismic action according to (EN 1998, cl 4.3.2).
- Car ramps in basement levels are not modeled in this stage of design. In this step we are concerned only about lateral load bearing system.

Two 3D views of structural model are shown in figures 6.2a and b. figure 6.2a includes all structural elements and figure 6.2b illustrates only cores. Figure 6.2 c and d shows the mesh pattern of hole structure and cores respectively.

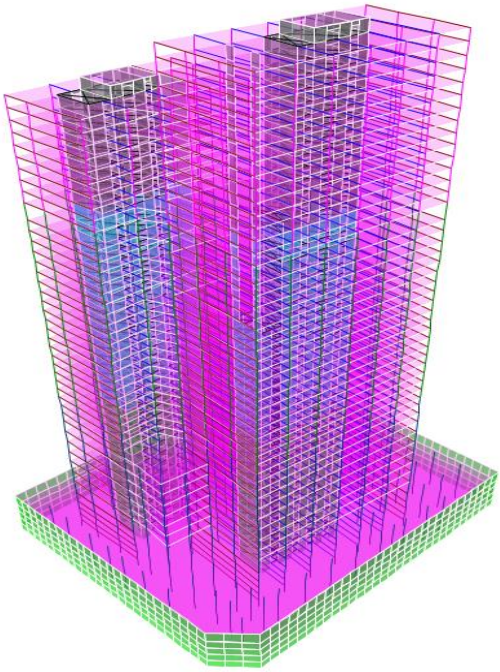

(a)

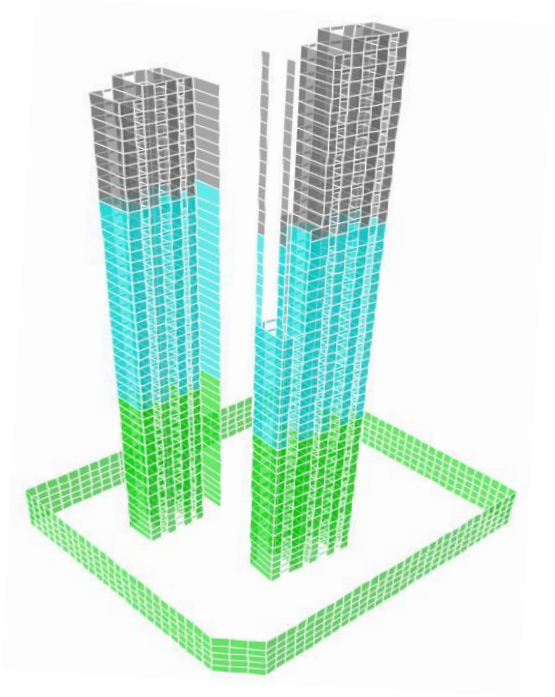

(b)

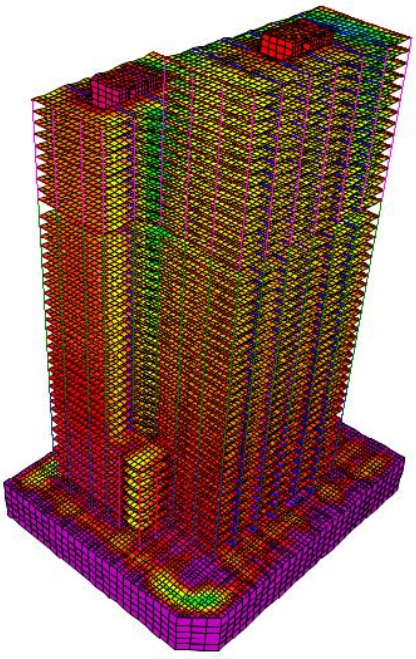

(c)

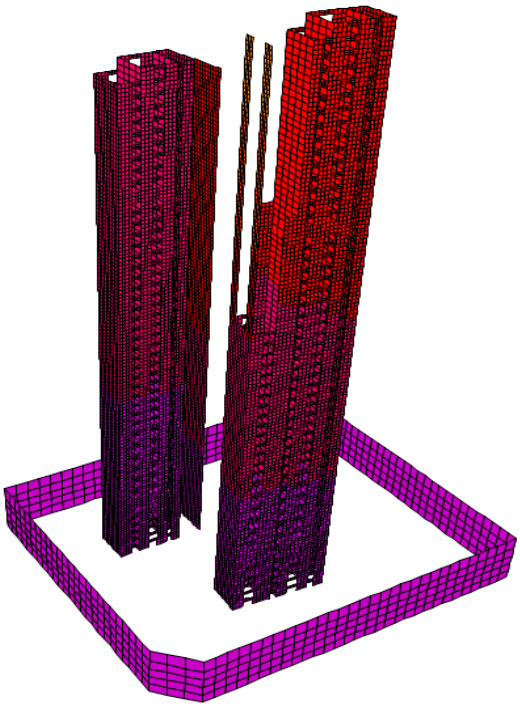

(d)

Figure 6.2: a) 3D view of structural elements; b) shear wall system; (c) analysis mesh of building; (d) analysis mesh of cores

6.2 Preliminary Analysis

A linear elastic analysis based on simple assumption for model parameters was performed for structure to see the behavior and the range of displacements, inter-story drifts and element internal forces. Structural system was composed of cores with periphery and middle columns. From the first analysis results it was made clear that the system is flexible in y direction and the drifts and displacements exceeds the requirements of Euro codes. Model has been improved to mitigate displacements and drifts which are described in next section.

6.3 Improved Structural System

In structures in which the flexural behavior dominates, the flexural displacement contribution in overall horizontal displacement is high. Core structures have flexural deflection mode acting as a cantilever, fixed at foundation and free at the other end. Frame structures have a shear deflection mode; this specification makes them be able to withstand lateral loads with less horizontal displacement at top. One of the mitigation measures to control the horizontal displacements in core structures could be the combination of the flexural deflection mode with shear deflection mode, by adding frames to preliminary system and forming a dual system.

Preliminary structural system was consisted of only cores as lateral load bearing system with a flexural deflection mode. To decrease the drifts and horizontal displacements, beams in Y direction were added later to form frames. These frames are coupled with shear walls at axes C, D, F, N and P, which compose wall-frame systems. Axes L, Q, B, G, H comprise only frames without shear walls. Additionally, a partition wall of sanitary rooms in axis P between axes 2 and 3 at tower 2 is changed to shear wall, this conversion doesn't distort the plan layout and is acceptable from architectural aspect. The columns at these two axes (P-2, P-3) are omitted, also columns at axes P-1 and P-4 are connected to shear wall through beams to have a wall-frame system. Additionally, to gain more stiffness in Y direction the columns at axes L, Q, B, H are rotated 90 degree in a way that have more moment of inertia about Y axes. To withstand high axial forces at internal columns and reducing drifts, Column dimensions and wall thicknesses are increased. Core wall layout has been changed and for more efficiency, the exterior flange walls are thicker and act as I flanges in tension and compression. The web walls, in contrast, are thinner and have 40 cm thickness to some shear forces. Table below summarize sizes of shear walls and columns.

Stories	Columns dimensions (cm)	*Core walls width* (cm)	
		Flange wall	Web wall
3rd basement to 15	150x90	60	40
16to 35	130x70	50	40
36 to 45	80x60	40	40

Table 6.1: Shear walls and typical column sizes

These changes are shown in figure 6.3 in comparison with an unchanged plan. As a typical floor plan story 21 is chosen for illustration purpose.

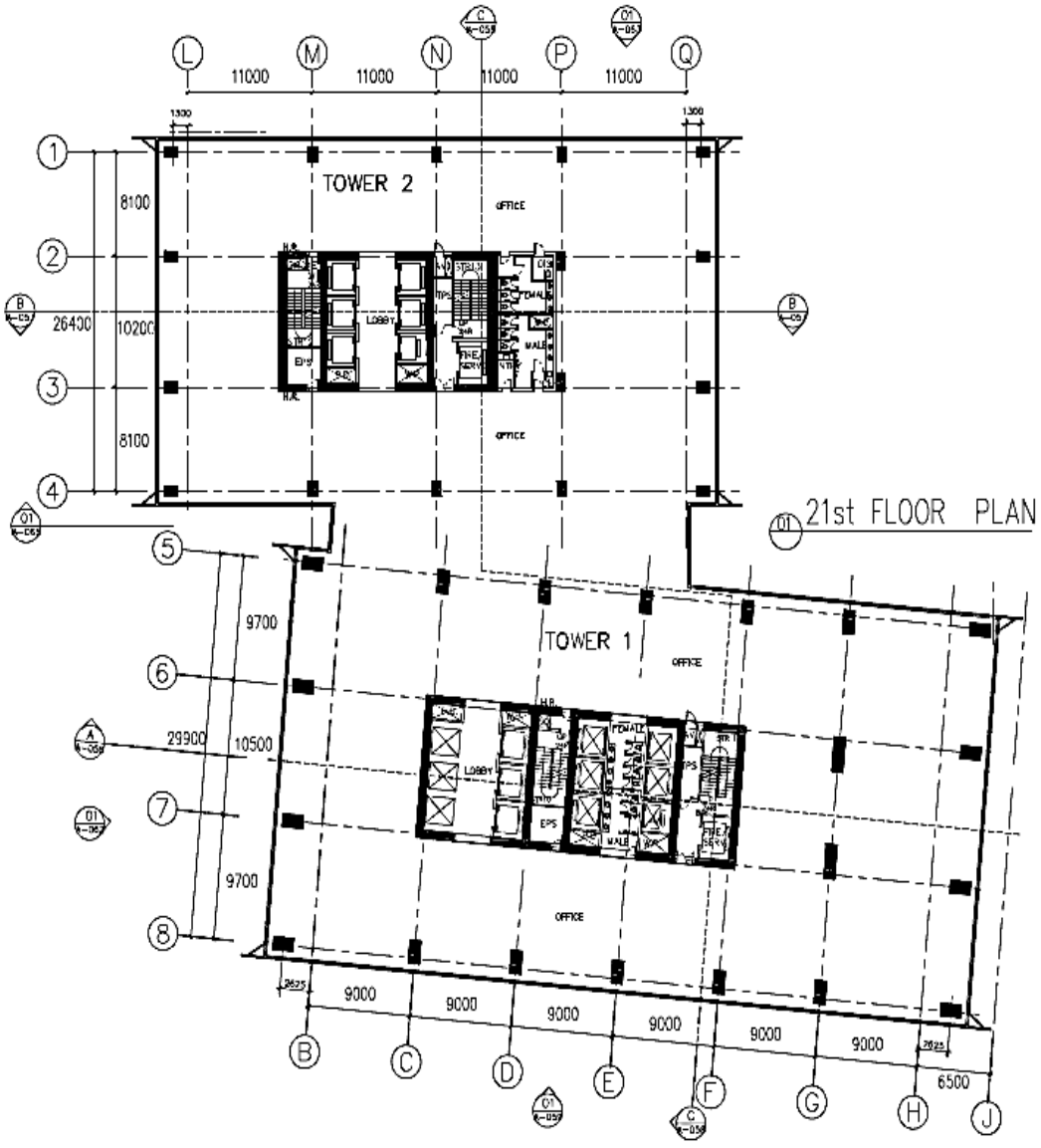

(a)

Figure 6.3(a): System without beams

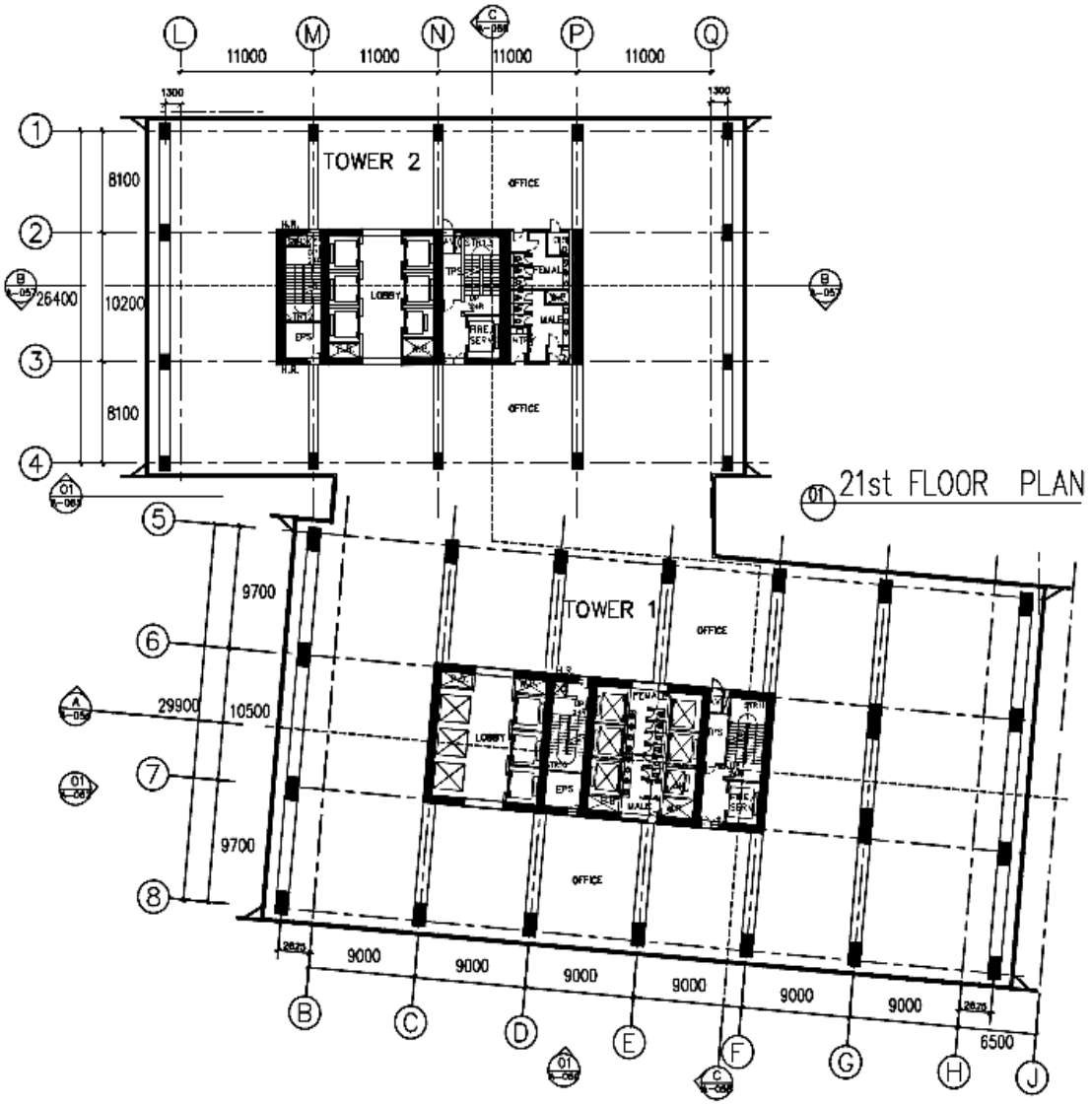

(b)

Figure 6.3(b): Stiffening the system in Y direction with beams and rotated columns

Figure 6.3: (a) System without beams; (b) Stiffening the system in Y direction with beams and rotated columns

6.4 Model Parameters

In this section parameters required for structural model is described. Most of parameters are necessary for dynamic analysis input of model. Earthquake engineering parameters are taken from EC 8, wind loading parameters from EC 1-4, parameters needed for gravity loading from EC 1-1 and material properties from EC 2. Some of important parameters are listed below.

6.5 Material Properties

Because of high axial loads in internal columns and to get more slender sections at lower stories concrete C70/85 is used. The corresponding modulus of elasticity amounts to E_{cm} = 41 GPa (EN 1992/Table 3.1). Poisson's ratio is taken equal to υ = 0 for cracked concrete and equal to υ = 0.2 for uncracked according to EN 1992 cl. 3.1.3(4). Steel BSt 500 Class B is used.

Effect of cracking is considered in structural elements (EN 1998-1, cl. 4.3.1(6)). When no accurate analysis of the cracked elements is performed, the elastic flexural and shear stiffness properties of concrete may be taken to be equal to one-half of the corresponding stiffness of the uncracked elements (EN 1998-1, cl 4.3.1(7)). It means that the moment of inertia and shear area of the uncracked section were multiplied by factor 0.5. Also the torsional stiffness of the elements has been reduced. Torsional stiffness of the cracked section was set equal to 10% of the torsional stiffness of the uncracked section. These modification factor only affect the analysis properties, they do not affect the design properties.

6.6 Effective Widths of Beams

The effective widths of beams b_{eff} were calculated according to EN 1992, cl. 5.3.2.1. For both tower effective widths was calculated based on their column spans, to be on the safe side, the minimum value was assigned to exterior and interior beams. A constant width was adopted over the whole span. In such a case the value of the b_{eff} applicable for the mid-span should be used (EN 1992 cl. 5.3.2.1(4)).

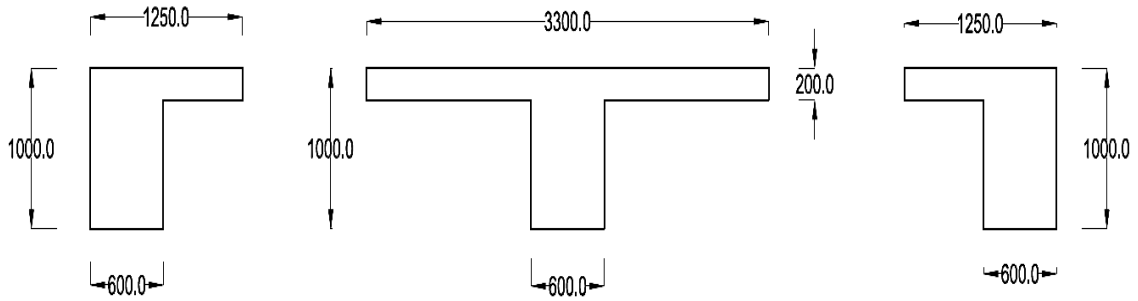

Figure 6.4: Effective widths of beams

6.7 Structural Regularity

In-plane regularity of building is checked based on section 4.2.3.2 of EC 8. From given architectural plan (figures 1.4 and 1.5) it is clear that the lateral stiffness and mass distribution of the structure is not symmetric with respect to two orthogonal principal axes. The plan configuration is not compact, i.e., each floor couldn't be delimited by a polygonal convex line. There are also some setbacks in core of tower 1 and all walls don't run without interruption from foundation to the top of building. Since all the requirements mentioned in section 4.2.3.2 should be met that the structure could be categorized as an in-plane regular structure the other requirements is not checked and investigated building is classified as in-plane irregular structure.

Regularity of building in elevation is checked due to criteria mentioned in section 4.2.3.3 of EC 8. Since we have unsymmetrical setbacks in some parts of plan from 8^{th} story to the up and also tower 1 is higher than tower 2 about 13m and also two towers are separate in some stories the building is assumed as irregular in elevation.

6.8 Structural Analysis Method

Table 4.1 of EC 8 gives analysis method for different levels of regularity. For more regular buildings also analysis of planner models is permitted which dependent on regularity, proper analysis method could be chosen. As investigated building is a high-rise building with irregular plan which higher modes could contribute significantly in structural behavior, more accurate method should be used. For this purpose multi modal response spectrum method is used which is applicable for all kinds of structures.

The results from modal analysis should be combined to get a final result. In the case of high-rise buildings there is always considerable number of modes and it is more probable that the natural periods of theses modes locate very closely together and mode dependency mentioned in 5.8.3.1 may not be satisfied (which is the case as will be shown in the results). For considering the modal dependency, CQC method which is more accurate combination method is used. Since we have the same response spectrum (without scaling) in both directions, directional combination of modes could be performed based on SRSS method but here we have used 30% rule, which apples 30% of the action from other direction. 40 modes have been considered in modal analysis. Modal analysis results in both horizontal directions were combined by 30% rule (EN 1998-1).

6.8.1 Seismic Parameters

As first parameter ground type was chosen from table 4.1of EC8 for construction site ground with consideration of a medium soil condition, hence ground type C is assigned. Since this building is a high-rise commercial and residential building the

collapse of such a structure is associated with serious consequences therefore the importance class III with corresponding importance factor 1.2 is considered.

For analysis purpose spectrum type 1 (M_s > 5.5) is used. The values of the periods T_B, T_C, T_D and of the soil factor S, which describe the shape of the elastic response spectrum, amount to T_B = 0.2 s, T_C = 0.6 s, T_D = 2.0 s and S = 1.15. Design ground acceleration was given as a_g =0.12g. The damping ratio is taken as 5% as for normal structures. For the design of the building the design response spectrum is used (i.e. elastic response spectrum reduced by the behaviour factor q). Determination of the behaviour factor q, which depends on the type of the structural system, regularity in elevation and plan, and ductility class, is described later.

6.8.2 Seismic Mass

Euro code 8 states that the masses to be used in a seismic analysis for calculating the inertial effects of the design seismic action, should be those associated with the load combination:

$$\sum G_{k,j} + \psi_{E,i} . Q_{K,i} \tag{6.1}$$

where $\psi_{E,i}$ is the combination coefficient for variable action i. $\psi_{E,i}$takes into account the likelihood of the variable load not being present over the entire structure during the earthquake. These coefficients could also account for a reduced participation of masses in the motion of the structure when they are not rigidly connected to the structure.

The combination coefficients $\psi_{E,i}$ for determination of the effects of the seismic actions shall be calculated from the following expression:

$$\psi_{E,i} = \varphi . \psi_{2,i} \tag{6.2}$$

With consideration of office category for building type from table 4.2 of EC8, parameter φ = 0,5 and $\psi_{2,i}$ = 0,3. With substituting of parameters in Eq. (6.2) gives: $\psi_{E,i}$ = 0,15. This coefficient is used in (6.1) for seismic mass definition.

6.8.3 Ductility Class

Two ductility classes are introduced in EC 8 for high seismicity areas, DCM (Ductility class medium) and DCH (ductility class high) depending on their hysteretic dissipation capacity. Both classes are enable to develop stable mechanisms associated with large dissipation of hysteretic energy under repeated reversed loading, without suffering brittle failures. The choice between two classes depends on costs and economical considerations, regional construction skill level and ductility demand. It is worth noting that the EC 8 DCH requirements for concrete are rather onerous and unlikely to be achieved with the construction skills available [29]. For

steel structures, DCH designing is likely to be more feasible. Investigated building is designed for DCM.

6.9 Structural Type and Torsional Rigidity

Due to EC 8 structural systems are classified into different types according to their behaviour under horizontal seismic actions. This classification is then used for determination of behavior factor which represents the ductility and energy dissipation amount of the structure. Structural types mentioned in EC 8 are as below:

1) frame system;
2) dual system (frame or wall equivalent);
3) ductile wall system (coupled or uncoupled);
4) system of large lightly reinforced walls;
5) inverted pendulum system;
6) torsionally flexible system.

The first four system types (i.e. frame, dual and wall systems of both types) should have a minimum torsional rigidity that satisfies expression (2.3) in both horizontal directions [15].

$$r_x \geq l_s \quad \text{and} \quad r_y \geq l_s \tag{6.3}$$

where

r_x is “torsional radius”; and

l_s is the radius of gyration of the floor mass in plan (square root of the ratio of (a) the polar moment of inertia of the floor mass in plan with respect to the center of mass of the floor to (b) the floor mass).

Due to EC8 section 4.2.3.2 in single storey buildings the torsional radius r_x (r_y) is defined as the square root of the ratio of the global torsional stiffness K_M to the global lateral stiffness in one direction $K_{Fx,i}$($K_{Fy,i}$).

$$r_{x,i} = \sqrt{\frac{K_{M,i}}{K_{Fx,i}}} \quad \text{and} \quad r_{\mathrm{y},i} = \sqrt{\frac{K_{M,i}}{K_{Fy,i}}} \tag{6.4}$$

EC 8 doesn’t provide any procedure for determining center of stiffness and torsional stiffness for example in case of core structures. In multi-storey buildings only approximate definitions of the center of stiffness and torsional radius are possible [15]. When the center of rigidity is subjected to lateral loading, the floor diaphragm will undergo only translational displacement. Other levels are free to translate and rotate since behavior is coupled both in plan and along height [31]. As a structural property, center of rigidity is independent of loading. Coordinate of center of rigidity for each floor is reported in program ETABS, but the torsional radius should be determined.

The procedure for obtaining of the torsional and lateral stiffness is similar to that for the determination of structural eccentricity [28]. Three static load cases are defined

for the highest storey level of typical stories, and loads are represented by F_{Tx}, F_{Ty} and M_T, respectively the forces and moment are applied in the center of stiffness. The torsional and lateral stiffness for both directions are calculated as below

$$K_{M,i} = \frac{1}{R_{z,i}(M_{T,i}=1)} \qquad K_{Fx,i} = \frac{1}{U_{x,i}(F_{Tx,i}=1)} \qquad K_{Fy,i} = \frac{1}{U_{y,i}(F_{Ty,i}=1)} \tag{6.5}$$

where $R_{z,i}(M_{T,i}=1)$ is the rotation of the storey i about the vertical axis due to unit moment M_T, $U_{x,i}(F_{Tx,i}=1)$ is the displacement at storey level i in direction x due to unit force F_{Tx} and $U_{y,i}(F_{Ty,i}=1)$ is the displacement in direction y due to unit force F_{Ty}.

The test structure has 4 different types of storeys, therefore 12 static load cases were defined in the 7th, 22nd, 39th, 44th, (highest storey floor levels of each type). If the torsional rigidity requirement of these storeys are satisfied other storeys under these storeys also passes this check. Values F_{Tx}=F_y=10^6 kN and M_T=10^6 kN.m were used as unit loads.

The radius of the gyration of the floor mass (l_s) should also be calculated. It is defined as the square root of the ratio of the polar moment of inertia of the floor mass in plan to the floor mass. Calculated values for torsional rigidity check and related values for test structure are tabulated:

Level	$U_{x,(FTx)}$ [m]	$U_{y,(FTy)}$ [m]	$R_{z,(MT)}$ [rad]	K_{Fx} [kN/m]	K_{Fy} [kN/m]	K_{MT} [kN.m/rad]	r_x	r_y	l_s
44	6.325	11.392	5.7E-05	1.58E+05	8.78E+04	2E+10	447	333	17.67
39	4.388	8.213	3.7E-05	2.28E+05	1.22E+05	3E+10	471	344	24.48
22	1.109	2.096	1.2E-05	9.02E+05	4.77E+05	8E+10	418	304	24.48
7	0.660	0.272	2.0E-06	1.52E+06	3.68E+06	5E+11	368	574	24.86

Table 6.2: The displacements and rotation due to F_{TX} = F_{TY} = 10^6 kN and M_T= 10^6 kN.m, the torsional (K_M) and lateral stiffness in both directions (K_{FX}, K_{FY}), torsional radius (r_x, r_y) and radius of gyration of the floor mass l_s

Obtained values in table 6.3 shows clearly that torsional radius in both directions is much higher than required and the structure is not flexible in torsion.

6.10 Behavior Factor

When designing structures for consideration of non-linear seismic response, a variety of analysis methods are available. The simplest and most widely used approach is to use the linear analysis methods, but with design forces reduced on the basis of a single, global behavior factor, q. Ec8 gives recommended values of q

for common structural forms. This approach is suitable for regular structures, where inelasticity can be expected to be reasonably uniformly distributed.

Procedure for calculating q is given in section 5.2.2.2 of EC8 as below,

$$q = q_0 . k_w \geq 1.5 \tag{6.7}$$

where

q_0 is the basic value of the behaviour factor, dependent on the type of the structural system and on its regularity in elevation

k_w is the factor reflecting the prevailing failure mode in structural systems with walls.

For buildings that are regular in elevation, the basic values of q_0 for the different structural types are given in 5.1 of EC8.

Based on EC8 recommendations, for non-regular structures in elevation the value of q_0 should be reduced by 20%.

Investigated test building is assumed as wall-equivalent dual systems which in this case due to table 5.1 of EC8, $q_0 = 3\alpha_u / \alpha_1$ in which for wall-equivalent dual, or coupled wall systems: α_u / α_1 = 1.2. Average of 1.2 value and 1,0 which is equal to 1,1 should be used in determination of q_0. From table 2.4 for dual systems and with consideration of irregularity in elevation gives:

$$q_0 = 3\alpha_u / \alpha_1 = 3 \times 1{,}1 \times 0{,}8 = 2{,}64 \tag{6.8}$$

The factor k_w reflecting the dominating failure mode in structure with walls shall be taken as follows:

$k_w =$	1,0 for frame and frame equivalent dual systems
	$(1+\alpha_0)/3 \leq 1$,but not less than 0,5 for wall, wall - equivalent and torsionally flexible systems

where α_0 is the aspect ratio of the walls of the structural system and is calculated with following expression:

$$\alpha_0 = \sum h_{wi} / \sum l_{wi} \tag{6.9}$$

Since the aspect ratio of walls in test building is very large, α_0 is taken equal to 1,0.

And therefore from equation (6.7):

$$q = 2{,}64 \tag{6.10}$$

6.11 Load Combination

The design load combinations are the various combinations of the load cases for which the structure needs to be checked. Load combinations for structural analysis and design in Ultimate limit state (ULS) are taken from EN 1990. For each critical load case, the design values of the effects of actions (E_d) could be obtained by

combining the values of actions that are considered to occur simultaneously. Combination of actions for persistent or transient design situations (fundamental combinations) is expressed as:

$$E_d = \sum_{j\geq 1} \gamma_{G,j}\, G_{K,j} \text{"+"} \gamma_P\, P \text{"+"} \gamma_{Q,1}\, Q_{K,1} \text{"+"} \sum_{i>1} \gamma_{Q,i}\, \psi_{0,i}\, Q_{K,i} \tag{6.11}$$

The combination of actions for seismic design situation is expressed as below:

$$E_d = \sum_{j\geq 1} G_{K,j} \text{"+"} P \text{"+"} A_{Ed} \text{"+"} \sum_{i>1} \psi_{2,i}\, Q_{K,i} \tag{6.12}$$

These combinations are used for Ultimate limit state (ULS). The values of the γ and ψ factors for actions is obtained from EN 1990 Annex A. Because of construction location climate, load case snow is not considered in combinations. Table A1.2(A) of EC0 is used for determination of coefficients for favorable and unfavorable design situations. If a structure is subjected to dead (D), live (L), wind (W), and earthquake (E) loads, and considering that wind and earthquake forces are reversible and should be considered in both orthogonal directions x and y, the following load combinations need to be considered if equation (6.11) and (6.12) are specified for generation of the load combinations (EC0 6.4.3):

$\gamma_{Gj,sup} D = 1{,}35D$

$\gamma_{Gj,sup} D + \gamma_{Q,1}\, L = 1{,}35D + 1.5L$

$\gamma_{Gj,sup} D \pm \gamma_{Q,1}\, W_i = 1{,}35D \pm 1.5W_i \quad , \quad i = x,y$

$\gamma_{Gj,inf} D \pm \gamma_{Q,1}\, W_i = D \pm 1.5W_i \quad , \quad i = x,y$

$\gamma_{Gj,sup} D + \gamma_{Q,1}\, L + \gamma_{Q,i}\psi_{0,i} W_i = 1{,}35D + 1.5L \pm 1{,}5 \times 0{,}6W_i \quad , \quad i = x,y$

$\gamma_{Gj,sup} D + \gamma_{Q,1}\, W_i + \gamma_{Q,i}\psi_{0,i} L = 1{,}35D + 1.5W_i + 1{,}5 \times 0{,}7L \quad , \quad i = x,y$

$D \pm 1{,}0E$

$D \pm 1{,}0E_i + \psi_{2,i} L = D \pm E_i + 0.3L \quad , \quad i = x,y$

7 Analysis Results and Design

7.1 Overview

After performing a multi-modal response spectrum analysis summary of results are shown in this chapter. The basic modal properties of the building are summarized here. Because the investigated structural system is too large it was not possible to show all internal forces graphically over the height of building in different elevations, therefore only some parts that will be designed in next chapter are illustrated graphically or tabulated. Also seismic requirements check due to EC8 and EC2 is performed and shown in this chapter.

7.2 Periods and Modal Shapes

For dynamic analysis 40 modes are considered and Ritz vectors are utilized for determining of periods and modal shapes. These values are obtained based on cracked section of members. The three fundamental periods of oscillation amount to 6.139, 4.477 and 3.412 seconds and is shown in figure 7.1. The effective masses from table 7.1 indicate that the first mode is predominantly translational in the Y direction, the second mode is translational in the X direction and the third mode is predominantly torsional. The sum of the effective modal masses amounts to more than 90% of the total mass of the structure and satisfy the requirements in EN 1998-1 cl. 4.3.3.3(3). Note that the first values of periods shows that the structure vibrates far from plateau level of response spectrum and therefore the structure is less subjected to ground acceleration.

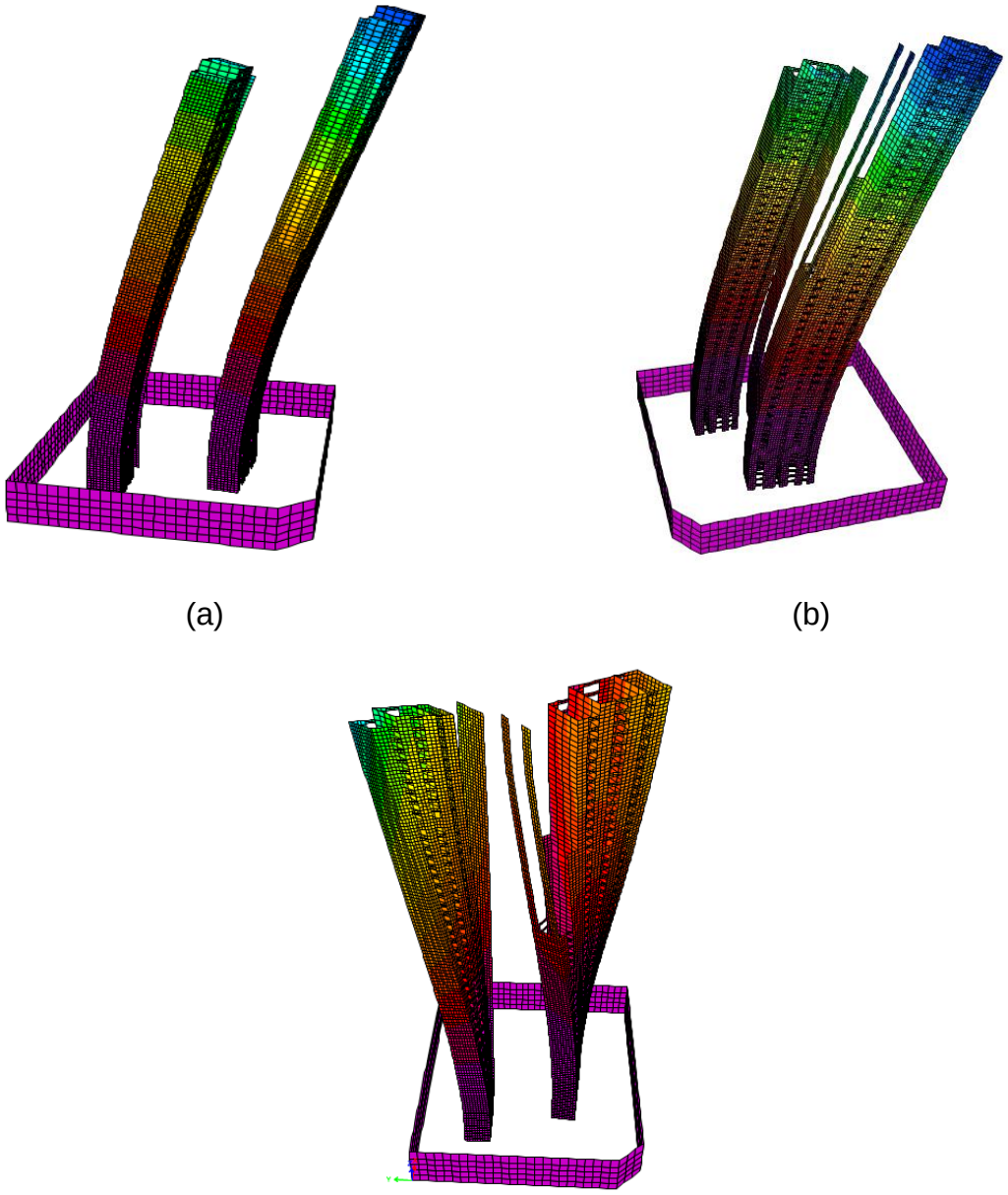

(a) (b)

(c)

Figure 7.1: First 3 modes of cores; (a) first mode translation in y direction; (b) second mode translation in x direction; (c) third mode, torsion about z axis

Mode	Period (sec)	$M_{eff,UX}$	$M_{eff,UY}$	$M_{eff,MZ}$	Sum $M_{eff,UX}$	Sum $M_{eff,UY}$
1	6.139	0.004	0.485	0.001	0.004	0.485
2	4.477	0.478	0.005	0.005	0.482	0.490
3	3.412	0.007	0.006	0.353	0.489	0.496
4	1.427	0.003	0.128	0.004	0.492	0.624
5	1.126	0.092	0.013	0.021	0.583	0.637
6	0.928	0.045	0.004	0.057	0.628	0.641
7	0.62	0.007	0.028	0.012	0.635	0.669
8	0.535	0.030	0.020	0.005	0.665	0.690
9	0.475	0.017	0.006	0.013	0.682	0.696
10	0.392	0.001	0.001	0.017	0.683	0.697
11	0.371	0.028	0.001	0.000	0.711	0.698
12	0.337	0.003	0.025	0.000	0.714	0.723
13	0.324	0.000	0.001	0.000	0.714	0.724
14	0.323	0.000	0.001	0.000	0.714	0.725
15	0.304	0.001	0.000	0.000	0.715	0.725
16	0.298	0.004	0.000	0.001	0.718	0.725
17	0.291	0.002	0.000	0.000	0.720	0.725
18	0.286	0.003	0.001	0.004	0.724	0.726
19	0.275	0.001	0.000	0.001	0.724	0.727
20	0.273	0.006	0.000	0.001	0.730	0.727
21	0.256	0.005	0.000	0.001	0.735	0.727
22	0.249	0.000	0.001	0.000	0.735	0.727
23	0.243	0.008	0.000	0.000	0.743	0.728
24	0.232	0.000	0.023	0.000	0.743	0.751
25	0.223	0.003	0.002	0.000	0.746	0.753
26	0.22	0.000	0.004	0.001	0.746	0.756
27	0.2	0.014	0.000	0.000	0.760	0.757
28	0.182	0.002	0.004	0.001	0.762	0.761
29	0.168	0.002	0.024	0.000	0.764	0.785
30	0.161	0.017	0.005	0.000	0.781	0.790
31	0.139	0.032	0.007	0.000	0.813	0.797
32	0.132	0.007	0.033	0.000	0.820	0.829
33	0.114	0.053	0.016	0.001	0.872	0.845
34	0.11	0.017	0.051	0.003	0.889	0.896
35	0.093	0.050	0.014	0.002	0.938	0.910
36	0.091	0.015	0.043	0.008	0.954	0.953
37	0.063	0.014	0.001	0.000	0.968	0.954
38	0.061	0.001	0.014	0.003	0.969	0.969
39	0.032	0.007	0.021	0.000	0.976	0.990
40	0.032	0.021	0.008	0.000	0.997	0.997

Table 7.1: The elastic periods (T), the effective masses and the effective mass moments (M_{eff})

7.3 Displacements

Obtained displacements from numerical calculation by modal response spectrum analysis are based on design response spectrum with included torsional effects. If linear analysis is performed according to EN 1998-1 (Equation 4.23) the actual displacements of the structural system (d_s) shall be calculated as a product of the behaviour factor q and the displacement of the same point. The displacements in the centers of masses (CM) are presented for both directions. Maximum displacement in seismic design situations occur under ($D+0,3.L+E_{y\ (\text{with 0,05 eccentricity})}+ 0,3E_x$) in y direction and for x direction under ($D+0,3L+E_{x\ (\text{with 0,05 eccentricity})}+ 0,3E_y$). Displacements, d_e and d_s, for this load combination are shown in Table 7.2. Naturally these displacements occur under ULS and cannot be used for SLS top displacement requirements which should be satisfied for occupants comfort. Displacement limitation for top of the building may be calculated for service loads with low period of return. Wind loads with ten year return period is used in most cases for deflection and acceleration control at top. Serviceability limit states are generally not included in building codes. Common criteria used for top deflection used in USA and Canada lies between h/500 and h/400 dependent on country. As a stringent criterion h/500 is used for wind in ULS for investigated building. Maximum top displacement for x direction occurs under load combination $D+1,5W_x$ and for y direction under load combination $D+1,5W_y$ as below, which is under limit.

Story	U_x (mm)	U_y (mm)	h/500 (mm)
45	156.5	313.3	320

It is clear that for a wind load with lower return period in SLS situation deflection limit is easily satisfied.

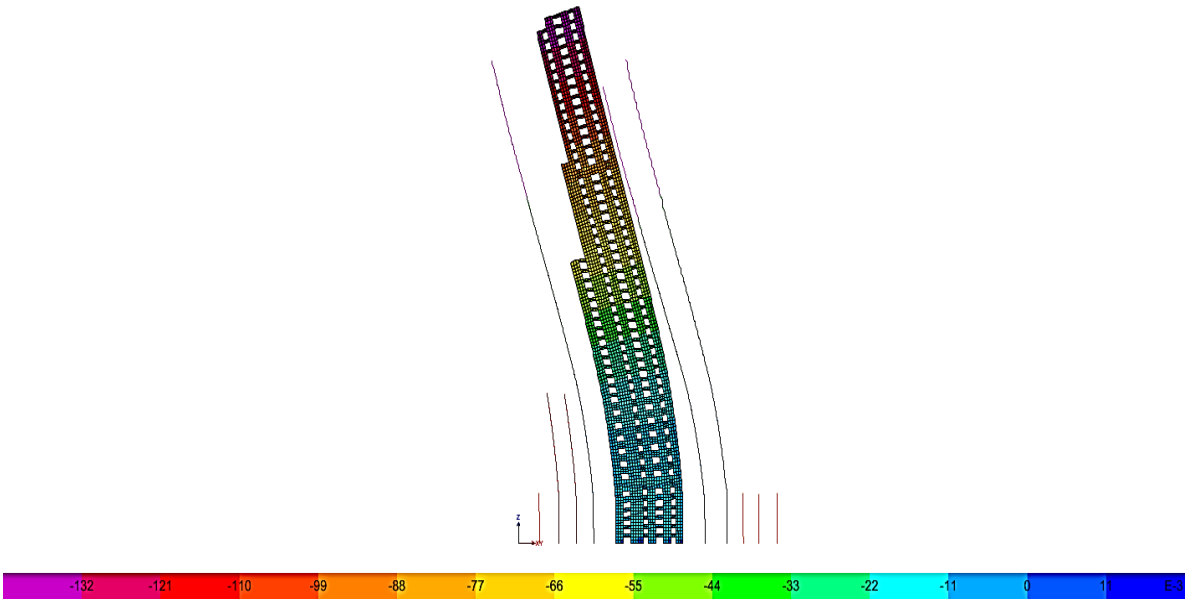

Figure7.2: Displacement of columns and core of tower 1 under design wind in elevation 7 in x direction

Story	d_{ex} (mm)	d_{ey} (mm)	q	d_{sx} (mm)	d_{sy} (mm)
45	241.60	398.7	2.64	637.82	1052.57
44	235.20	384.3	2.64	620.93	1014.55
43	229.10	375	2.64	604.82	990.00
42	223.00	365.4	2.64	588.72	964.66
41	216.70	355.8	2.64	572.09	939.31
40	210.50	346.2	2.64	555.72	913.97
39	193.20	321.7	2.64	510.05	849.29
38	180.30	319.8	2.64	475.99	844.27
37	174.80	312	2.64	461.47	823.68
36	169.10	302.7	2.64	446.42	799.13
35	163.50	293.4	2.64	431.64	774.58
34	157.80	284	2.64	416.59	749.76
33	152.10	274.7	2.64	401.54	725.21
32	146.40	265.3	2.64	386.50	700.39
31	140.80	256	2.64	371.71	675.84
30	135.20	246.6	2.64	356.93	651.02
29	129.70	237.3	2.64	342.41	626.47
28	121.30	222.5	2.64	320.23	587.40
27	115.90	213.3	2.64	305.98	563.11
26	110.50	204.1	2.64	291.72	538.82
25	105.10	194.9	2.64	277.46	514.54
24	99.70	185.8	2.64	263.21	490.51
23	94.50	176.8	2.64	249.48	466.75
22	89.30	167.8	2.64	235.75	442.99
21	84.40	159.2	2.64	222.82	420.29
20	79.70	150.5	2.64	210.41	397.32
19	75.10	141.8	2.64	198.26	374.35
18	70.50	133.2	2.64	186.12	351.65
17	65.90	124.7	2.64	173.98	329.21
16	61.50	116.4	2.64	162.36	307.30
15	57.10	108.2	2.64	150.74	285.65
14	52.70	100.2	2.64	139.13	264.53
13	48.50	92.4	2.64	128.04	243.94
12	44.30	84.7	2.64	116.95	223.61
11	40.30	77.3	2.64	106.39	204.07
10	36.30	70.1	2.64	95.83	185.06
9	32.50	63.1	2.64	85.80	166.58
8	28.90	56.4	2.64	76.30	148.90
7	25.50	50	2.64	67.32	132.00
6	22.30	44.1	2.64	58.87	116.42
5	18.50	36.1	2.64	48.84	95.30
4	14.80	28.7	2.64	39.07	75.77
3	11.50	21.9	2.64	30.36	57.82
2	8.40	15.8	2.64	22.18	41.71
1	5.60	10.5	2.64	14.78	27.72

Table 7.2: Actual displacements in CM of each storey above ground

7.4 Damage Limitation

The damage limitation requirement is expressed in terms of interstorey drift d_r in (EN 1998-1 cl.4.4.3.2) using equation

$$d_r \, v / h \leq 0,005 \tag{7.1}$$

Where

d_r is the design interstorey drift;

h is the storey height;

v is the reduction factor which takes into account the lower return period of the seismic action associated with the damage limitation requirement

Storey drift d_r is evaluated as the difference of the average lateral displacements d_s in center of mass at the top and bottom of the storey (EN 1998-1 cl.4.4.2.2(2)). In EN 1998, it is not clarified how the "average" value should be determined. It is reasonable to assume the values in center of mass as the average values. Storey drifts have to be determined for each vibration mode and combined according to a combination rule, e.g. CQC. In program ETABS interstorey drifts are reported for the center of mass for every floor diaphragm.
The value of v depends on the importance class of the building. Test building is classified as importance class II (EN 1998-1, Table 4.3) and the associated reduction factor v is equal to 0.5 (EN 1998-1 cl.4.4.3.2(2)). Term vd_r/h has limitations in accordance with non-structural elements and their arrangements into the structure. For buildings having non-structural elements of brittle materials attached to the structure vd_r/h should be smaller than 0,005, for buildings having ductile non-structural elements this limitation amounts to 0,0075 and for buildings having non-structural elements fixed in a way so as not to interfere with structural deformations, or without non-structural elements, limitation is equal to 0,01.
All parameters necessary for the verification of the damage limitation are obtained and illustrated in Table 7.3 for both orthogonal directions. It is obvious from the table that the most severe drift limit condition (0.005, for building having non-structural elements of brittle materials attached to the structure) is in the required range.

Story	d_{rx}	d_{ry}	h	$v.d_{rx}/h$	$v.d_{ry}/h$	limit
44	16.10	24.55	3300	0.0024	0.0037	0,005
43	16.10	24.55	3300	0.0024	0.0037	0,005
42	16.63	25.34	3300	0.0025	0.0038	0,005
41	16.37	25.34	3300	0.0025	0.0038	0,005
40	45.67	25.34	3300	0.0069	0.0038	0,005
39	34.06	64.68	3300	0.0052	0.0045	0,005
38	14.52	5.02	3300	0.0022	0.0008	0,005
37	15.05	20.59	3300	0.0023	0.0031	0,005
36	14.78	24.55	3300	0.0022	0.0037	0,005
35	15.05	24.55	3300	0.0023	0.0037	0,005
34	15.05	24.82	3300	0.0023	0.0038	0,005
33	15.05	24.55	3300	0.0023	0.0037	0,005
32	14.78	24.82	3300	0.0022	0.0038	0,005
31	14.78	24.55	3300	0.0022	0.0037	0,005
30	14.52	24.82	5250	0.0022	0.0038	0,005
29	22.18	24.55	3300	0.0021	0.0023	0,005
28	14.26	31.07	3300	0.0022	0.005	0,005
27	14.26	24.29	3300	0.0022	0.0037	0,005
26	14.26	24.29	3300	0.0022	0.0037	0,005
25	14.26	24.29	3300	0.0022	0.0037	0,005
24	13.73	24.02	3300	0.0021	0.0036	0,005
23	13.73	23.76	3300	0.0021	0.0036	0,005
22	12.94	23.76	3300	0.0020	0.0036	0,005
21	12.41	22.70	3300	0.0019	0.0034	0,005
20	12.14	22.97	3300	0.0018	0.0035	0,005
19	12.14	22.97	3300	0.0018	0.0035	0,005
18	12.14	22.70	3300	0.0018	0.0034	0,005
17	11.62	22.44	3300	0.0018	0.0034	0,005
16	11.62	21.91	3300	0.0018	0.0033	0,005
15	11.62	21.65	3300	0.0018	0.0033	0,005
14	11.09	21.12	3300	0.0017	0.0032	0,005
13	11.09	20.59	3300	0.0017	0.0031	0,005
12	10.56	20.33	3300	0.0016	0.0031	0,005
11	10.56	19.54	3300	0.0016	0.0030	0,005
10	10.03	19.01	3300	0.0015	0.0029	0,005
9	9.50	18.48	3300	0.0014	0.0028	0,005
8	8.98	17.69	3300	0.0014	0.0027	0,005
7	8.45	16.90	4500	0.0013	0.0026	0,005
6	10.03	15.58	4500	0.0011	0.0017	0,005
5	9.77	21.12	4500	0.0011	0.0023	0,005
4	8.71	19.54	4500	0.0010	0.0022	0,005
3	8.18	17.95	4500	0.0009	0.0020	0,005
2	7.39	16.10	4500	0.0008	0.0018	0,005
1	6.34	13.99	6000	0.0007	0.0016	0,005

Table 7.3: Story drifts check for both directions

7.5 Shear Forces

Shear force at the base of the structure obtained by modal response spectrum analysis for X direction amounts to Fb_X = 82092 kN at the base.The corresponding base shear ratio (base shear force versus total weight of the structure above level 0) is equal to 82092 / (2581895) =3.1%. For Y direction, the base shear force and base shear ratio are smaller, they amount to Fb_Y =79370 kN and 3%, respectively.

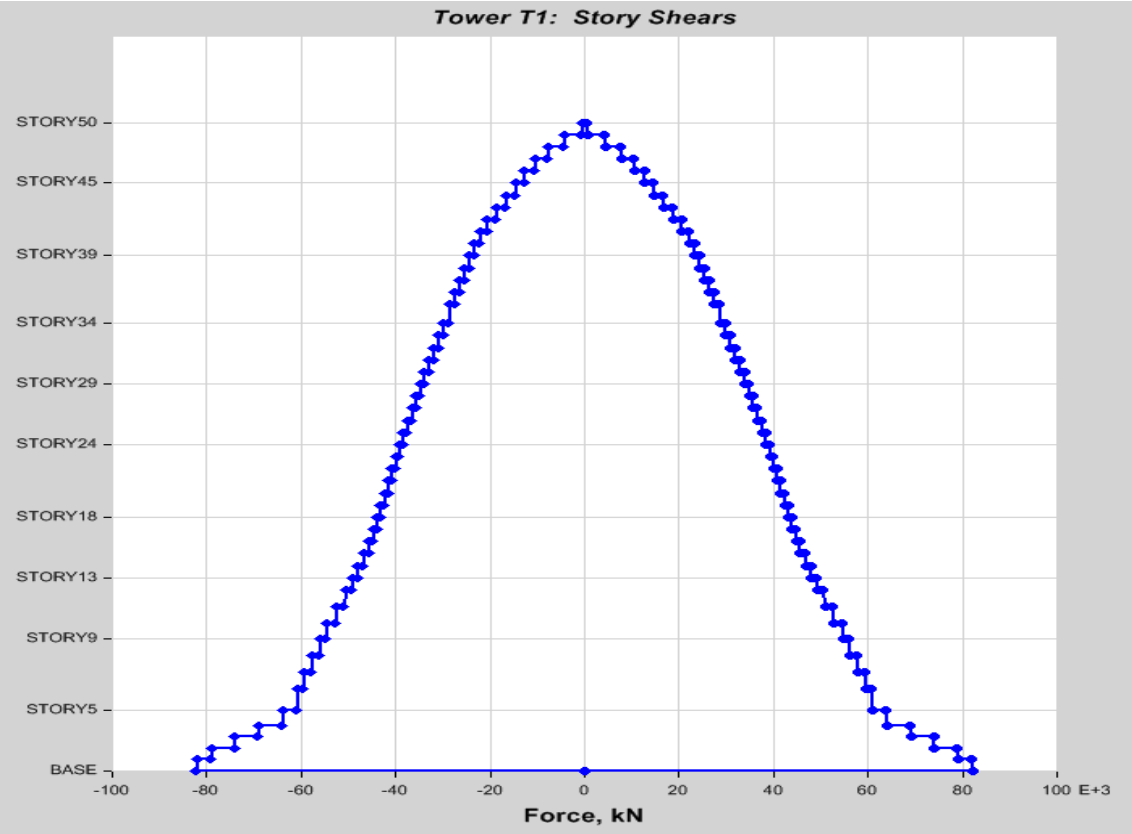

Figure 7.3: Story shear force in x direction

Calculated base shear can be checked by comparing it with the upper bound value for the base shear, which can be obtained by multiplying the total mass with the design spectral acceleration at the fundamental period in the relevant direction. Since structure calculated period for both directions lies far away from plateau level of spectrum, having very small amount, the minimum of $\beta.a_g$ from Eq. 3.16 of EC8 is used. Considering M = 263190 ton and $S_{d,min}$=*0,28 m/s*^{2} for both directions, the upper and lower bounds values for base shear, shown in Table 7.4 are obtained. The lower bound values can be obtained in a similar way, but considering the effective mass for the relevant fundamental mode (48,5% and 48,2% of the total mass above the basement in direction X and Y, respectively) instead of the total mass.

Base shear	Lower bound kN	Calculated value kN	Upper bound kN
Direction X	35520	82092	939964
Direction Y	35741	79370	939964

Table7.4: Base shear forces

7.6 Second Order Effects

Second-order or $P–\Delta$ effects criterion is based on interstorey drift sensitivity coefficient θ, which is expressed with equation (EN 1998-1/4.4.2.2(2))

$$\theta = \frac{P_{tot}.d_r}{V_{tot}.h} \tag{7.2}$$

where

θ is the interstorey drift sensitivity coefficient;

P_{tot} is the total gravity load at and above the storey in the seismic design situation (G + 0.3Q,);

d_r is the design interstorey drift, evaluated as the difference of the average lateral

displacements ds at the top and bottom of the storey;

V_{tot} the total seismic storey shear; obtained by modal response spectrum analysis

h is the interstorey height.

Due to EC8,If $\theta \leq 0{,}1$ there is no need to considered second order effect, if 0,1≤ θ ≤ 0,2 second order effect may be taken into account by amplifying the effects of seismic action by 1/(1- θ), for 0,2 ≤θ ≤0,3 second order effect must be account for by an analysis including second order effect explicitly. Values more than 0,3 is not permitted for θ.

From table 7.5 it is obvious that second order effect could be ignored for x direction and for y direction amplification factor of 1/(1 - 0,14) = 1,16 should be taken into account. For design purpose this factor is rounded to 1.2 and actions will amplify 20%.

This coefficient is not calculated for basement because of high stiffness of basement which deflects negligibly.

Story	P kN	V_x kN	V_y kN	$d_{r,x}$ (mm)	$d_{r,y}$ (mm)	H (mm)	θ_x	θ_y
1	1467272.2	60979.1	58642.6	6.336	13.992	6000	0.0254	0.058
2	1416419.7	59511.2	57064.2	7.392	16.104	4500	0.0391	0.089
3	1371473.9	57857.3	55420.8	8.184	17.952	4500	0.0431	0.099
4	1326528.1	56267.7	53847.6	8.712	19.536	4500	0.0456	0.107
5	1281582.2	54719	52378.4	9.768	21.12	4500	0.0508	0.115
6	1236636.4	52881.2	50817.6	10.03	15.576	4500	0.0521	0.084
7	1191690.5	50890	49187.9	8.448	16.896	4500	0.0440	0.091
8	1146728.5	49150.6	47692.2	8.976	17.688	3300	0.0635	0.129
9	1111303.9	47981.7	46683.2	9.504	18.48	3300	0.0667	0.133
10	1075879.4	46817.7	45757	10.03	19.008	3300	0.0699	0.135
11	1040454.8	45710.6	44894.4	10.56	19.536	3300	0.0728	0.137
12	1007270.3	44744	44079.7	10.56	20.328	3300	0.0720	0.141
13	974085.7	43905.5	43300	11.09	20.592	3300	0.0745	0.140
14	940901.2	43131.3	42586.8	11.09	21.12	3300	0.0733	0.141
15	907716.6	42340	41937.2	11.62	21.648	3300	0.0755	0.142
16	874532.1	41526.2	41313.7	11.62	21.912	3300	0.0741	0.141
17	841347.6	40736.3	40667.6	11.62	22.44	3300	0.0727	0.141
18	808163	39985	39963.8	12.14	22.704	3300	0.0744	0.139
19	774978.5	39226	39190.5	12.14	22.968	3300	0.0727	0.138
20	741794	38403.8	38353.1	12.14	22.968	3300	0.0711	0.135
21	708609.4	37513.1	37461.5	12.41	22.704	3300	0.0710	0.130
22	675424.9	36597.9	36521.1	12.94	23.76	3300	0.0723	0.133
23	642253.6	35705.3	35537.2	13.73	23.76	3300	0.0748	0.130
24	609045.1	34811.9	34495.4	13.73	24.024	3300	0.0728	0.129
25	575836.5	33881.2	33405.8	14.26	24.288	3300	0.0734	0.127
26	542628	32893.9	32289.8	14.26	24.288	3300	0.0713	0.124
27	509419.5	31865.6	31173.2	14.26	24.288	3300	0.0691	0.120
28	476210.9	30823.8	30076.3	14.26	31	3300	0.0667	0.149
29	443002.4	29779.6	29011.3	22.18	24.552	3300	0.1000	0.114
30	409793.9	28705.6	27959.7	14.52	24.816	5250	0.0395	0.069
31	371009.4	27431.2	26703.5	14.78	24.552	3300	0.0606	0.103
32	339828.4	26404.5	25703.4	14.78	24.816	3300	0.0577	0.099
33	308615.8	25373.7	24747.8	15.05	24.552	3300	0.0555	0.093
34	277405.1	24360.1	23790.7	15.05	24.816	3300	0.0519	0.088
35	246192.4	23312.8	22741.1	15.05	24.552	3300	0.0482	0.081
36	214981.7	22115	21496.4	14.78	24.552	3300	0.0436	0.074
37	183769.1	20650.7	19984	15.05	20.592	3300	0.0406	0.057
38	152558.4	18868.6	18195.2	14.52	5.016	3300	0.0356	0.013
39	121347.7	16799.1	16204.8	34.06	64.68	3300	0.0745	0.147
40	90135	14575	14199	45.67	25.344	3300	0.0856	0.049
41	70574.1	12770.6	12604.9	16.37	25.344	3300	0.0274	0.043
42	53571.5	10586.5	10600	16.63	25.344	3300	0.0255	0.039
43	36568.9	7810	7955.2	16.1	24.552	3300	0.0228	0.034
44	19565.8	4422.2	4594.1	16.1	24.552	3300	0.0216	0.032

Table 7.5: Sensitivity coefficient θ for both directions from first story up to 44

7.7 Shear Wall and Spandrel Positions

Sample checks are carried out on structural typical walls and are intended to show the requirements for design and detailing of critical regions. Design has been performed in three level namely, first at ground floor, second at story 20, and third at story 44. All checks are done only for core of tower 1 because of complexity and irregularity of this core, which is because of wall curtailments in different levels of this core. This core is illustrated again with wall numbers that we will refer to later. Letter W in figure refers to walls and S to coupling beams or spandrels. Each wall internal forces is derived from analysis and have been designed alone. The core is assumed as assemblies of rectangular walls and not assemblies of U shape or I shape walls. This assumption makes the design procedure easier and haven't any effect on final result of design.

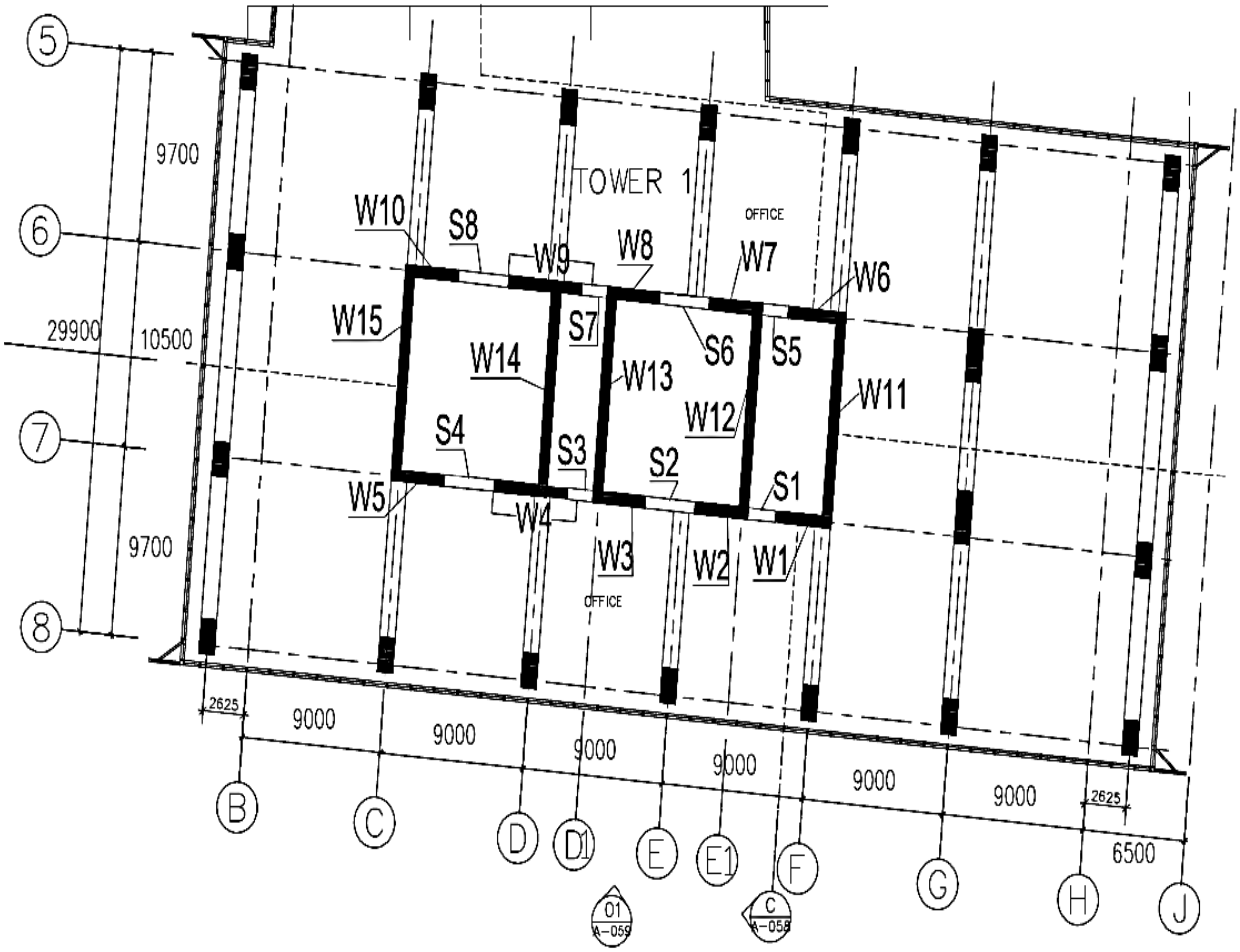

Figure 7.4: Wall and spandrel positions of tower 1

7.8 Internal Forces from Dynamic Analysis

The shear forces and bending moments obtained by the modal response spectrum analysis (RSA) are presented in the following figures. The results are shown for elevation 7 which have wall curtailments along the height. Figure 7.5 shows the layout of coupled shear walls and spandrels. In figure 7.6, 7.7 and internal forces are shown, since the system is too large forces are shown only schematically.

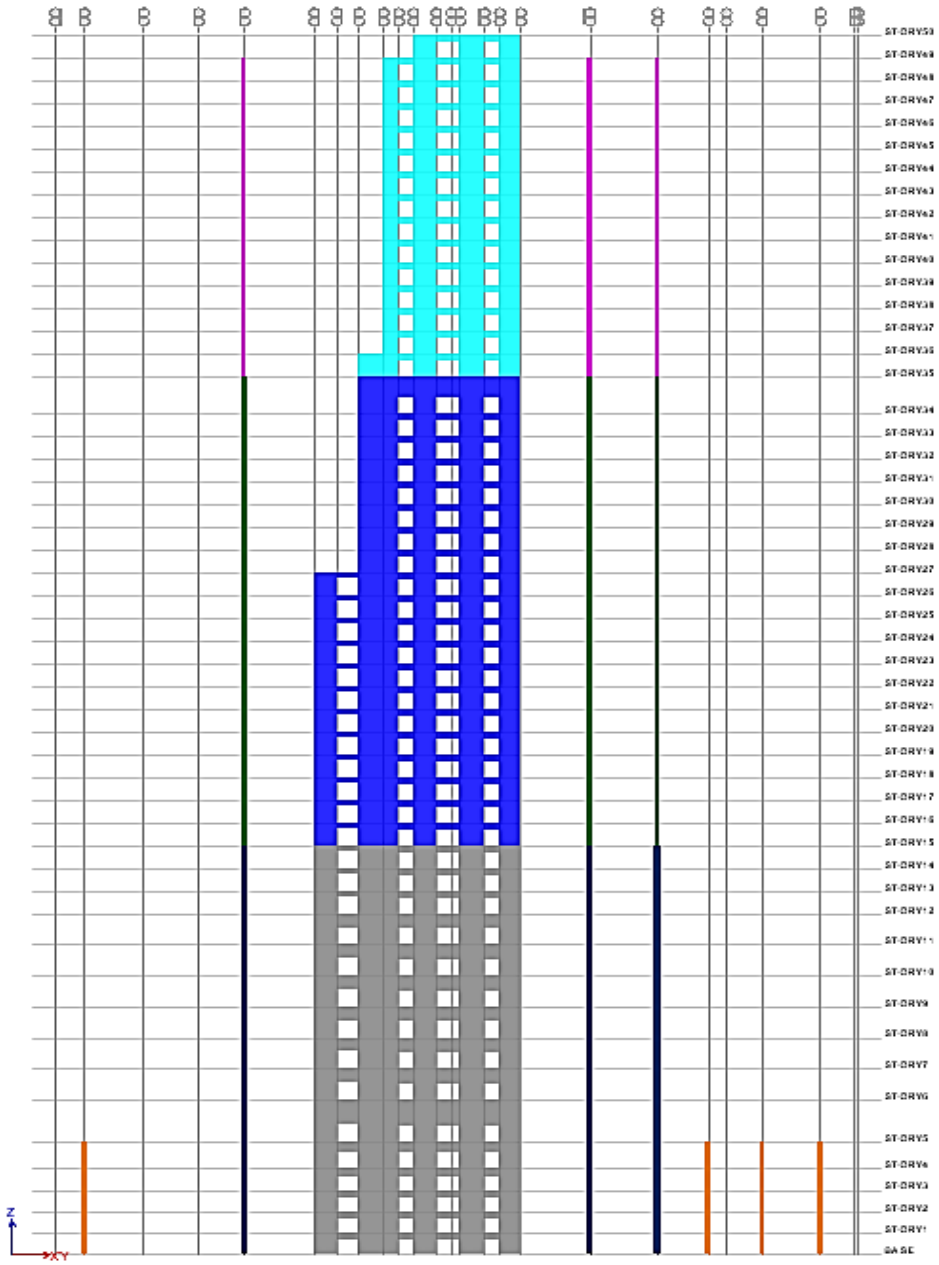

Figure 7.5: Coupled shear wall layout, elevation 7

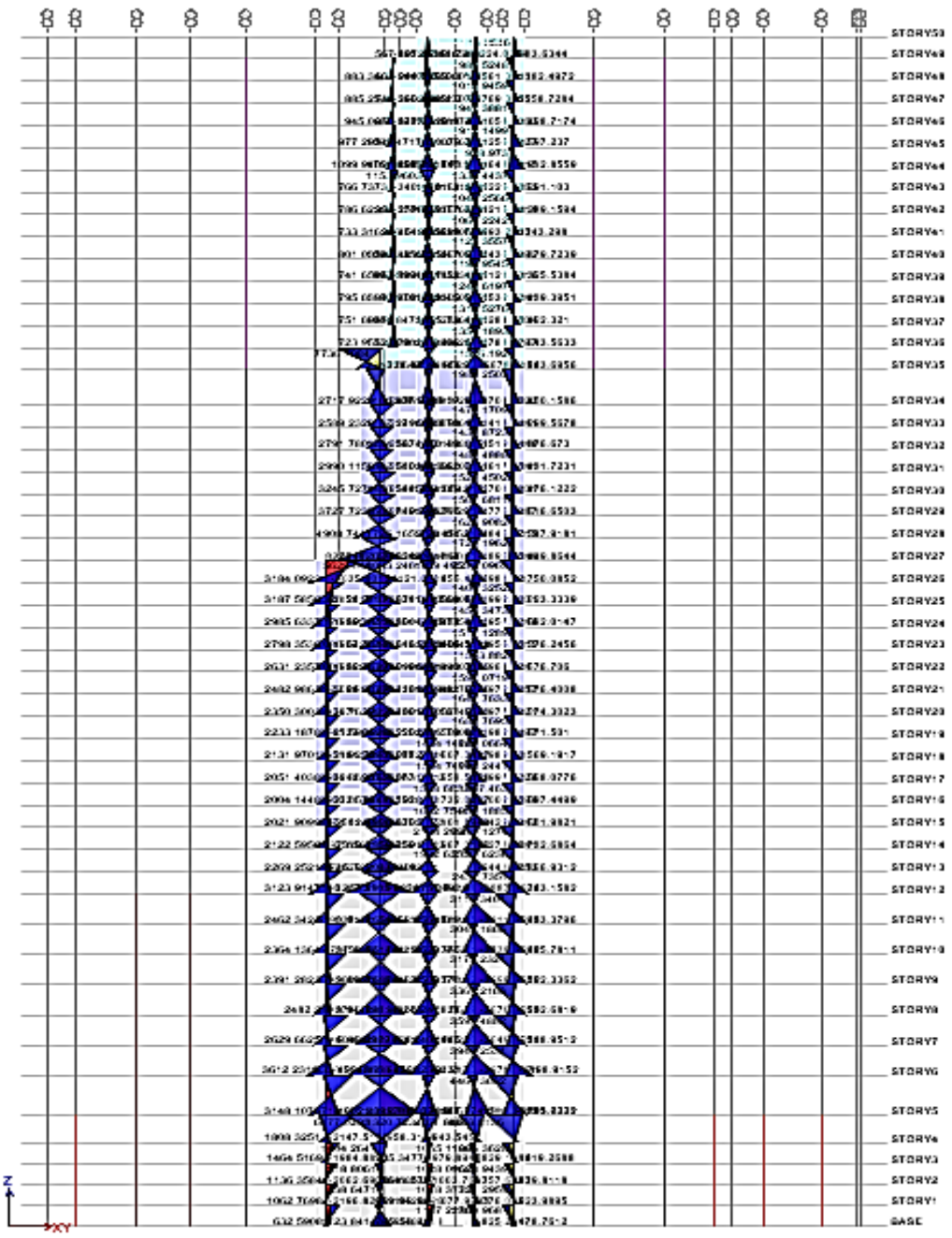

Figure 7.6: Bending moment of coupled walls in seismic situation, elevation 7

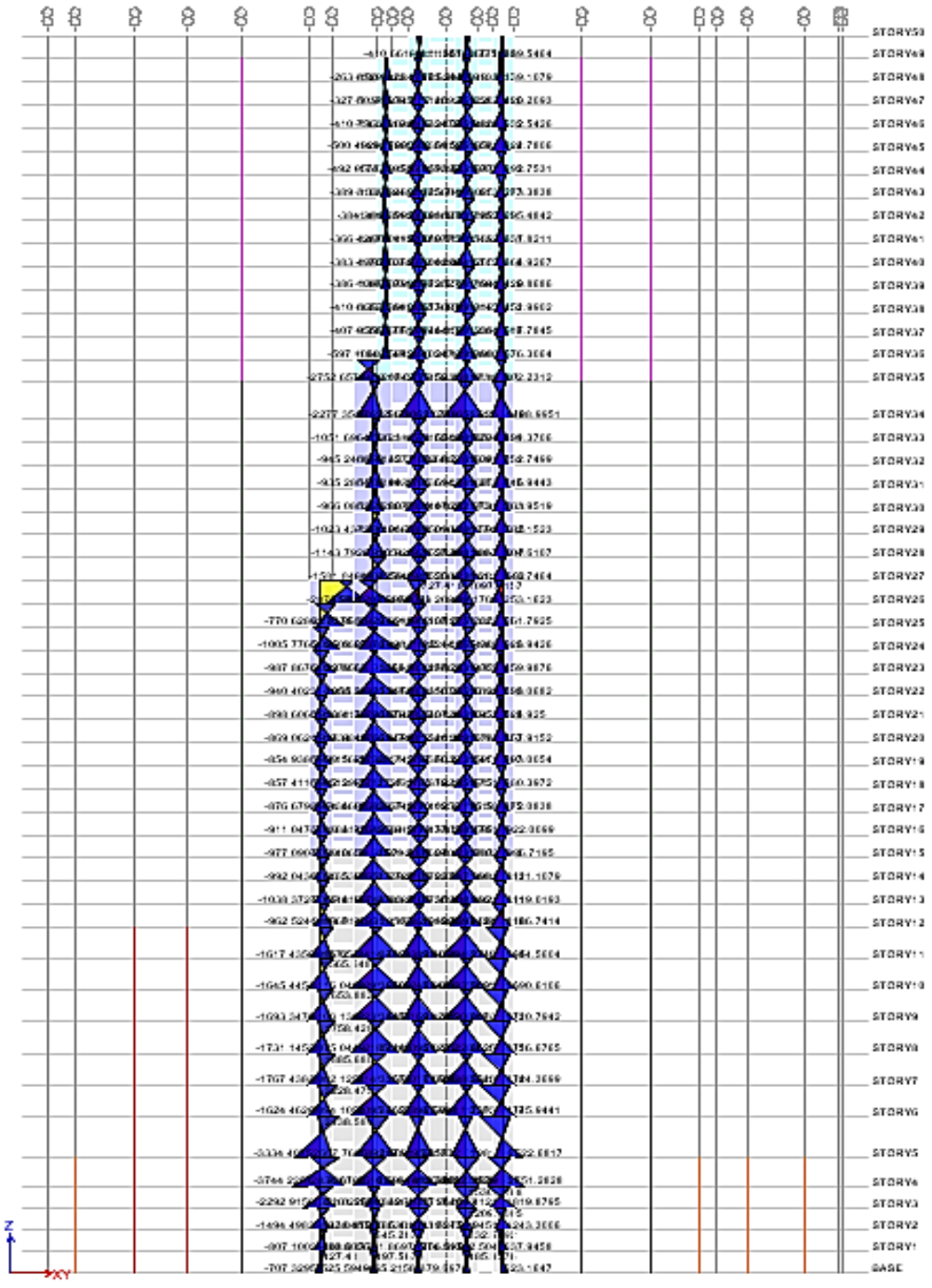

Figure7.7: Coupled walls shear forces in seismic situation, elevation 7

7.9 Internal Force Pattern

The variation of internal forces along the height of building is more complex in coupled walls. Walls in axis 6 and 7 are coupled with spandrels. The bending moment and shear force variation are shown in figures 7.8 and 7.9 respectively. The walls could be classified based on their behavior and level of forces for the purpose of design. For coupled walls their design envelope is illustrated for selected walls later to show the procedure of design due to EC8. As it is clear from figures 7.8 and 7.9, pairs of walls facing together in axis 5 and 6 have same behavior. These walls are (W10, W5), (W9, W4), (W3, W8), (W2, W7), (W1, W6) and are written in pairs for clarity. Each pair in parenthesis could be classified as one group and their envelope could be drawn for design purpose because their internal forces follow almost the same pattern.

Some jumps occur in internal force diagrams at different levels in walls which could be interpreted as below:

[1] The first jump occurs at transition from basement to the tower at ground level because of high stiffness of basement.
[2] Second jump happens at story 8 where the tower setbacks occur at both side of building and 8 columns and their tributary areas are omitted.
[3] Third jump appears in story 12 where the first reduction in cross section of columns and thickness of flange and coupled walls happens.
[4] Fourth main jump appears at story 23 where core curtailment takes place. Walls W5, W10 are omitted and W15 is changed to two columns. Beside these W9 and W4 are shortened. These curtailments are shown in figure 1.7 earlier. Due to these wall curtailments redistribution of forces happens and big interaction forces arise in the floor slabs and coupling beams which transfer them to the other walls. At this level the moment and shear force of curtailed elements redistribute between other vertical elements.
[5] Next jump occurs at story 31 where the cross sections of column and the thickness of all flange and coupled walls are reduced as a second reduction. This change in stiffness causes a redistribution of forces which appears in the form of jump in graphs.
[6] Sixth jump at story 40 is due to ending of tower 2 at this level, so there is no more interaction between two towers through floor slabs. After this level tower 1 continues till story 45.
[7] The last jump occurs due to curtailment of shear wall at story 45 where tower 1 ends.

Normally these jumps are caused by interaction forces between walls which are transmitted by coupling beams and are traceable one or two stories before or after change level which redistribution occurs and later normal pattern are continued again.

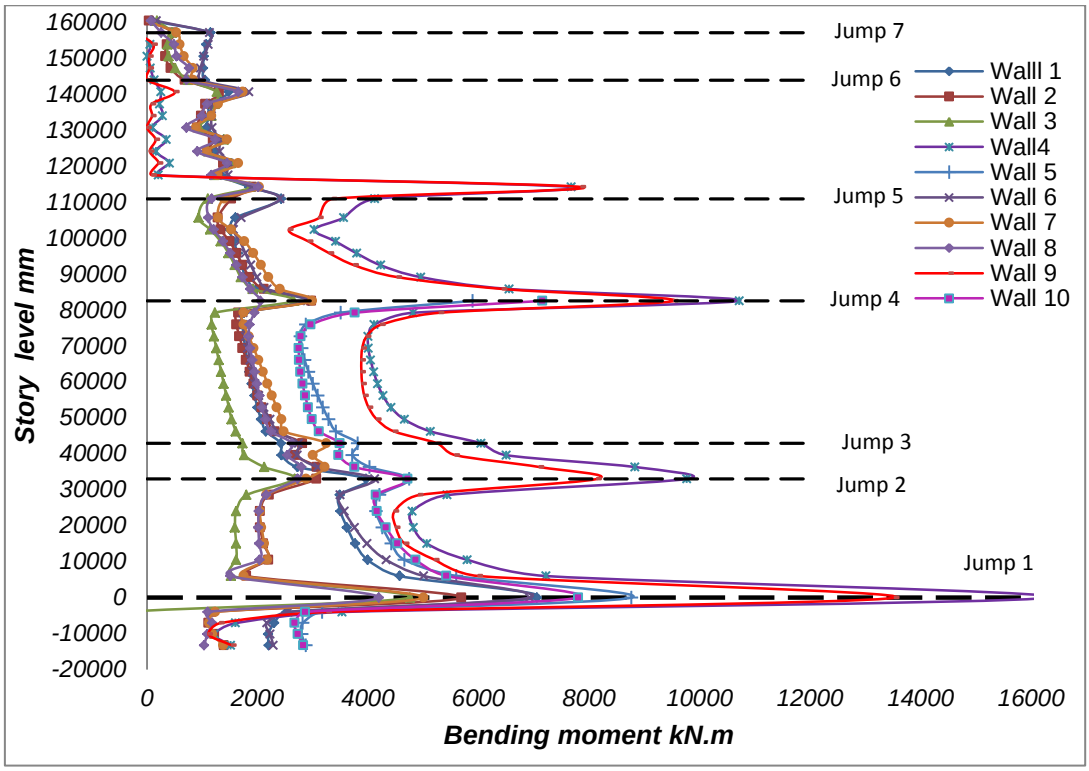

Figure 7.8: Bending moment variation of coupled walls at axis 6 and 7

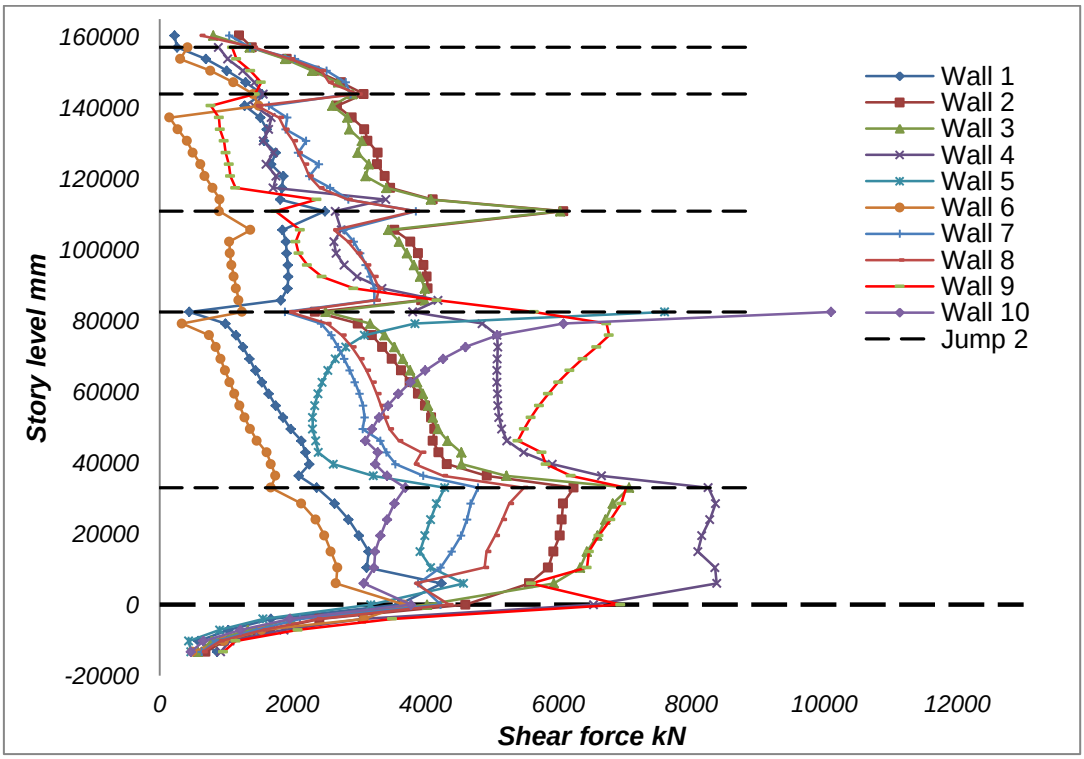

Figure 7.9: Shear force variation of coupled walls at axis 6 and 7

Design of coupling beams is based on their shear force, therefore the diagram of their internal shear is illustrated in figure 7.10. In the investigated building the coupling beams have different depths in different levels. First story with 6 m height have a coupling beam with 3.7 m depth. Story 2 to 7 have a story height of 4.5 m with coupling beams of 2.2 m depth. Story 30 which is assigned for mechanical facilities has a height of 5.25 m with a coupling beam of 2.95 m depth. The rest of stories with 3.3 m height have coupling beams with a height of 1 m. the height of openings is considered to be 2.3 m.

Normally the maximum shear force in coupling beams occurs at one third of building height in a regular wall and spandrel pattern with no change over height. But here because of irregularity this pattern is not traceable.

Spandrels are also classified for design purpose based on their internal force levels. From figure 7.15 spandrel pairs (1,5), (2,6), (3,7), (4,8) are classified to be designed in same group.

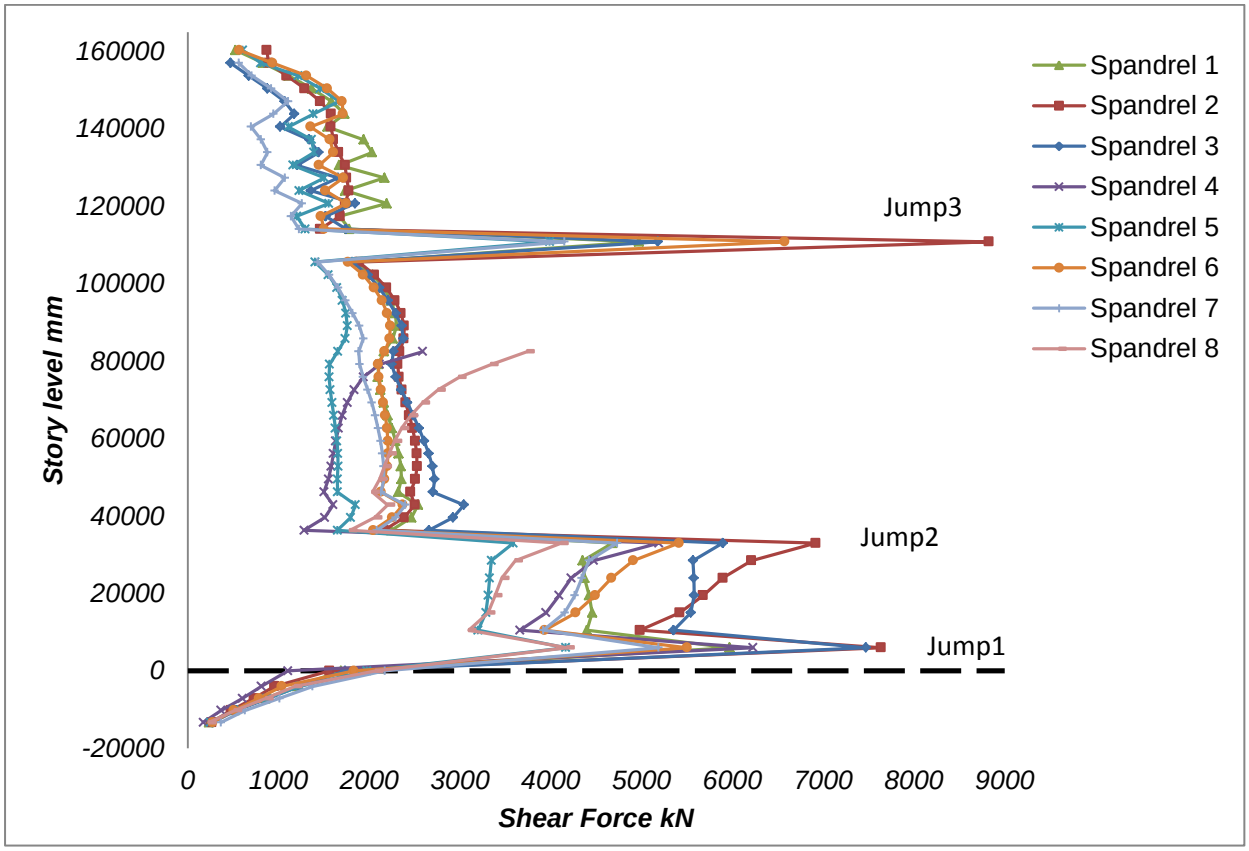

Figure 7.10: Coupling beams shear forces

As shear walls there is also jumps in shear force diagram of coupling beams caused by stiffness differences of coupling beams and could be interpreted as below.

[1] First jump occurs at the transition from tower to basement and because of stiffness difference. Other reason is that in the first floor the coupling beam depth is higher than those above (3.7 m at this story and 2.2 above this story up to story 7). The great depth of coupling beams in first 7 stories leads to high stiffness in these regions which attract more forces and is clear in figure 7.10.
[2] Second jump occurs at story 7 where coupling beams depth is reduced from 2.2 m to 1 m.
[3] Third Jump is because of change of coupling beam depth suddenly from 1 m to 2.95 m.

7.10 Design Envelopes

Due to the plastic hinge forming at the base it is better to avoid the soft story mechanism at the rest of wall at the upper stories. The elastic parts of the walls tend to behave as rigid body above the flexible zone of the hinge at the base which causes relatively uniform inter storey drift throughout the height of structure. This minimize the local ductility demand in frames and hence the extent of non-structural damage, for the same global ductility of the building.

Unlike frames, the bending moment diagram of walls does not change sign between successive floor levels, which creates uncertainties in moment distribution along the wall. To prevent yielding above the base hinge, EC8 suggests an envelope for bending moment diagram calculated from analysis, which is shown below.

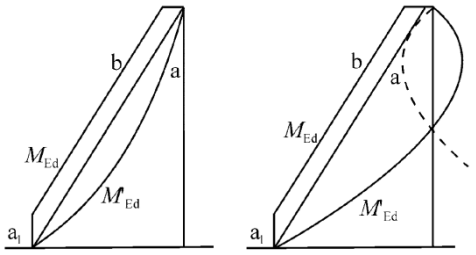

Figure 7.11: Bending moment envelope suggested by EC8 for structural walls

In figure 7.11 diagram a is moment diagram from analysis, diagram b is design envelope and a_1 is the tension shift. a_1 is dependent on compression strut inclination considered in shear verification in ULS situation. a_1 is defined as $a_1=z.\cot\theta$ where z is the effective depth at the base of the wall and θ is the strut angle in shear strength calculation [29]. For three uncurtailed and uncoupled walls, moment diagram and their envelope due to EC8 is shown below. With assumption of $\cot\theta=2$

and z=8.64 m, a_1 is calculated to 17.28 m, and with rounding this value to 19.5 m it covers the first 5 stories. For tension shift in basement first two stories under ground level with a height of 7.1 m has been taken into account for basement stories. Walls (12, 13, 14) and walls (11,15) have been selected to be designed as groups for the same internal forces.

Walls 12, 13, 14 acts as web in multicellular core of tower 1 and walls 11, 15 acts as flange, in which wall 15 is curtailed at story 22. Both of walls 11 and 15 alter in thickness from 60 cm at the base to 40 cm at the top. The bending moment diagram and their design envelope are illustrated in figure 7.13 and 7.14.

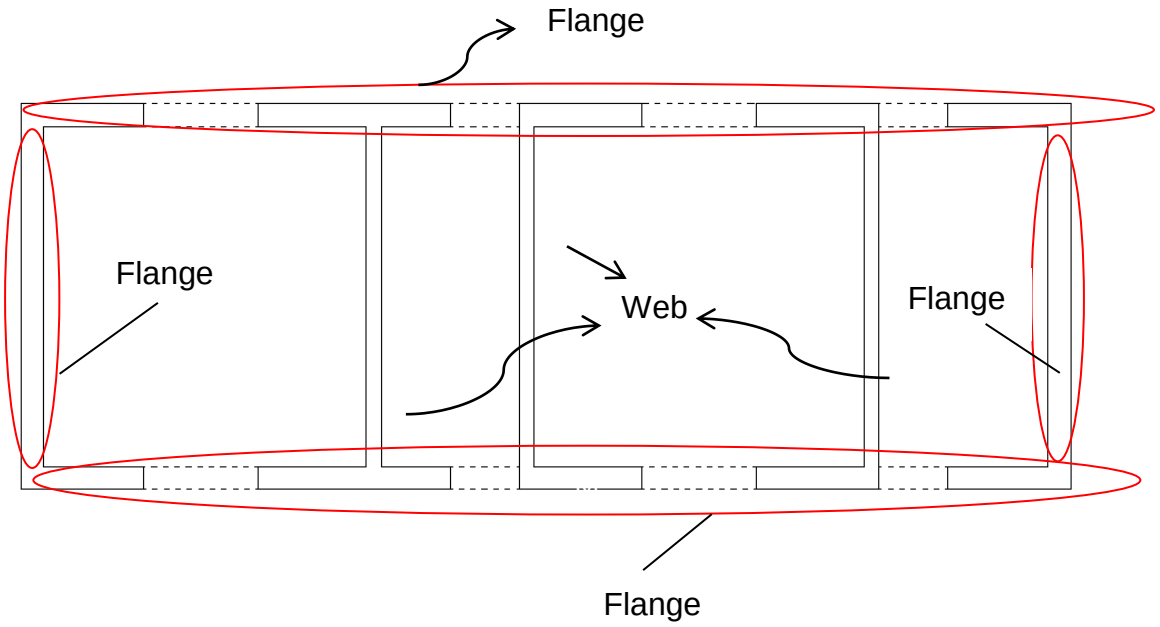

Figure 12: Web-flange action of wall assemblies

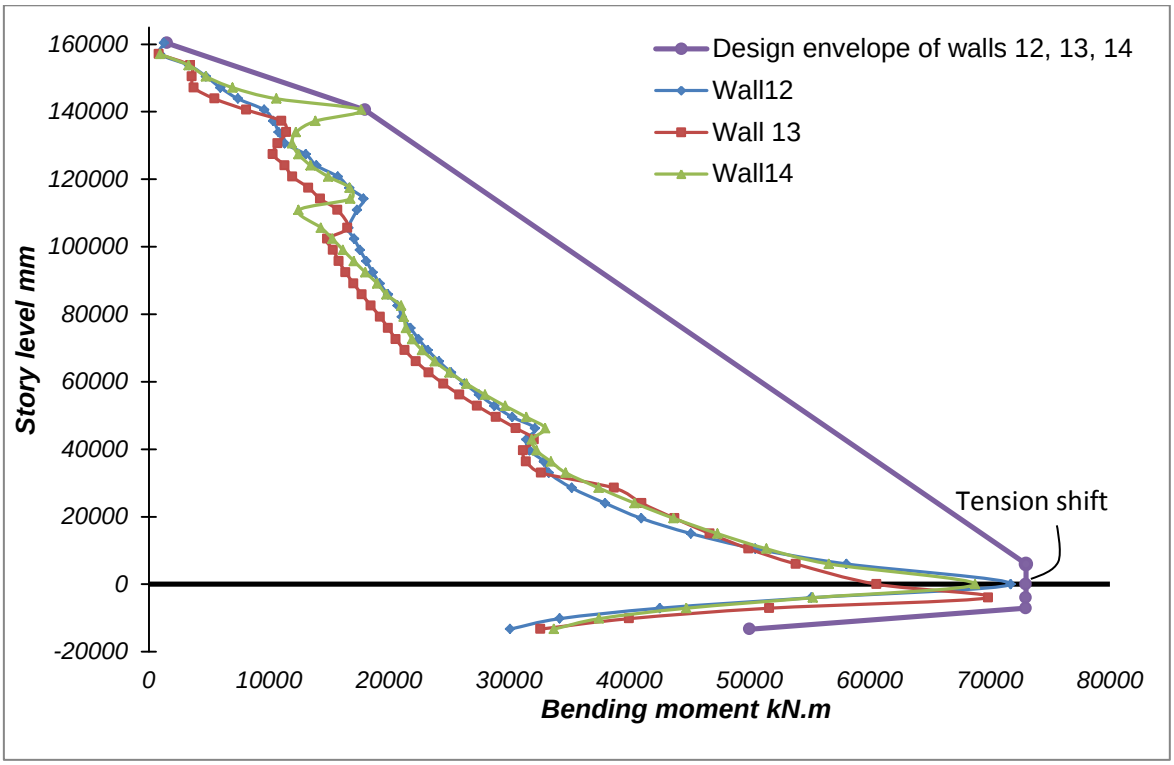

Figure 7.13: Bending moment of walls 12, 13, 14 and design envelope in y direction

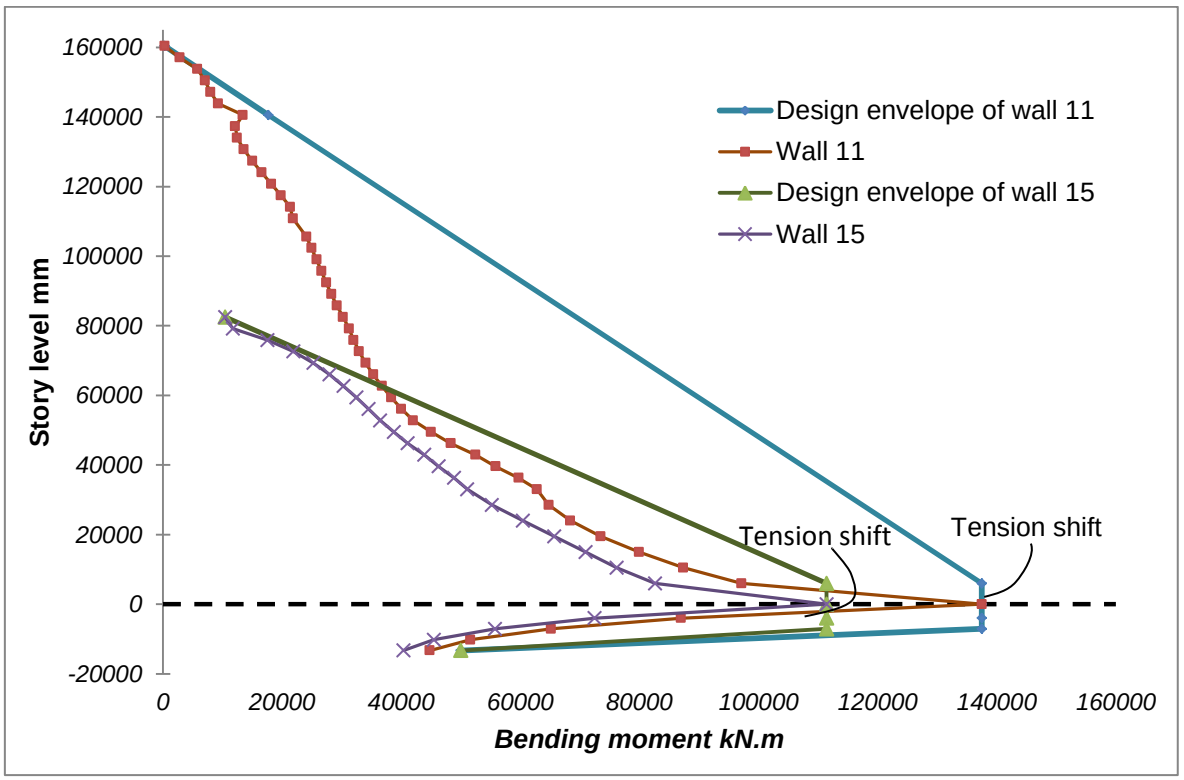

Figure 7.14: Bending moment of walls 11, 15 and design envelope in y direction

For shear design there is also provisions in EC8 to cover uncertainties of analysis. Since the bending moments in the wall at different stages of hinge development are not known it is not possible to derive shear based on equilibrium conditions. To prevent shear failure considering: 1) possible bending moments at the base section being greater than one used to determine the flexural reinforcement, 2) possible variation of the distribution of dynamic forces in the non-linear range 3) effect of higher oscillation modes [29], EC8 suggests to magnify the shear force from analysis by a factor 1.5, which is mentioned in section 5.4.2.4(7). For shear forces derived from analysis first an envelope of shears multiplied by 1.5 at each level is derived and illustrated, then an envelope suggested by EC8 is drawn in the same graph.

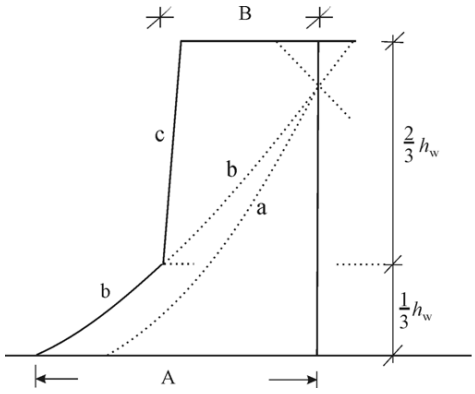

Figure 7.15: Design envelope of shear forces of dual systems in EC8

For three uncurtailed shear walls 12, 13, 14 which their bending moment is shown earlier, the shear force distribution and their envelope along the height is illustrated in figure 7.16. Shear force distribution and corresponding envelopes of walls 11, 15 are shown in figure 7.17. Shear wall 15 is curtailed at story 23. Both maximums of shear force and bending moment occurs at transition from basement to the first floor which there is a big jump in stiffness.

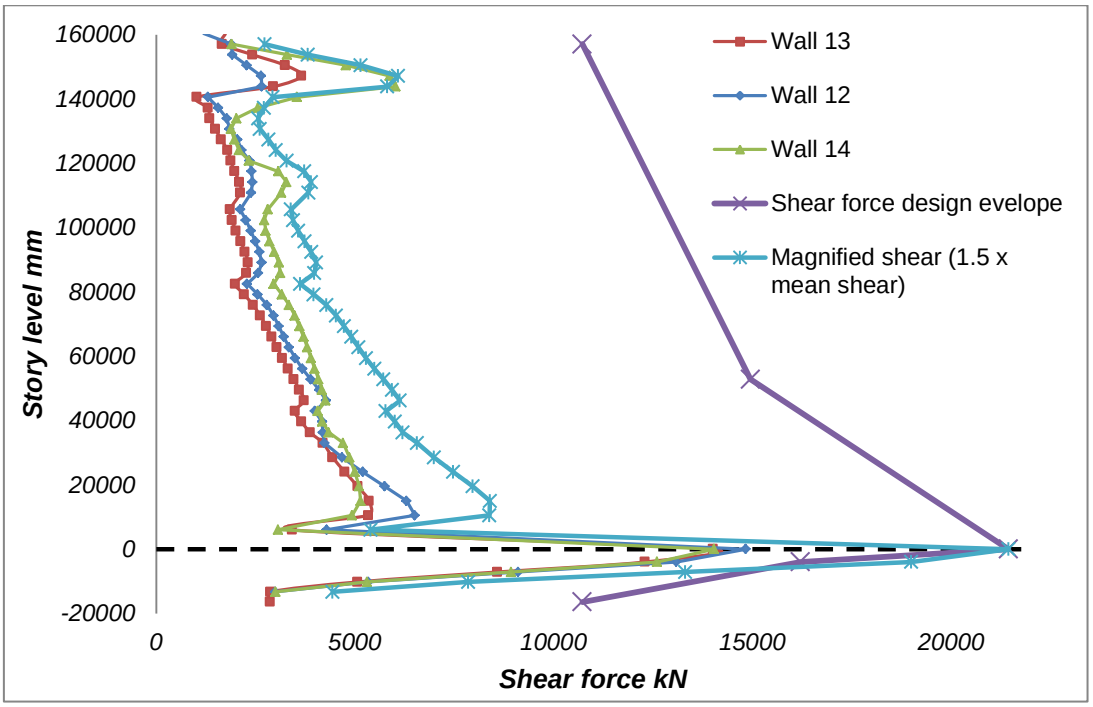

Figure 7.16: Shear forces and their design envelope due to EC8 for walls 12, 13, 14 in y direction

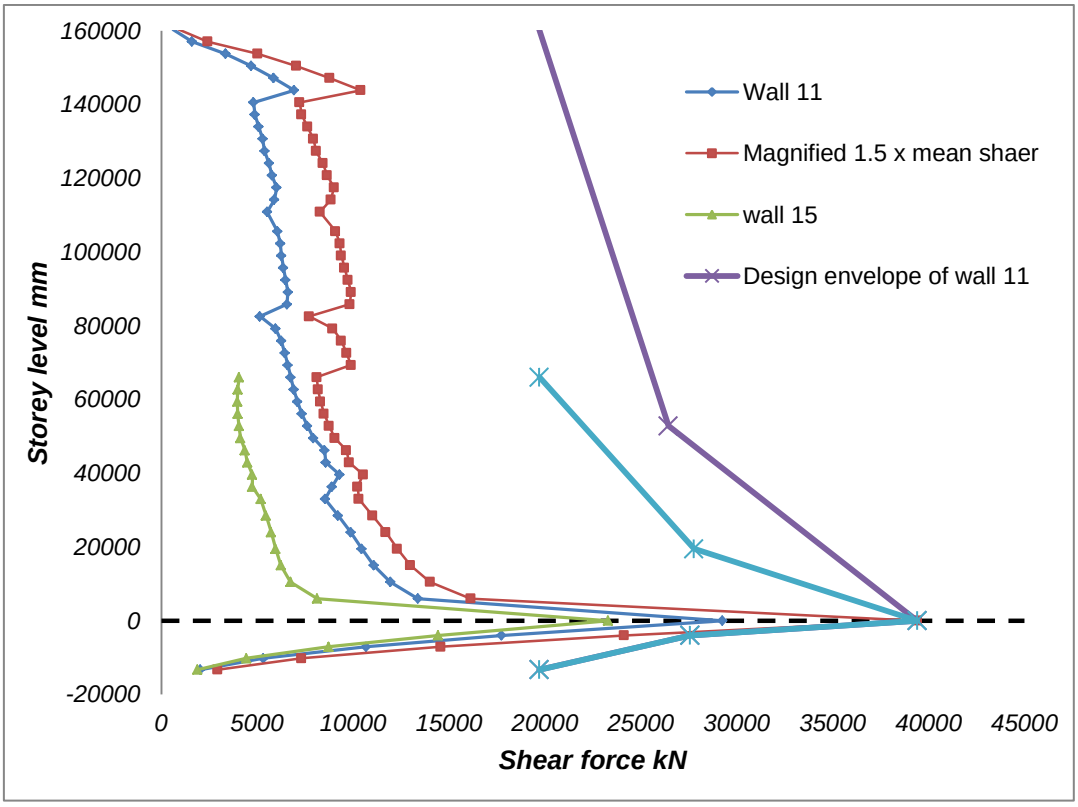

Fig 7.17: Shear forces and their design envelope due to EC8 for walls 11, 15 in y direction

7.11 Failure Modes of Structural Walls

The first step in a sound design is knowledge about the behavior of element and its failure modes which helps to take proper measures against failure phenomenon. Most cantilever walls could be considered as ordinary reinforced concrete beam-columns. Lateral loads are introduced by means of a series of point or line loads through the floors acting as diaphragms. Floor diaphragms stabilize the walls against buckling and allow relatively thin sections. To have a ductile wall, flexural yielding in clearly defined plastic hinge zones should govern the strength, and energy should be dissipated through inelastic deformation of these hinges. To prevent brittle failure mode the element should be designed based on capacity design procedure to ensure the location and formation of probable plastic hinges.

The primary failure mode and the main source of energy dissipation in a laterally loaded cantilever wall is the yielding of the flexural reinforcement in the plastic hinge regions located normally at the base of wall as shown in figure 7.18(b) and (e). Other failure modes which should be prevented are diagonal tension failure (Fig. 7.18(c)) or diagonal compression failure due to shear. Instability of thin walled sections or instability of the reinforcement under compression could also happen which should be prevented by altering the thickness of the wall and using enough hoops in the compressive zones. Sliding shear along construction joints, and shear or bond failure along splices or anchorage, illustrated in Fig. 7.18(d) are other modes of failure [26].

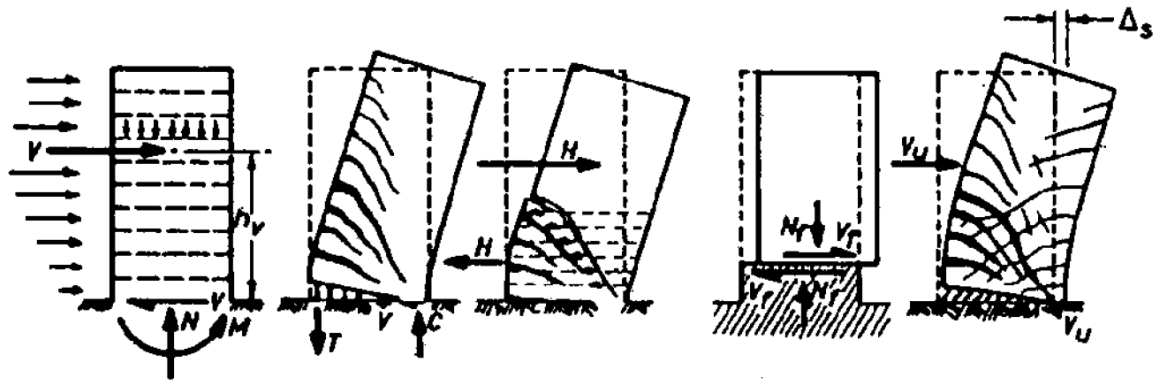

(a) (b) (c) (d) (e)

Figure7.18: Shear wall failure modes [26]

7.12 Local Ductility Parameter

Local ductility in critical regions is needed to ensure sufficient curvature in these regions of primary elements and also preventing of local buckling of compressed steel within plastic hinges. This ductility demand is fulfilled by special rules for

confinement of critical regions, especially at the base of columns, within beam/column joints and boundary elements of ductile walls. For this purpose EC8 introduces local ductility curvature factor $\mu_{\phi,}$ which is defined as:

$$\mu_\phi = 2q_0 - 1 \qquad if \qquad T_1 \geq T_C \tag{7.3}$$

where q_0 is the basic behavior factor before any reductions due to lack of structural regularity. For test building basic value of q_0 before reduction amounts to 3.3, then

$$\mu_\phi = 2 \times 2.64 - 1 = 4.28 \qquad with \qquad T_1 = 6.13 \geq T_C = 0.6 \tag{7.4}$$

7.13 Design of Walls at Base Section

Shear walls of investigated structure will be designed for DCM. Due to EC8 investigated building is categorized as wall equivalent dual system. Every part of flanged wall has been considered separately and designed as a straight wall. For example a U shape wall is assumed to be composed from three walls as shown in figure 7.19 and designed separately for its portion of load from total load delivered on entire cross-section.

Walls 11 and 15 have been grouped to be designed for same forces. Design procedure is shown for these walls and for the rest of the walls the results are reported in tabulated way. At last the section of walls has been detailed. As a feasibility study only walls of tower 1 are designed in three sections, firs at ground level second story 20 and last one story 44. Tower 1 is chosen for sample checks at preliminary design stag because of its irregularity and different curtailments of walls over the height. Tower 2 has no curtailments and is assumed to be sufficient in dimensions if tower 1 passes the checks.

7.14 Boundary Elements

Base section of wall is the region that plastic hinge develops. In this critical part special confinements should be provided in boundary elements if the normalized axial force exceeds 0,2 in DCM walls.

For design purpose every U or I shape wall has been defined as three individual straight walls in numerical model and the loads for each leg is derived separately. This makes the definition and calculation of boundary element length easier and design of wall assemblies could be done straight forward.

As dimension of walls the lengths of centerlines in numerical model have been used. Dimensions of center lines of Walls 3, 8 are L=300 cm, h= 60 cm.

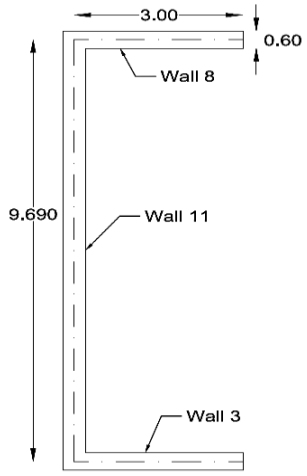

Figure7.19: Dimensions of walls 3, 8, 11 in numerical model

Calculated axial load amounts to 1782 kN. Axial normalized load due to vertical action (D+0,3L) is calculated as [Clause 5.4.3.4.1(2) of EC8]

$$f_{cd} = \frac{\alpha_{cc} \times f_{ck}}{\gamma_c} = \frac{0,85 \times 70}{1.5} = 39,7 \tag{7.5}$$

$$\nu = \frac{N}{\mathrm{b}.h.f_{cd}} = \frac{1782000}{600 \times 3000 \times 39.7} = 0,249 \tag{7.6}$$

$\nu \le 0,4 \Rightarrow$ The design axial force does not exceed the maximum limit for DCM structures.

$\nu \ge 0,2 \Rightarrow$it is necessary to design boundary elements explicitly for ductility according to EC8 Clause 5.4.3.4.2(12).

Before detailing the number and diameter of flexural reinforcement, the length of boundary elements will be determined. This is because flexural reinforcement should be distributed in this length and cannot be distributed arbitrary. Even it is better to concentrate it near the extremities.

Minimum length of boundary element due to Clause 5.4.3.4.2(6) of EC8 is

$$l_{\min} = \begin{cases} 0,15 l_w \ \ or \\ 1,5 b_w \end{cases} \Rightarrow l_{\min} = \begin{cases} 0,15 \times 3 = 0,45\ m \\ 1.5 \times 0,6 = 0,9\ m \end{cases} \tag{7.7}$$

The length of boundary elements h_0 could be determined as below [EC8 5.4.3.4.2(4,5,6)]:

$$h_0 = x_u \times (1 - \varepsilon_{cu2} / \varepsilon_{cu2,c}),\ \varepsilon_{cu2} = 0,0035 \tag{7.8}$$

$$\varepsilon_{cu2,c} = 0,0035 + 0,1 \alpha \omega_{wd} \tag{7.9}$$

$$x_u = (\nu_d + \omega_v)\varepsilon_{sy,d}\frac{l_w b_c}{b_0} \tag{7.10}$$

$$\alpha\omega_{wd} \geq 30\mu_\varphi(\nu_d + \omega_v)\varepsilon_{sy,d}\frac{b_c}{b_0} - 0,035 \tag{7.11}$$

where

b_0 is the minimum dimension of concrete core, measured to centerline of the hoops

x_u is the depth of compression zone

ε_{cu2} is the maximum strain of unconfined concrete

$\varepsilon_{cu2,c}$ is the maximum strain of confined concrete

α is the confinement effectiveness factor

ω_{wd} Is the mechanical ratio of confinement reinforcement $\omega_{wd} = \frac{V_{conf.reinf.}}{V_{concretecore}}\frac{f_{yd}}{f_{cd}}$.

Assuming a concrete cover of 50 mm to the main flexural reinforcement and φ =10 mm hoops:

$$b_0 = 600 - 2\times 50 + 10 = 510 \tag{7.12}$$
$$b_c = 600$$

Assuming that M_{rd}=M_{Ed} and from Eq. 7.4 we have

$$\mu_\phi = 5.6$$
$$\varepsilon_{sy,d} = \frac{435}{200000} = 0,002175 \tag{7.13}$$

For calculation of mechanical ratio of vertical web reinforcement first the amount of web steel is evaluated from Clause 9.6.2 of EC2 which gives the minimum amount of vertical web reinforcement as

$$A_{s,v\min} = 0,002A_c = 0,002\times 600\times 1000 = 1200\ mm^2/m = 12\ cm^2/m \tag{7.14}$$

To supply this amount of steel rebar ϕ12@15 on two faces of wall with A_s=15.08 cm^2/m is used. After this step ω_{wd} could be estimated as below

$$\omega_{wd} = \rho_v\frac{f_{yd,v}}{f_{cd}} = \frac{1508}{600\times 1000}\times\frac{435}{39.7} = 0.0275 \tag{7.15}$$

With ω_{wd} in hand equations (7.8) to (7.11) are evaluated

$$\alpha\omega_{wd} = 30\times 4,28(0,249 + 0,0275)\times 0,002175\times\frac{600}{510} = 0,0559 \tag{7.16}$$

$$\varepsilon_{cu2,c} = 0,0035 + 0,1 \times 0.056 = 0.0091 \quad (7.17)$$

$$x_u = (0,249 + 0,0275) \times \frac{3000 \times 600}{510} = 977.37 \quad (7.18)$$

$$h_0 = 977.37 \times (1 - 0,0035 / 0,009) = 601.4\ mm = 60\ cm \quad (7.19)$$

The length of boundary element is calculated to 60 cm on both sides of walls 3 and 8.

The boundary length of other walls is calculated in same way and tabulated below.

Wall	b_w (mm)	l (mm)	b_0 (mm)	N (kN)	ν_d	ω_v	$\alpha\omega_{wd}$	$\varepsilon_{cu2,c}$	x_u	h_0 (mm)
1,6	600	3000	510	15049	0.226	0.0275	0.0482	0.0083	833.99	483
2,7	600	3000	510	16497	0.231	0.0275	0.0499	0.0085	911.98	536
3,8	600	3000	510	17821	0.249	0.0286	0.0563	0.0091	981.37	605
4,9	600	3000	510	27208	0.228	0.0275	0.0491	0.0084	1505.80	879
5,10	600	3000	510	27208	0.228	0.0275	0.0466	0.0082	876.13	500
11,15	600	9690	510	56156	0.221	0.0275	0.0540	0.0089	3087.49	1873
12,13,14	400	9690	310	34719	0.226	0.0219	0.0542	0.0089	3095.08	188.

Table 7.6: Calculated parameters for boundary element length determination

The calculated amount of boundary element length is shown in table for different wall groups. For practice use they are adopted with detailing requirements. For walls 1, 6 a length of 54 for walls 2, 3, 5, 7, 8, 10 a length of 64 cm and for walls 4,9 a length of 108 cm is considered. For walls 11, 15 adopted length amounts to 200 cm and for walls 12, 13, 14 is equal to198 cm. this length is measured between the center lines of confining hoops. In figures concrete cover is also considered for these lengths.

After critical region of plastic hinge there the rules of EC2 should be met and there is no need for boundary elements. The proposed boundary element details meet EC8 and EC2 requirements.

7.15 Flexural Design

For flexural design under axial load and biaxial bending moment interaction surface were generated for every wall based on strain compatibility and force equilibrium. ETABS program generates a three-dimensional interaction surface with reference to the P, M_2 and M_3 axes. The surface is developed using a series of interaction curves that are created by rotating the direction of the wall neutral axis in equally spaced increments around a 360-degree. Each interaction diagram in a specific angle is determined by using the requirements of force equilibrium and strain compatibility to determine the nominal axial load and moment strength (N_r, M_{2r}, M_{3r}) of the wall. The coordinates of these points are determined by rotating a plane of linear strain on the section of the wall as illustrated below.

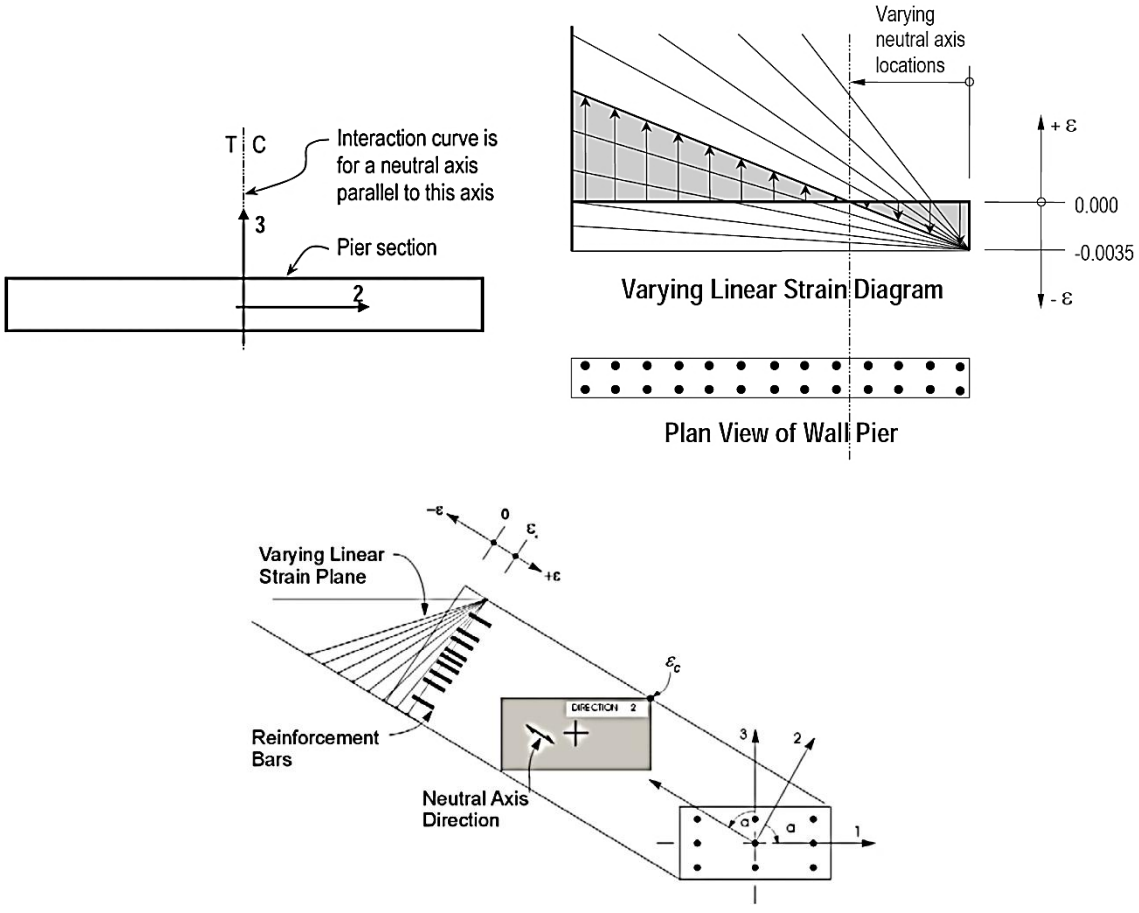

Figure 7.20: Determination of interaction Surface points coordinates by varying strain plane and natural axis rotation [72]

In addition to axial compression and biaxial bending, the formulation allows for axial tension and biaxial bending considerations. A typical interaction surface is shown below.

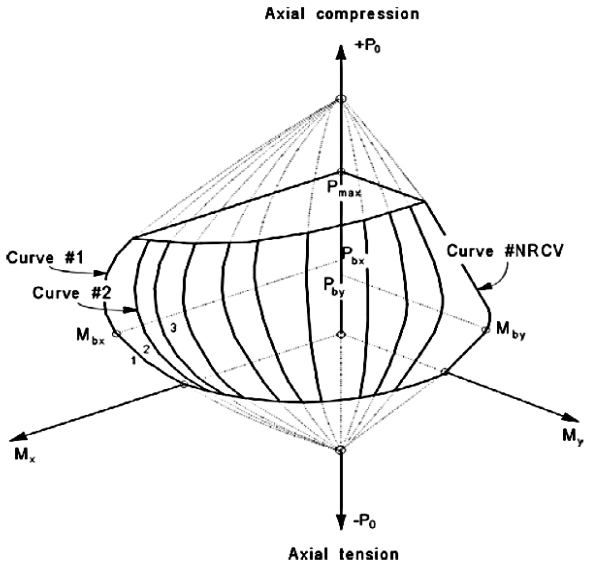

Figure 7.21: Typical interaction surface [72]

After generating interaction surface Demand/Capacity ratio is calculated for given load combination N_{Ed}, M_{2Ed} and M_{3Ed}. The point L, defined by (N_{Ed}, M_{2Ed}, M_{3Ed}), is placed on the interaction space, as shown below.

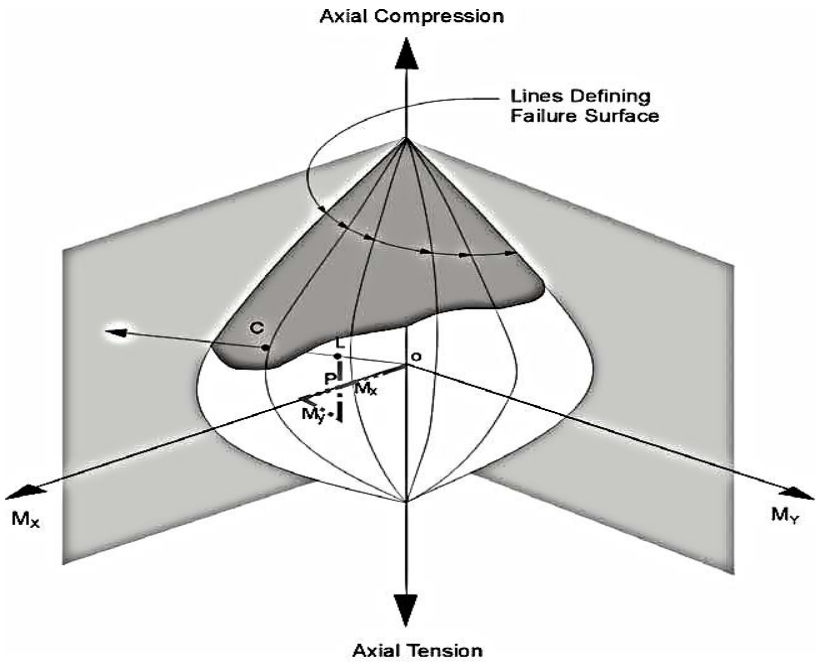

Figure 7.22: Geometric representation of wall capacity ratio [72]

As a measure of the stress condition in the wall section, the program evaluates a stress ratio. The ratio is estimated by plotting the point L and determining the location of point C. The point C is defined as the point where the line OL (extended outward if needed) reaches the interaction curve. This point is determined by three-dimensional linear interpolation between the points that define the failure surface, as

shown in Figure 7.22. The capacity ratio, CR, is given by the ratio OL/OC. The demand/capacity ratio, D/C, is defined as D/C = OL / OC where OL is the "distance" from point O (the origin) to point L and OC is the "distance" from point O to point C.

- If OL = OC (or D/C = 1), the point (N_{Ed}, M_{2Ed}, M_{3Ed}) lies on the interaction curve and the wall pier is stressed to capacity.
- If OL < OC (or D/C < 1), the point (N_{Ed}, M_{2Ed}, M_{3Ed}) lies within the interaction curve and the wall pier capacity is adequate.
- If OL > OC (or D/C > 1), the point (N_{Ed}, M_{2Ed}, M_{3Ed}) lies outside of the interaction curve and the wall pier is overstressed.

The flexural reinforcement is tried to be concentrated at extremities within boundary elements to gain higher flexural capacity (for the same amount of reinforcement) and higher curvature ductility, this is due to reduction of the compressive zone dimension [29].

First for all walls reinforcement is assigned and then D/C ratio is optimized. It has been tried to keep this ratio about 0,8 to 0,95. The D/C ratio for all walls and the reinforcement used in boundary elements and webs is shown in table 7.7. Yielding stress of rebars after consideration of safety factors is equal to 435 MPa for steel BSt500.

	Inside Boundary Element		**Between Boundary Element**		
Wall	Rebar	As (cm^2)	Web Rebar (on both face)	As (cm^2/m)	D/C Entire wall
1	30 x Ø32	240	Ø12@15	15.08	0.73
2	22 x Ø28	135.3	Ø12@15	15.08	0.86
3	18 x Ø25	88.2	Ø12@15	15.08	0.93
4	41 x Ø 25	200.9	Ø12@15	15.08	0.93
5	30 x Ø32	240	Ø12@15	15.08	0.9
6	30 x Ø32	240	Ø12@15	15.08	0.93
7	22 x Ø28	135.3	Ø12@15	15.08	0.87
8	18 x Ø25	88.2	Ø12@15	15.08	0.9
9	41 x Ø25	200.9	Ø12@15	15.08	0.85
10	30 x Ø32	240	Ø12@15	15.08	0.8
11	30xØ32+32xØ25+2xØ12	399.06	Ø12@15	15.08	0.82
12	40 x Ø14	48.4	Ø10@19	8.26	0.88
13	40 x Ø14	48.4	Ø10@19	8.26	0.77
14	40 x Ø14	48.4	Ø10@19	8.26	0.7
15	30xØ32+32xØ25+2xØ12	399.06	Ø12@15	15.08	0.81

Table 7.7: Supplied Flexural rebars in boundary elements and walls utilization factor

7.16 Shear Design

In shear design because of high shear forces in walls it has been assumed that walls cant withstand the shear without shear reinforcement and $V_{Rd,c}$ based on EC2 is not calculated for walls. The capacities of diagonal compressive struts have been checked due to EC2. Lower bound and upper bound values are calculated based on

different compressive strut angle. Upper bound evaluation is based on θ=45° with tanθ= cotθ=1 and lower bound based on θ=31° with tanθ= 0,6.

To calculate the concrete compressive struts strength Clause 6.2.3(3) of EC2 is used

$$V_{Rd,\max} = \frac{\alpha_{cw} b_w z \nu_1 f_{cd}}{\cot\theta + \tan\theta} \tag{7.22}$$

$$z = 0,9d = 0,9 \times (0,9 l_w) = 0,81 l_w \tag{7.23}$$

$$\nu_1 = 0,6 \times \left[1 - \frac{f_{ck}}{250}\right] = 0,6 \times \left[1 - \frac{70}{250}\right] = 0,432 \tag{7.24}$$

α_{cw} for non-prestressed structures is equal to 1.

Wall	α_{cw}	b_w (mm)	z (mm)	v	f_{cd}	θ Deg.	tanθ	cotθ	V_{Rdmax} (kN)
1,2,3,5,6,7,8,10	1	600	2400	0.432	39.7	31	0.6	1.67	10879
1,2,3,5,6,7,8,10	1	600	2400	0.432	39.7	45	1	1	12348
4,9	1	600	4000	0.432	39.7	31	0.6	1.67	18132
4,9	1	600	4000	0.432	39.7	45	1	1	20580
11,15	1	600	7848.9	0.432	39.7	31	0.6	1.67	35580
11,15	1	600	7848.9	0.432	39.7	45	1	1	40383
12,13,14	1	400	7848.9	0.432	39.7	31	0.6	1.67	23720
12,13,14	1	400	7848.9	0.432	39.7	45	1	1	26922

Table 7.8: Upper bound and lower bound of compressive strut strength

A comparison is made between shear design action and compressive strut strength for classified walls in table below.

Wall	$V_{Rd,max}$(kN) Upper Bound	$V_{Rd,max}$(kN) Lower Bound	V_{Ed} (kN)
1,6	12348.3	10879.5	7809
2,7	12348.3	10879.5	8346
3,8	12348.3	10879.5	10595
4,9	20580.5	18132.6	12592
5,10	12348.3	10879.5	9248
11,15	40383.5	35580.2	39378
12,13,14	26922.4	23720.1	22256

Table 7.9: Comparison of design value of shear force and compressive strut strength

Shear resistance associated with failure in shear by diagonal tension could be supplied by stirrups as below

$$\frac{A_s}{s} = \frac{V_{Ed}}{z.f_{ywd}.\cot\theta} \tag{7.24}$$

To be on the safe side upper bound angle is used for determination of stirrups with θ=45°. The minimum horizontal wall reinforcement is also calculated for comparison purpose as below

$$A_{sh,\min} = \begin{cases} 0,25 \times A_{sv,\min} \\ 0,001 \times A_c \end{cases} \tag{7.25}$$

Wall	V_{Ed} (kN)	z (mm)	f_{ywd} (Mpa)	cotθ	A_s/s (cm^2/m) Required	Used Rebar on both faces	A_s/s (cm^2/m) Supplied	$A_{sh,min}$	
								$0.25A_{svmin}$ (cm^2/m)	$0.001A_c$ (cm^2/m)
1,6	7809	2430	435	1	73.9	Ø26@14	75.9	3.77	6
2,7	8346	2430	435	1	79.0	Ø28@15	82	3.77	6
3,8	10595	2430	435	1	100.2	Ø30@14	101	3.77	6
4,9	12592	4000	435	1	72.4	Ø26@14	75.8	3.77	6
5,10	9248	2430	435	1	87.5	Ø30@16	88.36	3.77	6
11,15	39378	7849	435	1	115.3	Ø30@12	117.8	3.77	6
12,13,14	22255	8232	435	1	62.2	Ø25@15	65.3	2.07	4

Table 7.10: Calculated shear reinforcement and assigned reinforcement

7.17 Detailing for Local Ductility

Height of plastic hinge above the base of the wall for the purpose of providing confinement reinforcement is calculated based on Clause 5.4.3.4.2 of EC8

$$h_{cr} = \max\left[l_w, h_w / 6\right] = \max\left[9.69, 160.35 / 6\right] = 26.7m \tag{7.26}$$

$$\begin{cases} h_{cr} \le 2.l_w = 2 \times 9,69 = 19.38m \\ h_{cr} \le 2.h_s = 2 \times 6 = \underline{12m} \end{cases} \tag{7.27}$$

The spacing of hoops in boundary element region is same as columns given in Clause 5.4.3.2.2(11-a) of EC8

$$s = \min\left\{\frac{b_0}{2}; 175; 8d_{bl}\right\} = \left\{\frac{600}{2}; 175; 8 \times 25\right\} = 175mm \tag{7.28}$$

The minimum rebar size is chosen for hoops in all walls. Due to same Clause part b "The distance between consecutive longitudinal bars engaged by hoops or cross-ties does not exceed 200 mm" and due to EC2 Clause 9.5.3(6) no bars in compression zone shouldn't be spaced more than 150 mm from an engaged bar.

To prevent buckling of flexural bars in boundary element zone and fixing the bars that locate in middle layers at this zone in their place, all rebars are engaged with hoops or cross ties. To provide an effective confinement and to avoid inconvenient of having zones with different level of confinement near the extremity of the wall,

overlapping the inner hoops could be a solution. This provides a uniform distribution of available strain ductility in the edge member.

Over the critical height the rules of EC2 should be met and there is no need for confinement. In other codes like ACI-318 a transition zone with larger hoops spacing is considered between dense confinement zone and no-confinement zone, but such a transition zone is not clearly discussed in EC8.

Detailed wall sections are shown in figure 7.23 to 7.26 for base section.

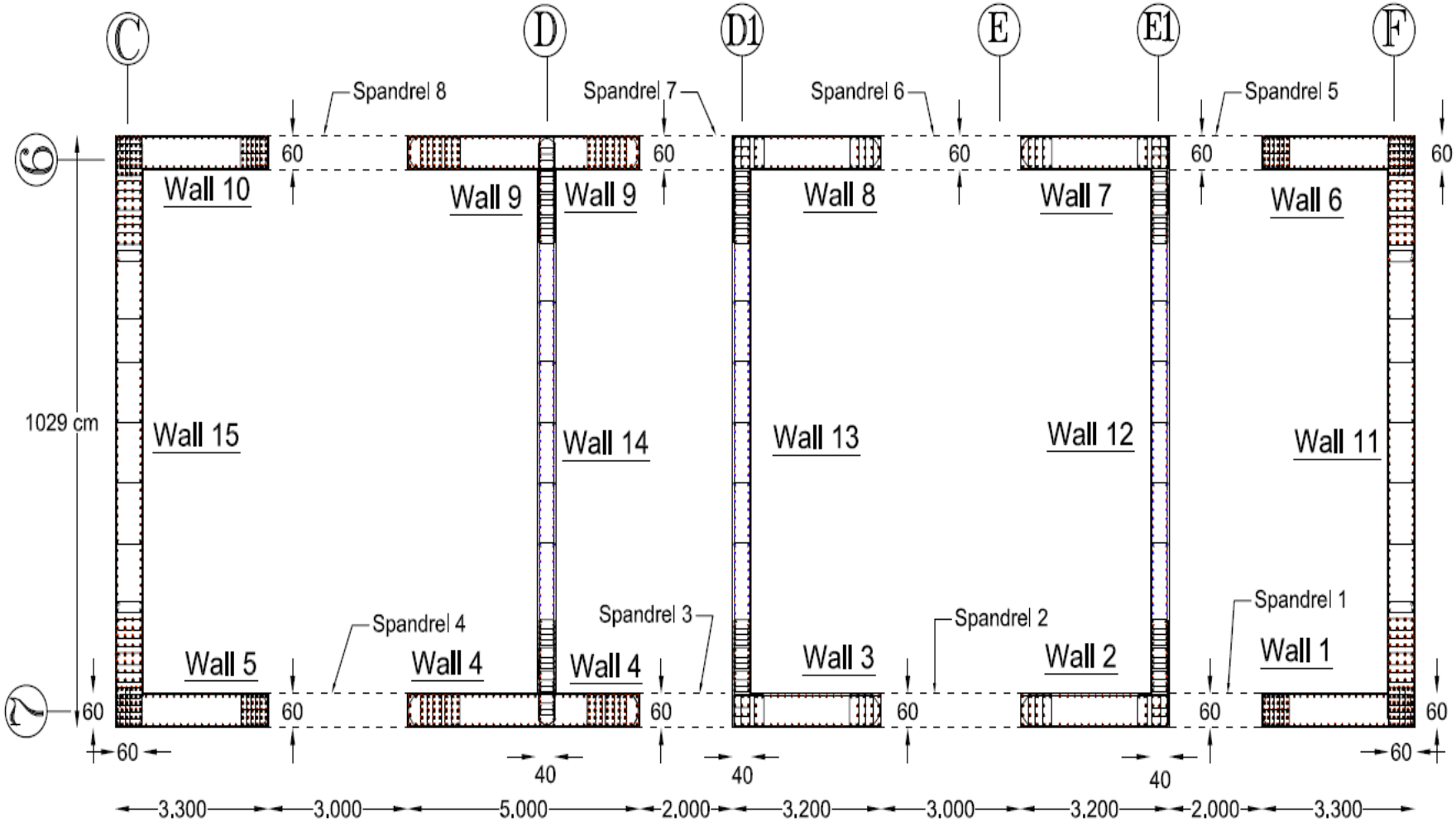

Figure 7.23: Wall axis and dimensions with spandrel positions (dimensions in cm)

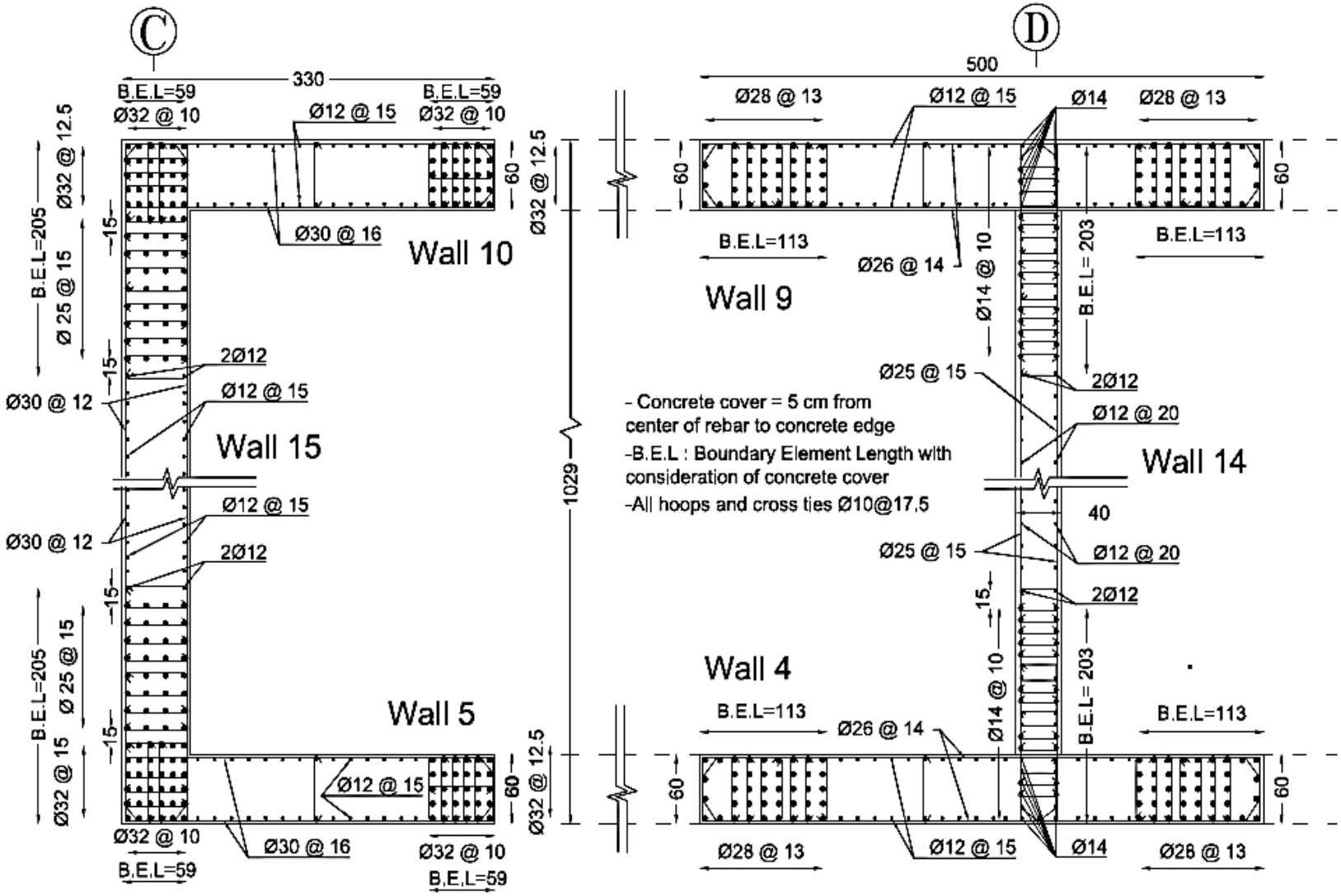
C
D
330
500
B.E.L=59
Ø32 @ 10
Ø12 @ 15
Ø32 @ 12.5
Ø30 @ 16
Wall 10
Wall 15
Wall 5
Wall 9
Wall 14
Wall 4
B.E.L=205
Ø 25 @ 15
2Ø12
Ø30 @ 12
1029
60
15
- Concrete cover = 5 cm from center of rebar to concrete edge
-B.E.L : Boundary Element Length with consideration of concrete cover
-All hoops and cross ties Ø10@17.5
Ø28 @ 13
Ø14
B.E.L=113
Ø26 @ 14
Ø14 @ 10
B.E.L= 203
Ø25 @ 15
Ø12 @ 20
40
Ø28 @ 13

Figure 7.24: Reinforcement detail of axis C and D

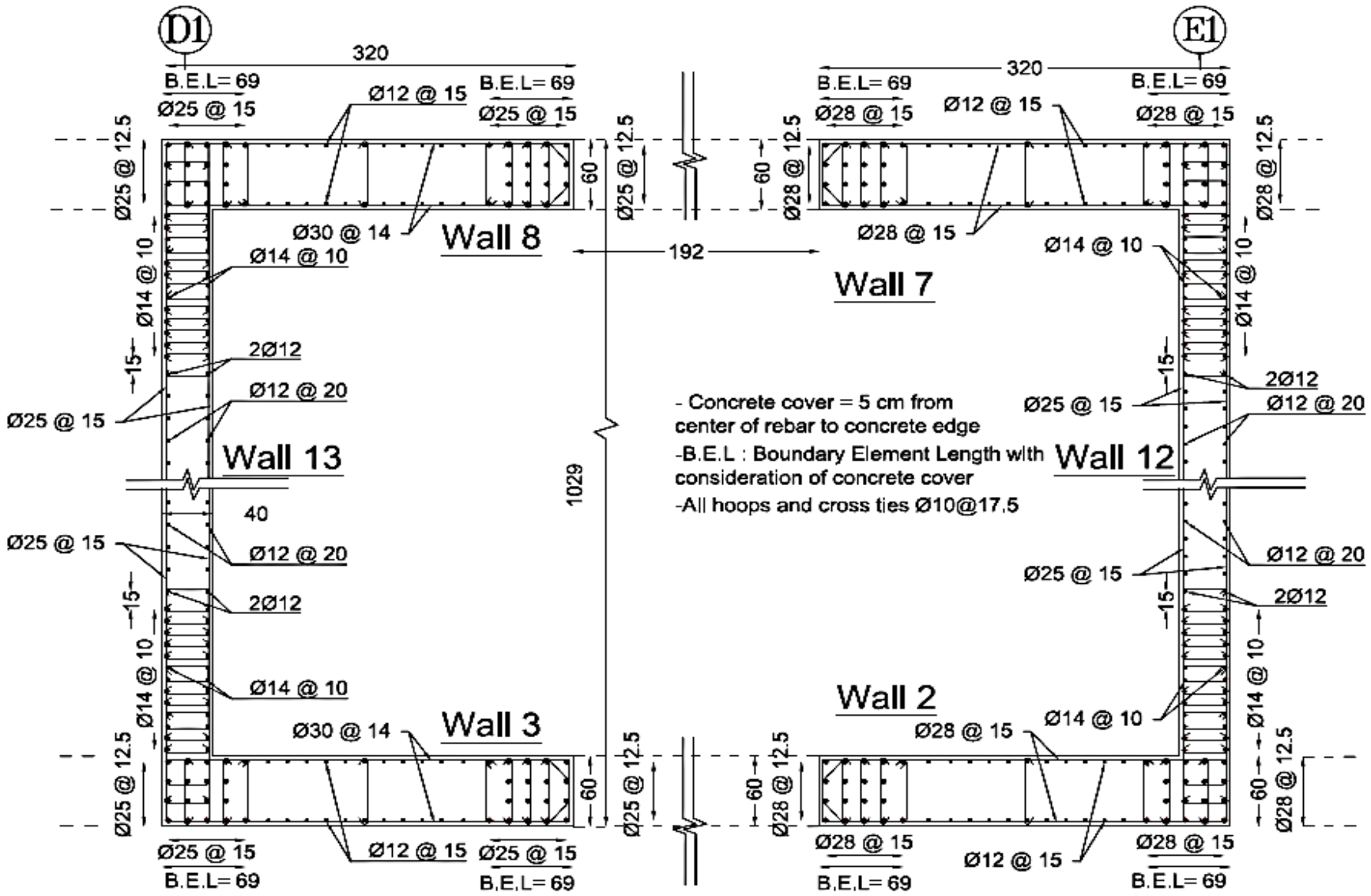
D1
E1
320
320
B.E.L= 69
Ø25 @ 15
Ø12 @ 15
B.E.L= 69
Ø25 @ 15
B.E.L= 69
Ø28 @ 15
Ø12 @ 15
B.E.L= 69
Ø28 @ 15
Ø25 @ 12.5
60
Ø25 @ 12.5
60
Ø28 @ 12.5
Ø28 @ 12.5
Ø30 @ 14
Wall 8
192
Ø28 @ 15
Ø14 @ 10
Wall 7
Ø14 @ 10
Ø14 @ 10
15
2Ø12
Ø12 @ 20
Ø25 @ 15
Wall 13
1029
- Concrete cover = 5 cm from center of rebar to concrete edge
-B.E.L : Boundary Element Length with consideration of concrete cover
-All hoops and cross ties Ø10@17.5
Wall 12
Ø25 @ 15
2Ø12
Ø12 @ 20
40
Ø25 @ 15
Ø12 @ 20
2Ø12
Ø25 @ 15
Ø12 @ 20
2Ø12
Ø14 @ 10
Ø14 @ 10
Wall 2
Wall 3
Ø30 @ 14
Ø28 @ 15
Ø14 @ 10
Ø25 @ 12.5
60
Ø25 @ 12.5
60
Ø28 @ 12.5
Ø28 @ 12.5
Ø25 @ 15
B.E.L= 69
Ø12 @ 15
Ø25 @ 15
B.E.L= 69
Ø28 @ 15
B.E.L= 69
Ø12 @ 15
Ø28 @ 15
B.E.L= 69

Figure 7.25: Reinforcement detail of axis D1 and E1

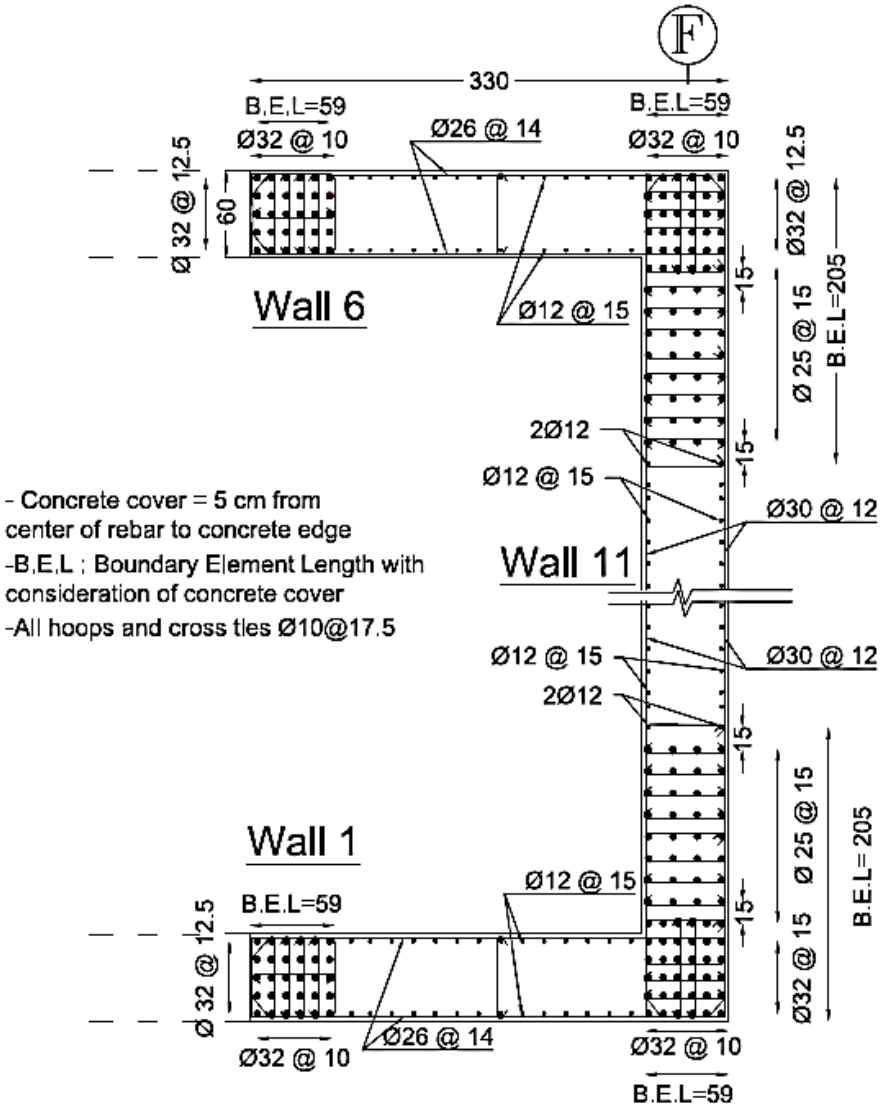

Figure 7.26: Reinforcement detail of axis F

7.18 Failure Mechanisms and Behavior of Coupling Beams

The primary goal of beams between coupled walls during earthquake is the transfer of shear from one wall to the other, as shown in Fig. 7.27(c). Many coupling beams have been designed as conventional flexural members with stirrups and with shear resistance allocated to the concrete. Such beams will inevitably fail in diagonal tension, as reported in many earthquakes. This phenomenon is shown in Fig. 7.27(a) [26].

It is obvious that the principal diagonal failure crack will divide a relatively short beam into two triangular parts. Unless the shear force associated with flexural overstrength of the beam at the wall faces can be transmitted by vertical stirrups only, a diagonal tension failure will result. In such beams it is difficult to develop full flexural strength even under monotonic loads, and therefore such conventional coupling beams are quite unsuitable for energy dissipation [26].

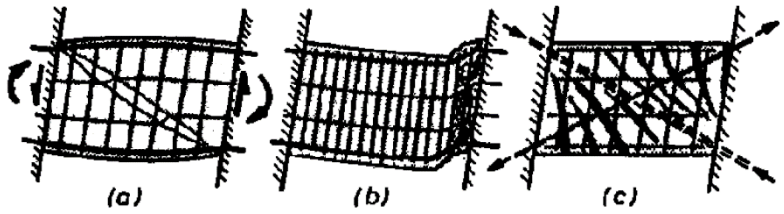

Figure 7.27: Shear resistance mechanism in coupling beams [26]

With conventional shear reinforcement based on capacity design principles, some limited ductility can be achieved. However, after only a few load reversals, flexural cracks at the boundaries will interconnect and a sudden sliding shear failure, such as shown in Fig. 7.27(b), will occur [26].

Under reversal cyclic loading it is hard to maintain the high bond stresses along the horizontal flexural reinforcement which is necessary to sustain the high rate of changes of moment along the short span. Such horizontal bars, shown in Fig. 7.27(a) and (b), tend to develop tension over the entire span, so that shear is transferred primarily by a single diagonal concrete strut across the beam. This consideration leads to the use of a bracing mechanism that uses diagonal reinforcement in coupling beams as shown in Figs. 7.27(c) 7.28 [26].

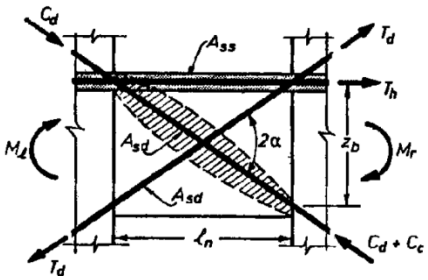

Figure 7.28: Analytical model of coupling beam and forces of diagonal reinforcement [26]

.In EC8 walls with an aspect ratio of 3 or less should be designed with diagonal reinforcement. The amount of diagonal reinforcement is calculate due to Clause 5.5.3.5 (a)

$$A_{si} = \frac{V_{Ed}}{2 f_{yd} . \sin \alpha} \tag{7.29}$$

where

V_{Ed} is the design shear force in the coupling element ;
A_{si} is the total area of steel bars in each diagonal direction;
α is the angle between the diagonal bars and the axis of the beam.
f_{yd} Is considered to be 435 MPa for steel B500

Minimum skin reinforcement is also calculated based on EC2 annex J and distributed on the surface of coupling beams equal to $A_{s,surf} = 0{,}01A_{ct,ext}$. Coupling beams of tower 1 at story 2 are designed at base section. At the next step coupling beams of story 25 and 44 are designed for comparison.

Spandrel	**h** [cm]	**l** [cm]	**sinα**	**V_{Ed}** [kN]	**A_{si}** [cm^2]	**Rebar used**	**A_s supplied** [cm^2]
1,5	220	200	0.76	4398	66.51	16Ø30	76.69
2,6	220	300	0.59	4931	96	16Ø28	98.4
3,7	220	200	0.76	5584	84.5	12Ø30	84.84
4,8	220	300	0.59	4000	78	12Ø30	84.84

Table 7.11: Coupling beams reinforcement at story 2

Figures 7.29 and 7.30 show the details of spandrel beams.

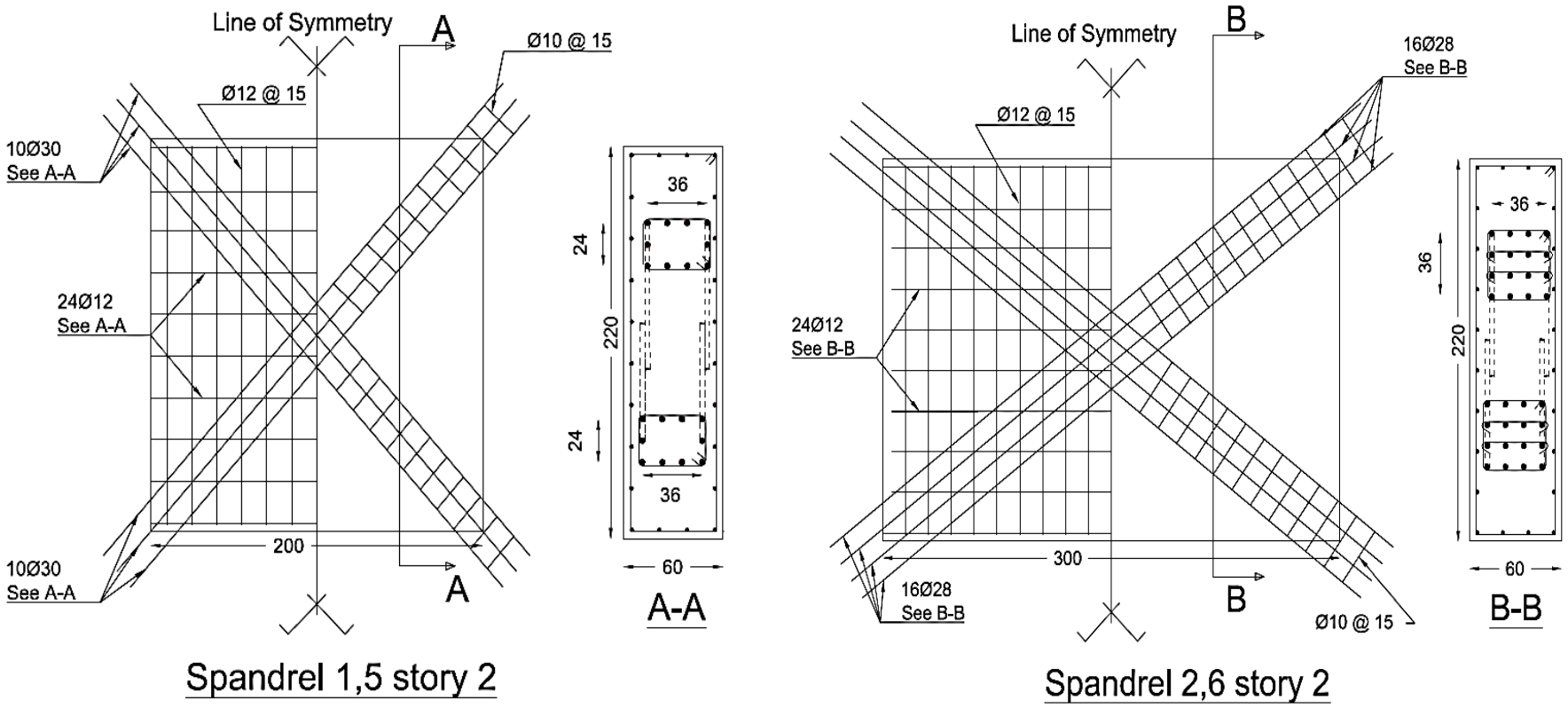

Figure 7.29: Spandrel 1,2,5,6, story2

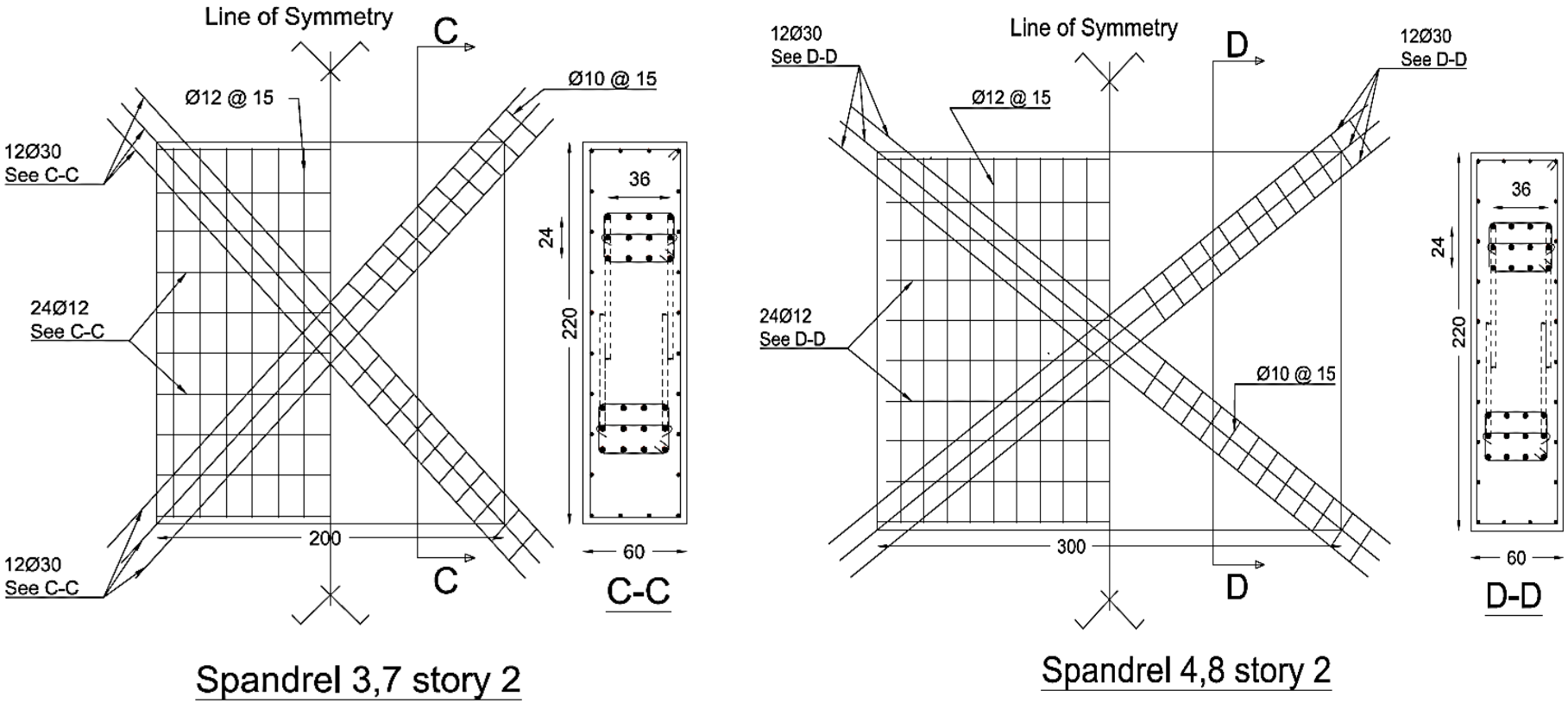

Figure 7.30: Spandrels 3,4,7,8 details at story 2

7.19 Wall and Spandrel Design at Midspan and Top of Building

The difference of wall design at the base section and upper stories is the confinement reinforcement which is used at the base to gain more ductility and preventing of buckling of flexural bars. At the base a dense volume of confinement is used to ensure formation of plastic hinge and preventing brittle failure. At the upper levels with reduction of axial force there is no need to confine concrete. The level of axial force which requires confinement varies in different codes. EC8 mentions that over the critical height of plastic hinge rules of EC2 could be applied.

Since internal forces diminishes rapidly with height, flexural design shows that only in some walls at story 20 flexural reinforcement more than minimum reinforcement is required. In other walls minimum web reinforcement is sufficient. Shear reinforcements is required also at these sections much more than minimum value required for shear and shows that shear force governs the design.

Figures 7.32 to 7.34 shows the wall sections and spandrel details at story 20, on axis 6. Because of symmetry only upper part is shown.

At top section only minimum reinforcement is requirde for flexural reinforcement, but shear design is exactly like story 20, because shear force envlope is the same. Only for flexural design minimum of 0,002Ac= 8cm2 is required which Ø10@18 could be used with As=8.72 cm2. At to section (story 44) axis C is omitted and walls 5,8,15 are curtailed also spandrels 4,8 are eliminated. Remaining spandrels have a less diagonal reinforcement and the same skin rebar as other spandrels. Therefore only section of these spandrels are shown and no wall detail is illustrated.

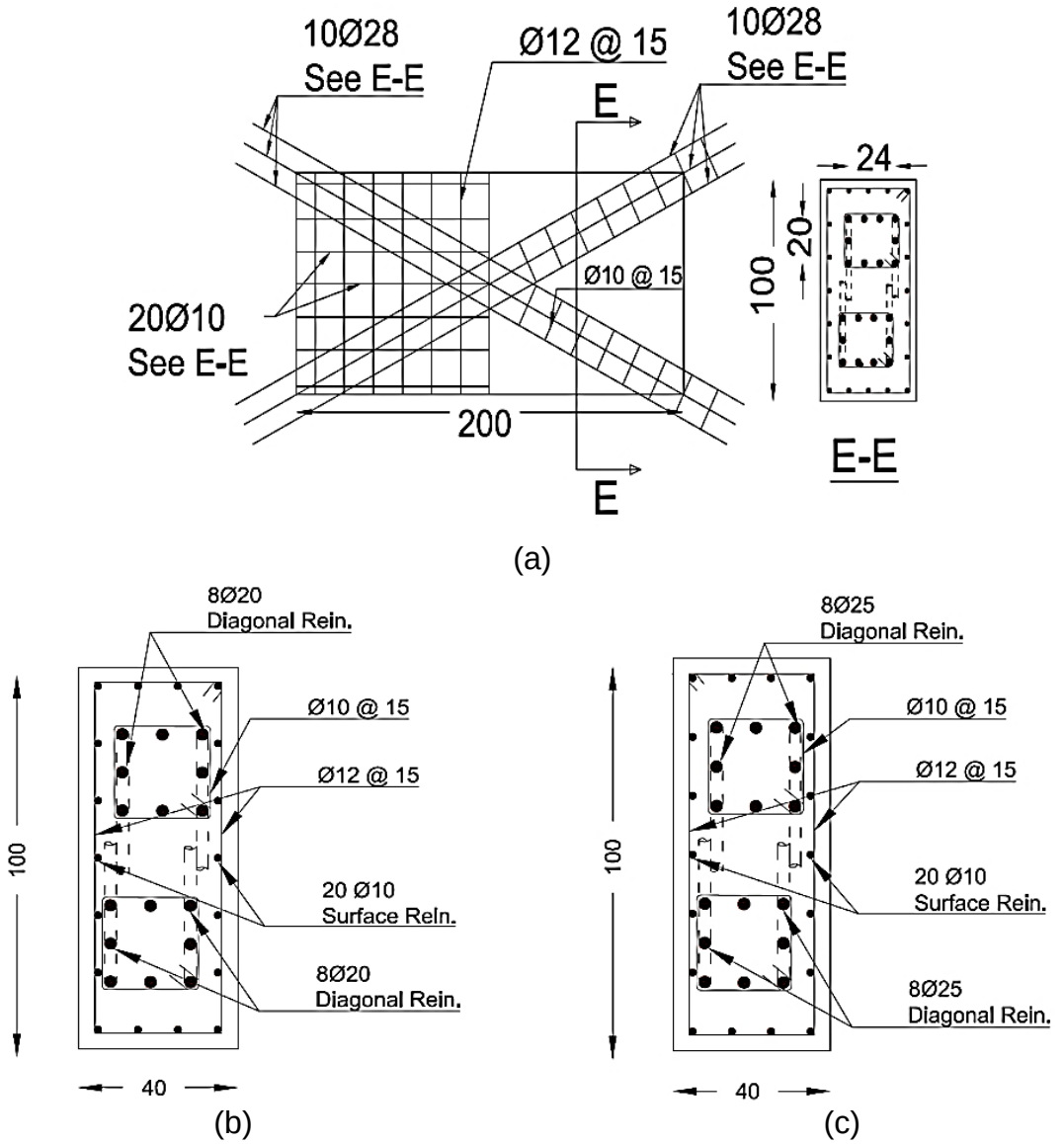

Figure 7.31: (a) Spandrel 3,7 story 20; (b) spandrel 1,3,5,7, story44; (c) spandrel 2,6 story44

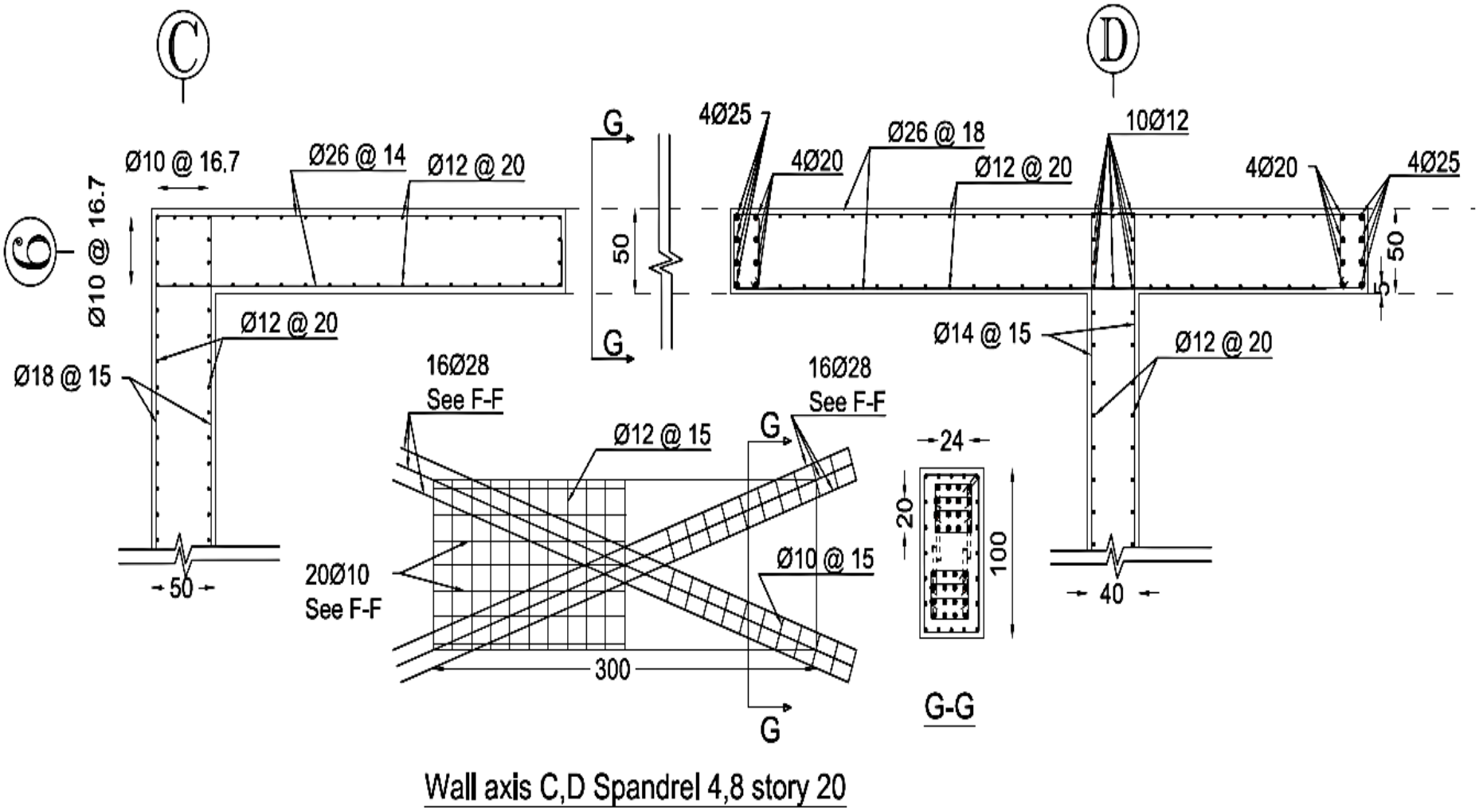

Figure 7.32: Wall section details between axis C,D on axis 6 at story 20 (because of symmetry only axis 6 is shown)

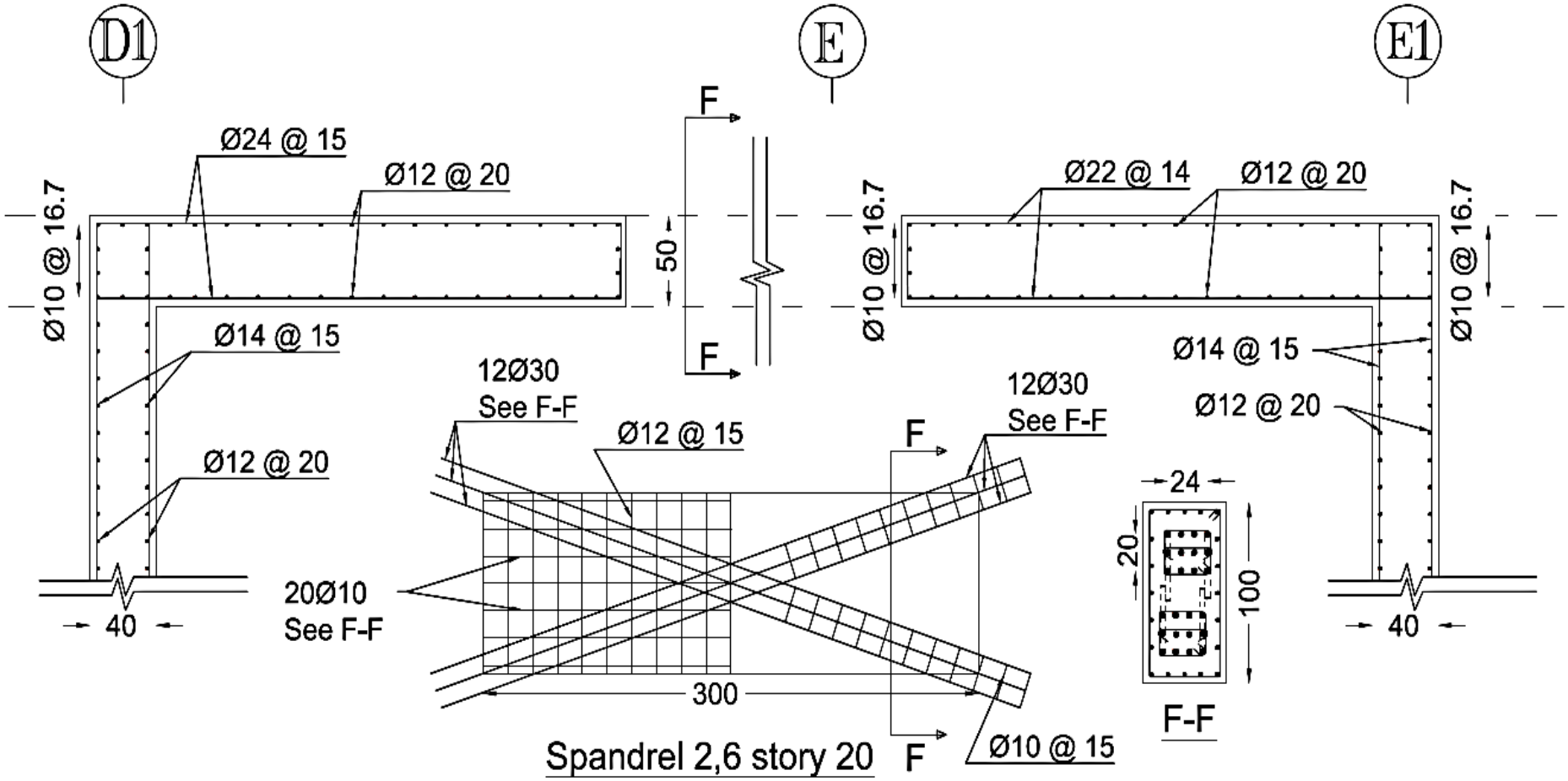

Figure 7.33: Wall sectio detail between axis D1,E1 on axis 6 at story 20 (because of symmetry only axis 6 is shown)

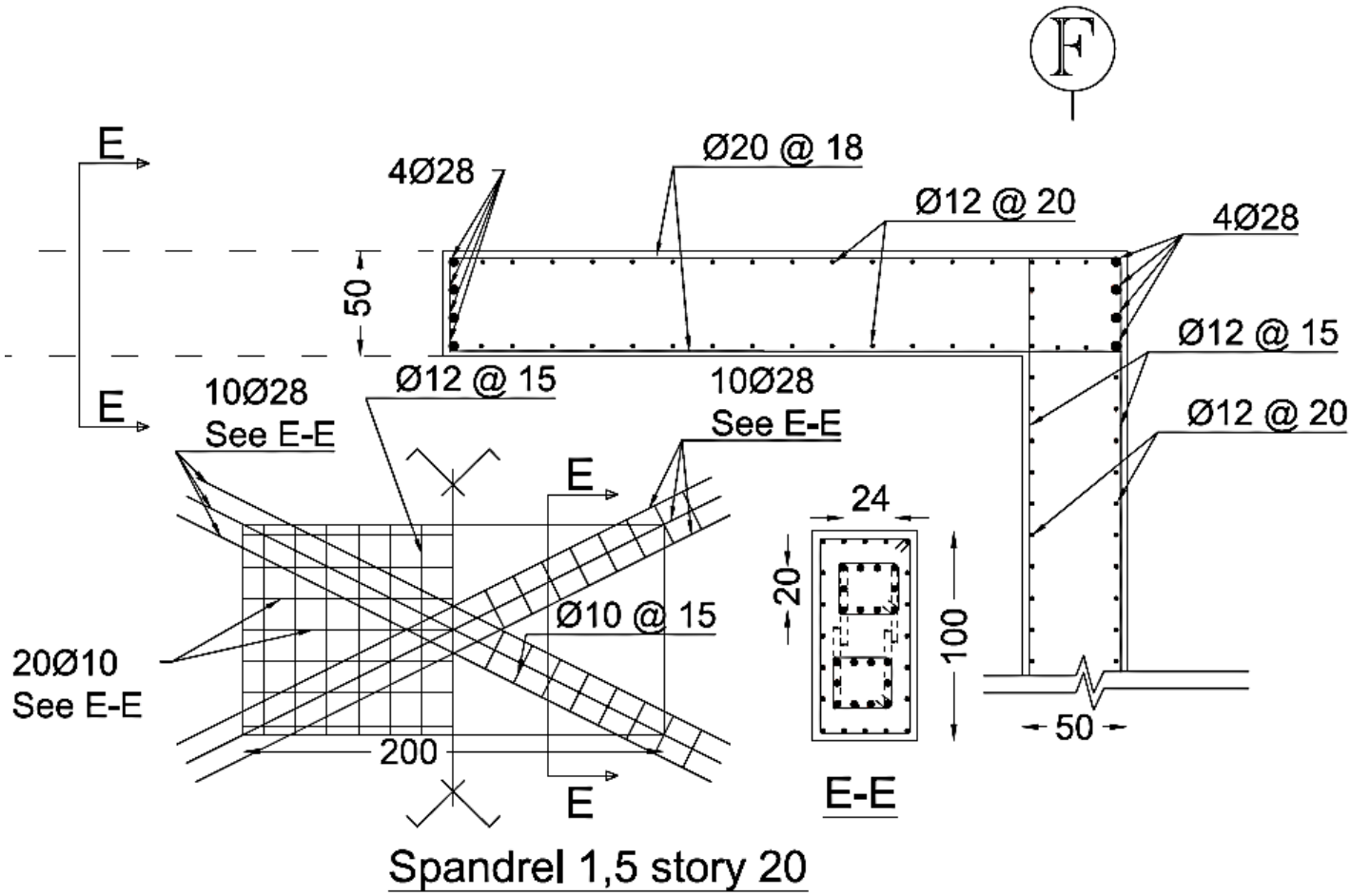

Figure 7.34: Wall section detail at axis F on axis 6 at story 20 (because of symmetry only axis 6 is shown)

8 Conclusions and Recommendations

In this project comparison of wind and earthquake loads shows that the earthquake is the governing load case for design in both shear and flexural demand.

As a result of high natrual period of structure the delivered acceleration lies far from plateua level of reponse specturm and is less prone to earthquake forces.

The analysis and design of this structure shows the feasibility of such a geometrical layout in plan after applying of improvements. Flexural demand could be easily met specially at the base section even for larger earthquakes. Design for shear forces in walls implies a dense shear reinforcement at base because of high shear forces. This shows a high compressive stress in compressive struts of concrete in shear design. For more conservative design or higher earthquake levels it could be necessary to thicken the walls or elongate them, but if the architectural plan is fixed only thicker walls could be more convenient solution.

Building regularity is not checked in plan and elevation because a multi modal response specrum analysis is used.

A concerete with less strength can be used for upper levels for more economical design, in two or three steps.

Since the coupling beams should withstand high shear forces eventuating in diagonal tension and on the other hand will undergo syclic loading a higher ductility demand is needed to ensure the concrete integrity in coupling beams and to keep the walls coupled in major earhtquake. Therefore these couplings are designed for DCH.

For decreasing torsional effect and resulted shear forces, it is more convenient to change the plan to more compact shape in which two towers have no offset from each other. If the latter case is not possible tower 1 could be rotate 5 degrees in plan in a way that axis B, C, D match and unify respectivly with axis M, N, P to form larger frames and to increse effective depth of structure. Another countermeasure may be adding frames in x direction to increase the distribution of torsion on frames and to improve torsional stiffnes.

There is no recommendation for Rotational capacity of coupling beams and their maximum rotation at both ends in eurocodes therefore these cases sould be checked due to other guidelines.

To provide a better insight into the torsionall response of building the nummber of modes should be increased in a way that the sum of effective torsional modal mass reaches 90% of total mass.

If water tanks will be implemented at the top, their effect soud be modeled as concentrated mass at the top and the dynamic response of building specially drifts and top deflection shoul be investigated.

The favorable effects of car ramps on lateral stiffness of basement could be neglected. Car ramps may be designed localy in a disassembled way to simplify the system and decreasing computing time, but their resulting loads should be considered in desing of main elements if they are connected to main load bearing structural elements.

It is better to use frames with higher redundancy at axis G so the loads could be redistributed efficiently and have an alternative load pass in a case when a column goes damge and is eliminated from system. To this aim, more columns may be used to increase redundancy or outrigger with belt-truss system is adviced to give gravity load an alternative load pass and to prevent a progressive collapse.

If in final design a higher earthquake level is considered, drift control could be properly done by adding outriggers in two or three levels like story 15, mechanical room at story 30 and at the top which interferes less the architectural plan.

9 Recommendations for Further Studies

- A nonlinear push-over analysis could be done to evaluate the behavior factor exactly and location of probable plastic hinges.
- A nonlinear dynamic analysis can be performed for consideration of exact behavior of structuer in nonlinear range with consideration of material nonlinearity.
- Second order iterative analysis may be used for estimating exact values of internal forces magnification under second order effect, and results could be compared with values sugessted in code for magnification factor .
- Alternative structural systems like core-outrigger systems could be examined for gaining better structural response or optimization of structural dimensions.
- The floor slabs strength should be checked in necked part of floor plan at upper stories between tower 1 and tower 2, also diaphragm action of slab shoul be checked.
- For more precise evaluation of overall wind forces and its turbulance effect on building also local effects of wind on cladding, wind tunnel test could be performed.

References

[1] Austrian Standard Institute, “Eurocode 1: Actions on structures, Part 1: Part 1-4: General actions - Wind actions.” ÖNORM EN 1991-1-4: 2005, Vienna, 2011.

[2] Austrian Standard Institute, “Eurocode 1: Actions on structures, Part 1-1: General actions - Densities, self-weight, imposed loads for buildings.” ÖNORM EN 1991-1-1: 2002, Vienna, 2011.

[3] Austrian Standard Institute, “Eurocode 1: Actions on structures, Part 1-3: General actions - Snow loads.” ÖNORM EN 1991-1-3: 2002, Vienna, 2005.

[4] Svend Ole Hansen, Claës Dyrbye, “ Wind Loads on Structures.” Copenhagen, John Wiley & Sons, 1999.

[5] Emil Simiu and Robert H. Scanlan, “Wind Effects on Structures: Fundamentals and Applications to Design.” 3rd ed. Baltimore, John Wiley & Sons, 1996.

[6] John D.Holmes, “Wind Loading of Structures.” 2nd ed. Abingdon, Taylor & Francis, 2007.

[7] Bungale s. Taranath, “Wind and Earthquake Resistant Buildings: Structural Analysis and Design.” New York, Marcel Dekker, 2005.

[8] T. Balendra, “Vibration of Buildings to Wind and Earthquake Loads.” Sinngapore, Springer, 1993.

[9] Rainer Flesch, Horst Pacht, “Baudynamik praxisgerecht: Band 1 Berechnungsgrundlagen.” Wien, Bauverlag, 2000.

[10] Klaus Holschemacher, “Lastannahmen nach neuen Normen: Grundlagen, Erläuterungen, Praxisbeispiele. Einwirkungen auf Tragwerke aus: Nutzlasten, Windlasten, Schneelasten, Erdbebenlasten.” Bauwerk, 2007.

[11] Konrad Bergmeister, Johann-Dietrich Wörner (Herausgeber), “Beton-Kalender 2003: Hochhäuser und Geschossbauten.” Ernst & Sohn, 2002.

[12] Ted Stathopoulos, Charalambos C. Baniotopoulos, “Wind Effects on Buidings and Design of Wind-Sensitive Structures.” Udine, Springer, 2007.

[13] Rosemeier, Gustav-Erich, “Windbelastung von Bauwerken: Hoch-und Brückenbauten; Schalen; Leichte Flächentragwerke; neue Windlastnorm DIN 1055-4; Baudynamik; Aerodynamik; Luftturbulenzen” 2 ed., Berlin, Bauwerk, 2009.

[14] P.D Cenek, J.H. Wood, “Brans Study Report: Designing Multi-Story Buildings for Wind Efffects.” NO.25, Building Research Association of New Zealand, 1990.

[15] Austrian Standard Institute, “ Eurocode 8: Design of Structures for Earthquake Resistance, Part 1: General Rules, Seismic Actions and Rules for Buildings.” ÖNORM EN 1998-1: 2004, Vienna, 2011.

[16] Anil K. Chopra, “Dynamics of Structures: Theory and Application to Earthquake Engineering.” Englewood Cliffs, Prentice Hall, 1995.
[17] Ray W. Clough, Joseph Penzien, “Dynamics of Structures.” 3rd ed., Berkley, Computers & Structures, Inc., 2003.
[18] Jimin He, Zhi-Fang Fu, “Modal Analysis.” Oxford, Butterworth-Heinemann, 2001.
[19] Rainer Flesch, “Baudynamik und Erdbebeningenieurwesen.” Script, Technical University of Graz, 2011.
[20] Leonard Meirovitch, “Elements of Vibration Analysis.” 2nd ed., McGraw-Hill, 1986.
[21] Konstantin Meskouris, Klaus-G. Hinzen, Christoph Butenweg, Michael Mistler, “Bauwerke und Erdbeben.” 2nd ed., Wiesbaden, Vieweg, 2007
[22] Helmut Kramer, “Angewandte Baudynamik: Grundlagen und Beispiele für Studium und Praxis.” Berlin, Ernst & Sohn, 2007.
[23] T. K. Datta, “Seismic Analysis of Structures.” Delhi, John Wiley & Sons, 2010.
[24] Comite Euro-International Du Beton, “Seismic Design of Reinforced Concrete Structures For Controlled Inelastic Response: Design Concepts.” Lausanne, Thomas Telford, 1997.
[25] Srinivasan Chandrasekaran, Luciano Nunziante, Giorgio Serino, Federico Carannante, “Seismic Design Aids for Nonlinear Analysis of Reinforced Concrete Structures.” Boca Raton, CRC, 2010.
[26] T. Paulay, M. J. N. Priestley, “Seismic Design of Reinforced Concrete and Masonry Buildings.” USA, John Wiley & Sons, 1992.
[27] C. E Beards, “Structural Vibration: Analysis and Damping.” Oxford, Butterworth-Heinemann, 1996.
[28] P. Bisch, E. Carvalho, H. Degee, P. Fajfar, M. Fardis, P. Franchin, M. Kreslin, A. Pecker, P. Pinto, A. Plumier, H. Somja, G. Tsionis, “Eurocode 8: Seismic Design of Buildings Worked examples.” Luxembourg, Publications Office of the European Union, 2012.
[29] Ahmed Y. Elghazouli, “Seismic Design of Buildings to Eurocode 8.” Abingdon, Spon Press, 2009.
[30] Müller F. P., Keintzel E. “Erdbebensicherung von Hochbauten.” Verlag Ernst und Sohn, Berlin, 1984
[31] Computers and Structures, Inc., “CSI Analysis Reference Manual.” Berkeley, 2013.
[32] A. K. Gupta, “Response Spectrum Method in Seismic Analysis and Design of Structures.” Black well Scientific Publications, Cambridge, Mass, 1990.
[33] E. L. Wilson, A. Der Kiureghian, and E. P. Bayo, “A Replacement for the SRSS Method in Seismic Analysis,” Earthquake Engineering and Structural Dynamics, Vol. 9, 1981.
[34] Rosenblueth, E., Elorduy, J. “Responses of linear Systems to certain transient disturbances.” 4. WCEE, Santiago, 1969

[35] NRC, “Combining Modal Responses and Spatial Components in Seismic Response Analysis,” Regulatory Guide 1.92, Revision 2, U.S. Nuclear Regulatory Commission, 2006.
[36] C. Menun and A. Der Kiureghian, “A Replacement for the 30%, 40%, and SRSS Rules for Multicomponent Seismic Analysis,” Earth quake Spectra, Vol. 14, No. 1, pp. 153-163, 1998.
[37] Fahjan, Y., Tuzun, C., Kubin, J., “An Alternative Procedure for Accidental Eccentricity in Dynamic Modal Analyses of Buildings.” First European Conference on Earthquake Engineering and Seismology, 1166, 2006.
[38] Institution of Structural Engineers/SECED/AFPS, “Manual for the seismic design of steel and concrete buildings to Eurocode 8.”, London, 2010.
[39] Bungale S. Taranath, “ Structural Analysis and Design of Tall Buildings: Steel and Composite Construction.” CRC Press, New York, 2012.
[40] Bryan Stafford Smith and Alex Coull, “Tall Building Structures: Analysis and Design.” John Wiley & Sons, USA, 1991.
[41] Bungale S. Taranath, “Structural Analysis and Desig of Tall Buildings.” McGraw-Hili, USA, 1988.
[42] Madison R Paulino, “Preliminary Design of Tall Buildings.” Master Thesis, Worcester Polytechnic Institute, 2010.
[43] www.bc.edu
[44] www.flickr.com
[45] Uniform Building Code, International Conference of Building Officials. Whittier, California, 1997.
[46] Goldberg. J. E. “Approximate methods in Stress and Stability Analysis of Tall Building Frames. “Proc. IABSE Regional Conference on Tall Buildings, Bankok, 1974.
[47] Robert E. Englekirk, “Seismic Design of Reinforced and Precast Concrete Buildings.” John Wiley & Sons, New Jersey, 2003.
[48] R. Park and T. Paulay, “Reinforced concrete structures.” John Wiley & Sons, 1975.
[49] James K. Wight, James J. MacGregor, “Reinforced Concrete: Mechanics and Design.” 5th ed., Pearsonn Prentice Hall, New Jersy, 2009.
[50] Xiangfu Chen, “Settlement Calculation on High-Rise Buildings: Theory and Application.” Springer, New York, 2011.
[51] Viet Tue Nguyen, “Stahlbetonbau.” Skriptum, Technische Universität Graz, Institute für Betonbau, Graz, 2011.
[52] Iain A. Mackleod, “shear wall frame interaction.” Special Publication Sp011.01D, Portland cement Association, Skokie IL, 1971, 62pp.
[53] Pala, S. And Ozmen, G., Effective stiffness of coupling beams in structural walls, Computer & Structures, V. 54, No. 5, pp. 925-931, 1995.
[54] Madison R Paulino, “Preliminary Design of Tall Buildings.” Master Thesis, Worcester Polytechnic Institute, 2010.

[55] Shervin Shahriari, “The Effect of Openings on the Performance Reinforce Concrete Walls,” Master Thesis, University of Salford, 2010.
[56] Rosman, R, "Laterally Loaded Systems Consisting of Wails and Frames." Tall Buildings, Pergamon Press Ltd., London, pp. 273-289, 1967.
[57] Coull, A., and Choudhury, J.R, "Stresses and Deflections in Coupled Shear Walls." ACI Proc., Vol. 64, No.2, pp.65-72, 1967.
[58] Heidebrecht, A.C. and Stafford Smith, B. “Approximate analysis of Tall Wall-Frame Structures.” J. Struct. Div., Proc. ASCE99, ST2. 199-21, 1973.
[59] Marie-José Nollet, “A Study of the Interactive Behaviour of Continuous and Discontinuous Wall-Frame Structures.” Dissertation, McGill University, Montreal, Canada, 1991.
[60] Nollet, M. –J. and Stafford Smith. B. “An Empirical Approach to the Evaluation of Shear Rigidity of a Wall-Frame with Rigidly Jointed Link Beams.” Structural Engineering Series Report No. 88-5. Department of Civil Engineering and applied Mechanics, McGill University. 1988.
[61] Mark Sarkisian, “Designing Tall Buildings: Structure as Architecture.” Routledge, New York, 2012.
[62] Vlaslov. V.Z, “ Thin-walled Elastic Beams.” 2nd ed. Office of Technical Service, Washington, D.C. 1961.
[63] Kollbrunner. C.F. and Basler. K., “Torsion in Structures, An engineering Approach.” Springer Verlag, New York, 1969.
[64] Stafford Smith. B. and Taranath. B.S. “Analysis of Tall Core-Supported Structures subjected to Torsion.” Proc. Inst. Civ. Engineers, 53, 173-187, 1972.
[65] Heidebrecht, A.C. and Stafford Smith. B. “Approximmate analysis of Open-Section Shear Walls Subjected to Torsional loading.” Proc. ASCE ST12, 2355-2373, 1973.
[66] Staford Smith. B. and jesien. W. “Two-column Method for Static Analysis of Monosymetric Thin-walled Beams.” Structural Engineering Report No.88-3. Department of Civil Engineering and Applied Mechanics. McGill University, 1988.
[67] Michael N. Fardis et al., “Designer’s guide to EN 1998-1 and EN 1998-5.” Thomas Telford, London 2005.
[68] Hugo Bachmann, “Kapazitaetbemessung und Plastisches Dynamisches Verhalten von Stahlbetontragwerken.” Ernnst & Sohn, Zürich, 1999.
[69] Hugo Bachmann, Thomas Paulay, “Kapazitätbemessung von Stahlbetontragwände unter Erdbebeneinwirkung.” Birkhhäuser Verlag, Zürich, 1990.
[70] Konrad Moser, Thomas Paulay, “Kapazitätbemessung erdbebenbeanspruchter Stahlbetonrahmen.” Birkhhäuser Verlag, Zürich, 1990.
[71] Hugo Bachman et al., “Erdbebengerechter Entwurf und Kapazitätbemessung eines Gebäudes mit Stahlbetontragwänden.” SIA, Zürich, 2002.

[72] Computers & Structures, Inc., “Shear Wall Design Manual Eurocode 2-2004 with Eurocode 8-2004 For ETABS® 2013” Berkeley, 2013.

List of Figures

Figure 1.1	3rd basement floor plan	2
Figure 1.2	Typical floor plan from 1st to floor plan	3
Figure 1.3	Typical floor plan from 2nd to 8th story	4
Figure 1.4	typical floor plan from 9th up to end story, excluded story 24,28, 32, 36, connected floor slabs	5
Figure 1.5	Typical separated floor slabs of 24, 28, 32, 36th floors	6
Figure 1.6	Elevation c-c	7
Figure 1.7	(a) Story 21 without setback; (b) shear wall setbacks at story 22; (c) curtailment at story 31 in tower 1(dimensions in mm)	9,10
Figure 2.1	Braced frame behavior, (a): flexural deformation, (b): shear deformation, (c): combined configuration	18
Figure 2.1	(a) Rigid frame, (b) assumption made at structural node in analysis	13
Figure 2.2	Response of rigid frame to lateral forces in shear mode	13
Figure 2.4	Forces and deformation under external moment in bending mode	14
Figure 2.5	(a) Deformation under shear load, (b) equivalent braced analogy	16
Figure 2.6	Sliding shear failure	16
Figure 2.7	(a) Shear wall structure [40], (b) common shear wall sections	17
Figure 2.8	(a) Proportionate wall system, (b) nonproportionate wall system	18
Figure 2.9	(a) Allocation of moments between walls, (b) resulting interactions	19
Figure 2.10	(a) Coupling of walls solely by slabs; (b) developed yield lines under horizontal loading	20
Figure 2.11	(a) Pin ended links; (b) moment resisting coupling	21
Figure 2.12	(b) True stress distribution on the wall based on superposition of stress distribution due to (c) composite and (d) independent action	22
Figure 2.13	Effect of shear wall deflections in coupling beam and induced internal forces	23
Figure 2.14	(a) Coupled shear wall; (b) mathematical model	24
Figure 2.15	Different cases in frame analogy method; (a) model with shallow coupling beams; (b) model with deep coupling beams; (c) solid wall	25
Figure 2.16	Representative wall-frame structure	26
Figure 2.17	Deflection modes and interaction between wall and frame	27

Figure 2.18	(a) Typical deflection of wall-frame system under horizontal static loading; (b) typical moment diagram of system; (c) typical shear diagram	27
Figure 2.19	(a) Planner wall frame structure; (b) continuum analogy for wall frame structure; (c) free body diagram of wall and frame	28
Figure 2.20	(a) Framed tube structure; (b) shear lag effect	30
Figure 2.21	(a) Stress distribution in bundled tube with two cells; (b) multi-cell bundled tube stress distribution	30
Figure 2.22	(a) Braced tube structure; (b) Tube in tube structure	31
Figure 2.23	(a) Open section core; (b) core partially closed by beams; (c) core partially closed by floor slabs	32
Figure 2.24	(a) Twisting of core under torque; (b) twisting shear Stress in open section; (c) shear stress in closed section	33
Figure 2.25	(a) Core under distributed torque; (b) stress distribution due to warping in core section; (c) rotation of core; (d) bimoment in core; (e) shear force in beams of partially closed core	35
Figure 2.26	Core and outrigger system: (a) centrally located core; (b) offset core	37
Figure 2.27	(a) Outrigger system under horizontal loading; (b) external moment diagram; (c) M_1 moment diagram caused by upper outrigger; (d) M_2 moment diagram caused by lower outrigger; (e) core resultant moment diagram	38
Figure 2.28	Belt truss system	45
Figure 2.29	(a) Extended diagonals as outrigger; (b) moment resistant connected girders acting as outrigger	39
Figure 4.1	Variation of wind velocity with time	43
Figure 4.2	Representation of wind pressure composed from two components	44
Figure 4.3	Assumption of EC1-4 for pressure distribution over height	48
Figure 4.4	Pressure zones and dimensions in wind from both x and y directions	48
Figure 4.5	Definition of reference height	50
Figure 4.6	Peak factor	56
Figure 4.7	Wind Pressure profile and its classification on test building due to [EC1-4] provisions	60
Figure 4.8	Wind streamlines and directions of along-wind and crosswind	61
Figure 4.9	Forming and shedding of vortices and equivalent loads	62
Figure 5.1	Response spectrum determination concept	68
Figure 5.2	Shape of the elastic response spectrum	70
Figure 5.3	Type 1 elastic response spectra	70
Figure 5.4	Type 2 elastic response spectra	71

Figure 5.5	Elastic and design response spectrum	72
Figure 5.6	Representing deflections as sum of modal components	75
Figure 5.7	Superposition of modes and phase shift between them	76
Figure 6.1	Model coordinate system	80
Figure 6.2	a) 3D view of structural elements; b) shear wall system; (c) analysis mesh of building; (d) analysis mesh of cores	82
Figure 6.3	(a) System without beams; (b) Stiffening the system in Y direction with beams and rotated columns	85
Figure 6.4	Effective widths of beams	86
Figure 7.1	First 3 modes of cores; (a) first mode translation in y direction; (b) second mode translation in x direction; (c) third mode, torsion about z axis	94
Figure 7.2	Displacement of columns and core of tower 1 under design wind in elevation 7 in x direction	95
Figure 7.3	Story shear force in x direction	100
Figure 7.4	Wall and spandrel positions of tower 1	103
Figure 7.5	Coupled shear wall layout, elevation 7	104
Figure 7.6	Bending moment of coupled walls in seismic situation, elevation 7	105
Figure 7.7	Coupled walls shear forces in seismic situation, elevation 7	106
Figure 7.8	Bending moment variation of coupled walls at axis 6 and 7	108
Figure 7.9	Shear force variation of coupled walls at axis 6 and 7	108
Figure 7.10	Coupling beams shear forces	109
Figure 7.11	Bending moment envelope suggested by EC8 for structural walls	110
Figure 7.12	Web-flange action of wall assemblies	111
Figure 7.13	Bending moment of walls 12, 13, 14 and design envelope in y direction	112
Figure 7.14	Bending moment of walls 11, 15 and design envelope in y direction	113
Figure 7.15	Design envelope of shear forces of dual systems in EC8	113
Figure 7.16	Shear forces and their design envelope due to EC8 for walls 12, 13, 14 in y direction	114
Figure 7.17	Shear forces and their design envelope due to EC8 for walls 11, 15 in y direction	114
Figure 7.18	Shear wall failure modes	115
Figure 7.19	Dimensions of walls 3, 8, 11 in numerical model	117
Figure 7.20	Determination of interaction Surface points coordinates by varying strain plane and natural axis rotation	120
Figure 7.21	Typical interaction surface	121
Figure 7.22	Geometric representation of wall capacity ratio	121

Figure 7.23	Reinforcement detail of axis C and D	126
Figure 7.24	Reinforcement detail of axis D1 and E1	127
Figure 7.25	Reinforcement detail of axis F	128
Figure 7.26	Shear resistance mechanism in coupling beams	129
Figure 7.27	Analytical model of coupling beam and forces of diagonal reinforcement	130
Figure 7.28	Spandrel 1,2,5,6, story2	130
Figure 7.29	Spandrels 3,4,7,8 details at story 2	132
Figure 7.30	(a) Spandrel 3,7 story 20; (b) spandrel 1,3,5,7, story44; (c) spandrel 2,6 story44	144 133
Figure 7.31	Wall section details between axis C,D on axis 6 at story 20 (because of symmetry only axis 6 is shown)	135
Figure 7.32	Wall sectio detail between axis D1,E1 on axis 6 at story 20 (because of symmetry only axis 6 is shown)	136
Figure 7.33	Wall section detail at axis F on axis 6 at story 20 (because of symmetry only axis 6 is shown)	137
Figure 7.34	Wall section detail at axis F on axis 6 at story 20 (because of symmetry only axis 6 is shown)	138

List of Tables

Table 1.1	Columns dimensions and walls width classification for preliminary model	8
Table 4.1	Terrain categories	45
Table 4.2	Pressure coefficients for wind blowing in x direction	49
Table 4.3	Pressure coefficients for wind blowing in y direction	49
Table 4.4	Calculated background factor for both direction and related parameters	51
Table 4.5	Power spectral density function and related parameters	52
Table 4.6	Force coefficients for x and y directions	54
Table 4.7	Values of δ_a in both directions	55
Table 4.8	Logarithmic decrement of damping	55
Table 4.9	Resonance response factor values in both directions	55
Table 4.10	Wind forces using force coefficient	57
Table 4.11	Wind forces using surface pressure coefficient	59
Table 4.12	Galloping effect parameters	63
Table 4.13	Parameters of standard deviation of the characteristic along-wind acceleration	65
Table 5.1	Importance classes and importance factors	67
Table 6.1	Shear walls and typical column sizes	84
Table 6.2	The displacements and rotation due to F_{TX} = F_{TY} = 10^6 kN and M_T = 10^6 kN.m, the torsional (K_M) and lateral stiffness in both directions (K_{FX}, K_{FY}), torsional radius (r_x, r_y) and radius of gyration of the floor mass l_s	90
Table 7.1	The elastic periods (T), the effective masses and the effective mass moments (M_{eff})	95
Table 7.2	Actual displacements in CM of each storey above ground	97
Table 7.3	Story drifts check for both directions	99
Table 7.4	Base shear forces	100
Table 7.5	Sensitivity coefficient θ for both directions from first story up to 44	102
Table 7.6	Calculated parameters for boundary element length determination	119
Table 7.7	Supplied Flexural rebars in boundary elements and walls utilization factor	122
Table 7.8	Upper bound and lower bound of compressive strut strength	123
Table 7.9	Comparison of design value of shear force and compressive strut strength	123
Table 7.10	Calculated shear reinforcement and assigned reinforcement	124
Table 7.11	Coupling beams reinforcement at story 2	131

Dies ist eine Veröffentlichung des

FACHBEREICHS INGENIEURBAUKUNST (IBK) AN DER TU GRAZ

Der Fachbereich Ingenieurbaukunst umfasst die dem konstruktiven Ingenieurbau nahe stehenden Institute für Baustatik, Betonbau, Stahlbau & Flächentragwerke, Holzbau & Holztechnologie, Materialprüfung & Baustofftechnologie, Baubetrieb & Bauwirtschaft, Hochbau & Industriebau, Bauinformatik und Allgemeine Mechanik der Fakultät für Bauingenieurwissenschaften an der Technischen Universität Graz.

Dem Fachbereich Ingenieurbaukunst ist das Bautechnikzentrum (BTZ) zugeordnet, welches als gemeinsame hochmoderne Laboreinrichtung zur Durchführung der experimentellen Forschung aller beteiligten Institute dient. Es umfasst die drei Laboreinheiten für konstruktiven Ingenieurbau, für Bauphysik und für Baustofftechnologie.

Der Fachbereich Ingenieurbaukunst kooperiert im gemeinsamen Forschungsschwerpunkt „Advanced Construction Technology“.
Dieser Forschungsschwerpunkt umfasst sowohl Grundlagen- als auch praxisorientierte Forschungs- und Entwicklungsprogramme.

Weitere Forschungs- und Entwicklungskooperationen bestehen mit anderen Instituten der Fakultät, insbesondere mit der Gruppe Geotechnik, sowie nationalen und internationalen Partnern aus Wissenschaft und Wirtschaft.

Die Lehrinhalte des Fachbereichs Ingenieurbaukunst sind aufeinander abgestimmt. Aus gemeinsam betreuten Projektarbeiten und gemeinsamen Prüfungen innerhalb der Fachmodule können alle Beteiligten einen optimalen Nutzen ziehen.

Durch den gemeinsamen, einheitlichen Auftritt in der Öffentlichkeit präsentiert sich der Fachbereich Ingenieurbaukunst als moderne Lehr- und Forschungsgemeinschaft, welche die Ziele und Visionen der TU Graz umsetzt.

Nummerierungssystematik der Schriftenreihe:

D – Masterarbeiten/Dissertationen | F – Forschungsberichte
S – Skripten, Vorlesungsunterlagen | V – Vorträge, Tagungen

Institutskennzahl:
1 – Allgemeine Mechanik | 2 – Baustatik | 3 – Betonbau
4 – Holzbau & Holztechnologie | 5 – Stahlbau & Flächentragwerke
6 – Materialprüfung & Baustofftechnologie | 7 – Baubetrieb & Bauwirtschaft
8 – Hochbau & Industriebau | 9 – Bauinformatik
10 – Labor für Konstruktiven Ingenieurbau

Fortlaufende Nummer pro Reihe und Institut / Jahreszahl